Optimizing immobilized cultivation of *Haematococcus pluvialis* for astaxanthin production

by

Alice Costa Kiperstok

Cologne, 2016

Optimizing immobilized cultivation of
Haematococcus pluvialis for astaxanthin production

Inaugural-Dissertation

zur

Erlangung des Doktorgrades

der Mathematisch-Naturwissenschaftlichen Fakultät

der Universität zu Köln

vorgelegt von

Alice Costa Kiperstok

aus Salvador, Brasilien

Berichterstatter: Prof. Dr. Michael Melkonian
(Gutachter)
                         Prof. Dr. Burkhard Becker

Tag der mündlichen Prüfung: 12.04.2016

Acknowledgments

Abstract

Astaxanthin production from *Haematococcus pluvialis* is one of the main branches of microalgal biotechnology. Commercial interest rises from its applications as a pigment in animal feed and more recently in human health, due to its potent antioxidant activity. However, challenges in large-scale production of *H. pluvialis*, associated to both algal metabolism and cultivation strategies, still limit the market of natural astaxanthin. Current cultivation technologies are based on suspension systems that have major drawbacks such as high water, energy and technical requirements. These problems can be avoided by immobilized cultivation, which is therefore receiving increased attention. In this study, *H. pluvialis* was cultivated under immobilized conditions, in a Twin-Layer PSBR. 26 different strains of *H. pluvialis* were capable of biofilm growth and astaxanthin production and CCAC 0125 was selected for process optimization. Biomass and astaxanthin production increased as a function of the light intensity, until up to 1,015 µmol photons m^{-2} s^{-1}, with no sign of photoinhibition. Maximum biomass productivity of 19.4 g m^{-2} d^{-1} was observed at high light. Nutrient limitation and salinity increased astaxanthin production but compromised biomass growth. Nevertheless, highest astaxanthin productivity of 0.507 g m^{-2} d^{-1} and content in biomass of 3.5% of dry matter was reported at high irradiance, under nitrogen and phosphorous depletion. These results strongly encourage the immobilized cultivation of *H. pluvialis* as an alternative to current technologies. Coupling high biomass and astaxanthin productivities under high light intensities was possible due to the biofilm organization. It can represent a breakthrough in the commercial production of *H. pluvialis* by exempting the need of pre-cultivation at low light and thereby, simplifying the costly two-step processes currently employed.

Zusammenfassung

Die Produktion von Astaxanthin mittels *Haematococcus pluvialis* ist eines der wichtigsten Fachgebiete der Mikroalgen Biotechnologie. Kommerzielles Interesse ist zurückzuführen auf dessen Anwendungen als Pigment in der Tierzucht und neuerdings auch im Bereich des Gesundheitswesens, begründet auf seiner starken anti-oxidativen Wirkung. Allerdings begrenzen die Herausforderungen in der industriellen Produktion von *H. pluvialis*, in Bezug auf den Metabolismus der Alge wie gleichermaßen auch die Kultivierungsstrategie, immer noch den Markt für natürliches Astaxanthin. Die derzeit gängigen Kultivationstechnologien basieren auf Suspensionssystemen, welche weitgehende Nachteile mit sich führen, wie hoher Wasser-, Energie und Technikaufwand. Diese Probleme können durch die Anwendung einer immobilisierten Kultivation vermieden werden, weshalb diesem Verfahren immer mehr Aufmerksamkeit zu Teil wird. In dieser Arbeit wurde *H. pluvialis* als immobilisierte Kultur in einem Twin-Layer PSBR verwendet. Insgesamt wurden 26 verschiedene Arten von *H. pluvialis* gefunden, die als Biofilm wachsen und Astaxanthin produzieren konnten, wobei der Stamm CCAC 0125 zur weiteren Optimierung des Prozesses ausgewählt wurde. Biomasse und Astaxanthin Produktion stiegen zunehmenden in Abhängigkeit zu der Lichtintensität, bis einschließlich 1,015 µmol Photonen m^{-2} s^{-1}, ohne Anzeichen von Photoinhibition. Maximale Biomasse Produktivität von 19.4 g m^{-2} d^{-1} wurde unter starken Lichtverhältnissen verzeichnet. Nährstofflimitierungen und Salinität unterstützen die Astaxanthin Produktion hinderten allerdings das Wachstum der Biomasse. Nichtdestotrotz, wurde die höchste Astaxanthin Produktivität von 0.507 g m^{-2} d^{-1} mit einem Biomasseanteil von 3.5% in der Trockenmasse durch starke Belichtung sowie Stickstoff- und Phosphatmangel erreicht. Diese Ergebnisse bestärken die Verwendung der immobilisierten Kultivation von *H. pluvialis* als Alternative zu den derzeitigen Technologien. Die Verknüpfung von hoher Biomasse mit der Produktion von Astaxanthin bei starkem Lichtintensitäten wurde nur durch die Anordnung in einem Biofilm ermöglicht. Es kann einen Durchbruch in der kommerziellen Herstellung von *H. pluvialis* darstellen, da hierbei das Vorziehen der Kulturen bei geringen Licht entfällt, was wiederum den derzeit verwendeten komplexen Zwei-Stufen Prozess stark vereinfacht.

List of Figures

List of Tables

Table of Contents

Intoduction

1.1 Astaxanthin: applications and markets

Astaxanthin is a keto-carotenoid (3,3'-dihydroxy-β,β-carotene-4,4'-dione; Figure 1.1) commonly known for eliciting the pinkish/red colour of salmonids and crustaceans. Such animals acquire astaxanthin from their food, since they are not capable of the *de novo* carotenoid synthesis. Therefore, astaxanthin is widely used as pigment in animal feed, mostly in aquaculture for salmon, trout and shrimps but it is also applied in poultry for better pigmentation of the egg yolk (Chien and Jeng, 1992; Christiansen et al., 1994; Foss et al., 1984; Johnson and Schroeder, 1995; Lorenz and Cysewski, 2000; Schiedt et al., 1989; Yamada, 1990). Astaxanthin has gained further attention in the past years due to its potent antioxidant activities (Naguib, 2000; Ranga Rao et al., 2010). Numerous studies are currently being conducted and astaxanthin is indicated to have a beneficial effect in immune response, cardiovascular system, cancer, diabetes and dermatitis among others (Dong et al., 2013; Gross et al., 2006; Park et al., 2010; Rao et al., 2013; Yoshihisa et al., 2016). However, at present astaxanthin is only commercialized for direct human consumption as a nutraceutical or cosmetic, mostly for antiaging and eye, joints and muscle health improvement (Ambati et al., 2014).

Global astaxanthin market is increasing rapidly and was estimated to be around US$ 400 million in 2014 with prediction of reaching US$ 1.1 billion by 2020 (BCC Research, 2015; Industry Experts, 2015). The major portion of this market is aquaculture, for which astaxanthin is sold at values around US$ 2.500 kg^{-1}, but is dominated by the synthetic version of the pigment (Lorenz and Cysewski, 2000), synthesized from crude-oil-derived carbon fragments (Baker and Saling, 2003). Natural astaxanthin synthesis occurs in some bacteria (Tsubokura et al., 1999; Yokoyama and Miki, 1995), fungi (Domínguez-Bocanegra et al., 2007; Johnson and Schroeder, 1996; Wang et al., 2006) and green algae (Droop, 1954; Ip and Chen, 2005; Řezanka et al., 2013; Zhang et al., 1997). However, the bacteria *Paracoccus carotinifaciens*, the yeast *Phaffia rhodozyma* and the green alga *Haematococcus pluvialis* are the most commonly used for commercial production of natural astaxanthin.
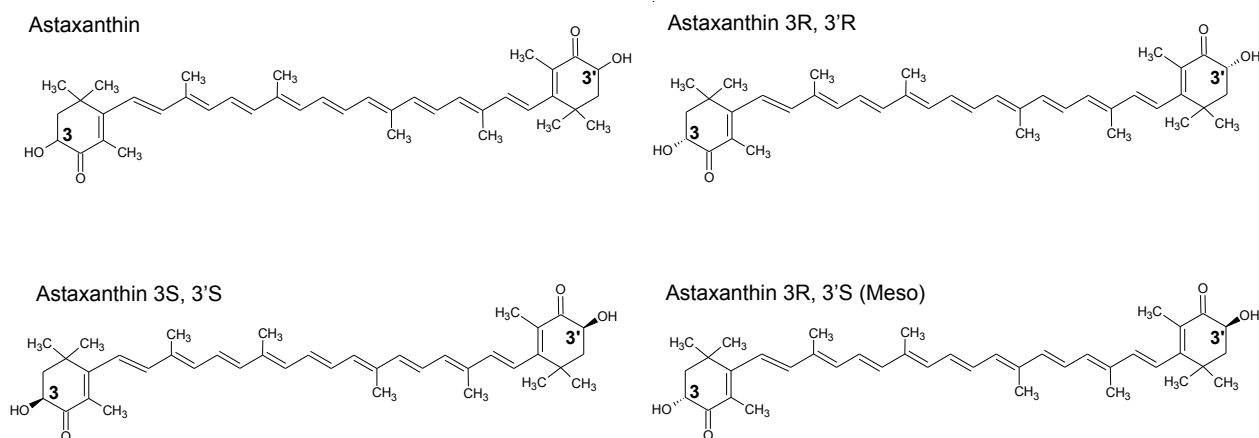
Figure 1.1 Astaxanthin structure and the different stereoisomers

Astaxanthin from different sources have distinct isomer compositions. The astaxanthin molecule contains two benzenoid rings with asymmetric carbons located at positions 3 and 3'. The attachment of the hydroxyl to the asymmetric carbons on S or R configurations determine the different enantiomers: 3R,3'R; 3S,3'S and 3R,3'S (meso), as seen on Figure 1.1. Astaxanthin synthesized by *H. pluvialis* has a 3S,3'S configuration, which is also the isomer observed in wild salmons (Andrewes et al., 1974; Turujman et al., 1997). The 3R, 3'R form accounts for over 92% of the astaxanthin produced by *Phaffia* (Andrewes and Starr, 1976), whereas the synthetic version of the pigment is a mixture of all three isomers in an approximate 1 3S,3'S: 2 meso: 1 3R,3'R relation (Turujman et al., 1997). Furthermore, astaxanthin is mostly esterified in mono and diesters in *H. pluvialis*, and free when produced by *Phaffia* and when chemically synthesized (Andrewes et al., 1976). The effect of the different astaxanthin composition on its accumulation in animal tissue and biological activity is controversial and seems to be species specific (Foss et al., 1987; Fujita et al., 1983; Tejera et al., 2007).

Synthetic astaxanthin is associated to lower production costs, however it is currently limited to applications in animal feed. With the exception of AstaSana from DSM (Herleen, The Netherlands) that is attempting direct human consumption, nutraceuticals are only prepared from natural sources. This market is increasing with a growing knowledge on axtaxanthin-associated health benefits and retail price of

nutraceutical grade astaxanthin is US\$ 15,000 kg^{-1} (Leu and Boussiba, 2014). In a similar health-concern framework, the commercial interest for salmon fed with natural astaxanthin is also enhanced.

H. pluvialis is considered the best source of natural astaxanthin because it is capable of accumulating the pigment in values around 4.5% of its biomass, more than 10-fold that observed in *Phaffia* (Boussiba and Vonshak, 1991; Kang et al., 2006b; Lorenz and Cysewski, 2000; Zhang et al., 2014). Moreover, the production process is less energy intensive and more eco efficient (Baker and Saling, 2003).

1.2 The green microalga *Haematococcus pluvialis* as a source for astaxanthin

Haematococcus pluvialis is a freshwater, unicellular and ubiquitous green microalga, typical of temporary water pools. Usual life cycle of this organism comprises green biflagellate cells, immotile green cells called palmellas and akinetes, a resting stage (Figure 1.2). Under favourable growth conditions – commonly established in laboratory as light intensity up to 100 µmol photons m^{-2} s^{-1}, temperature of 20 - 28 $^{\circ}$C and nutrient replete freshwater medium (Borowitzka et al., 1991; Fan, et al., 1994; Giannelli et al., 2015) -, flagellates are the most abundant form. They are pear-shaped vegetative cells with a cup-shaped chloroplast and the protoplast is connected to the cell wall by means of protoplasmic strands. If conditions become adverse, cells shed the flagella, forming non-motile palmella stages that have a similar protoplasm structure as the flagellates, but adhered to the cell wall. Both flagellates and palmellas are vegetative cells and undergo cell division. However, if environmental conditions continue to be adverse or aggravate, cell division is ceased as palmellas transform into astaxanthin-accumulating akinetes (Droop, 1953; Elliot, 1934; Hazen, 1899; Pocock, 1960). This transformation is accompanied by modifications in cell composition, mainly characterized by a dramatic increase in astaxanthin production, but also in cellular carbohydrate and lipid content and formation of a trilaminar sheath containing sporopollenin-like material (Boussiba and

Vonshak, 1991; Hagen et al., 2002; Santos and Mesquita, 1984). Under very specific circumstances such as akinete germination following adverse conditions, sexual reproduction can also be observed in *H. pluvialis* (Triki et al., 1997).
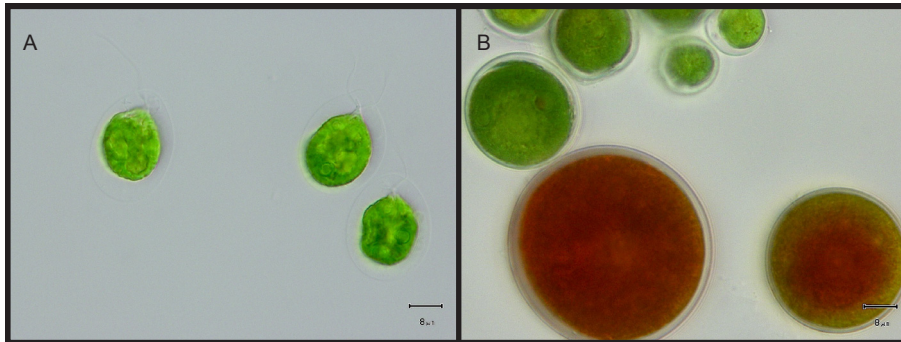
Figure 1.2. Micrographs of different life stages of *Haematococcus pluvialis:* **A** biflagellate cells, **B** palmellas (green round cells) and akinetes (red cells).

Carotenoids are synthesized from isopentenyl pyrophosphate in the chloroplasts, however astaxanthin accumulates in the cytoplasm. Grünewald and Hagen (2001) propose that β-carotene is transported from the chloroplast to the lipid bodies, where it undergoes oxygenation and hydroxylation, the final steps of astaxanthin biosynthesis. Fatty acids are esterified onto the hydroxyl group(s) of astaxanthin after biosynthesis of the carotenoid, forming mono and diesters and thereby increasing its lipid solubility and stability (Grung et al., 1992). Astaxanthin then accumulates in lipid droplets in the cytoplasm of *H. pluvialis*, initially surrounding the nucleus and then spreading through the entire cell (Santos and Mesquita, 1984).

The physiological role of astaxanthin in the *H. pluvialis* cell is still a topic of debate, but two major functions are considered. The first is its action as a light shield, protecting cell components from excessive and harmful irradiances, by absorbing light in the blue region (Hagen et al., 1994; Wang et al., 2003; Yong and Lee, 1991). The second and likely major function is protection against oxidative stress, either directly scavenging and quenching reactive oxygen species or indirectly, where the astaxanthin biosynthesis pathway consumes excessive electrons and molecular oxygen (Fan et al., 1998; Kobayashi et al., 1993; 1997; Li et al., 2008; Wang et al., 2003). Astaxanthin accumulation is, therefore, triggered by conditions that generate

light and/or oxidative stress, such as: high irradiance, nutrient deficiency, salinity and iron surplus (Boussiba and Vonshak, 1991; Boussiba et al., 1999; Droop, 1955; Goodwin and Jamikorn, 1954; Harker et al., 1996, 1995; Kobayashi et al., 1992a; Sarada et al., 2002). Light plays a key role in both growth and astaxanthin production, however, it is not mandatory. *H. pluvialis* can grow heterotrophically, with productivities similar to that of photoautotrophic cultures and growth rates can be increased in mixotrophic cultivation. Astaxanthin can also be produced in the absence of light, as long as an organic carbon source is provided (Droop, 1955, 1954; Jeon et al., 2006; Kobayashi et al., 1992b).

One of the major difficulties of scaling up astaxanthin production for commercial use is the metabolism itself. Even if growing flagellate cultures are capable of astaxanthin production (Grünewald et al., 1997; Lee and Soh, 1991), as it is a secondary metabolic compound, its accumulation is enhanced when the cell division slows down or ceases, in the akinete resting stage (Boussiba and Vonshak, 1991; Droop, 1954). Therefore, state-of-the-art cultivation of *H. pluvialis* for astaxanthin production is a two-step strategy. In the first step (green/growth phase), cultivation parameters are optimal for vegetative growth, reaching high cell densities. When sufficient biomass is obtained, the culture undergoes a stress/red phase, to enhance astaxanthin production and accumulation. In large-scale setups, this second phase is frequently performed outdoors taking advantage of natural sunlight, which reaches intensities of up to 2,000 μmol photons m^{-2} s^{-1}. However, maximum 150 μmol photons m^{-2} s^{-1} light intensities are necessary to maintain vegetative growth in suspension cultures and other parameters such as nutrients, temperature, CO_2 and pH should also be carefully monitored (Lorenz and Cysewski, 2000; Olaizola and Huntley, 2003). Thus, different systems are necessary for each phase and the vegetative growth is frequently conducted indoors, using artificial light. Higher technical efforts and energy inputs are, therefore, demanded in two-step cultivation systems. Moreover, it suffers from a non-astaxanthin-productive growth phase, which usually represents around half of the cultivation period (Aflalo et al., 2007; Suh et al., 2006).

1.3 Astaxanthin production by *H. pluvialis* on a technical scale

For a technical- or commercial-scale production of astaxanthin by *H. pluvialis* conventional suspension cultivation dominate *H. pluvialis* research and market. Suspension cultivation can be performed in open ponds or closed photobioreactors (PBRs). Open ponds are basically containers in which suspension cultures are kept exposed to the environment, constantly mixed and aerated by a paddlewheel. These are very simple and cheap constructions, however, they are easily contaminated. To reduce contamination and improve productivities, a range of closed PBRs was designed. In such systems, suspension cultures are grown in enclosed transparent structures (tubes, columns, flat plates, among others) and mixed by pumping and/or aeration. Environmental conditions can be better controlled in closed PBRs, but it comes at a high cost for both construction and operation (Acién Fernández et al., 2013; Brennan and Owende, 2010; Olivieri et al., 2014). Furthermore, biomass is highly diluted in suspension systems, representing only 0.05 – 0.6 % of the culture. Harvesting is then laborious and cost prohibitive (Gross et al., 2015).

Most of the commercial cultivation of *H. pluvialis* is performed under photoautotrophic conditions, in closed photobioreactors or open ponds. Tubular PBRs are the most commonly used enclosed systems and can be employed for both growth and stress phases. Open ponds are restricted to the stress phase, when extreme conditions can be applied and cultivation is performed for a short period, i.e. 4 - 6 days, thereby reducing contamination risks (Olaizola and Huntley, 2003). The choice of the cultivation system should be based on the final product that is aimed. Nutraceuticals have more demanding requirements with respect to contamination, but also higher market values, therefore, the use of expensive and energy intensive systems as closed PBRs can still be economically viable. On the other hand, when aiming at a bigger market with lower added value, such as animal feed, production costs should be maximally reduced in order to compete with the synthetic astaxanthin (Leu and Boussiba, 2014).

In spite of the intense basic and applied research, the market share of natural astaxanthin nowadays is still limited by the high costs associated to *H. pluvialis*

cultivation. It is speculated that the synthetic pigment production costs are below US$ 1,000 kg^{-1}. Hence, in order to compete with the synthetic version, 1 kg of *H. pluvialis* dry weight containing 3 – 4 % astaxanthin should be produced at the values of US$ 30 - 40 (Olaizola and Huntley, 2003). Meanwhile, Leu and Boussiba (2014) estimate costs of at least US$ 100 kg^{-1} in a small commercial plant with two-step cultivation but values lower than US$ 30 kg^{-1} could be reached in a much larger scale and with a one-step approach using tubular PBRs and an appropriate strain. Values could be further reduced in regions with cheaper lands and labour, as well as material and nutrients. Indeed, an economical assessment of a conceptual production plant in China estimated costs below US$ 20 kg^{-1} of *H. pluvialis* biomass and US$ 1,000 kg^{-1} astaxanthin for cultivation in a two-step system with closed PBRs and open ponds (Li et al., 2011).

Immobilized cultivation represents an alternative for simplifying microalgae production. By overcoming common problems associated with suspension culture such as high water and energy consumption; limitations in gas exchange and light dilution and shear stress, production costs can be reduced. It consists of biofilm-based cultivation systems in which harvesting can be performed simply by scraping off the biomass, which has a very low water content of about 70 – 85 %, over 100 fold higher than that of suspension cultures. This way, flocculation and/or centrifugation is exempted (Berner et al., 2014; Gross et al., 2015; Ozkan et al., 2012). Hence, immobilized cultivation has attracted a lot of attention in the past years and different biofilm-based PBRs have been developed in both stationary and rotating configurations (Blanken et al., 2014; Christenson and Sims, 2012; Genin et al., 2014; Gross et al., 2013; Mulbry and Wilkie, 2001; Schnurr et al., 2013). However, in all these systems the biofilm is submerged in the culture medium constantly or periodically, which can reduce algal immobilization and increase biomass detachment.

These problems are avoided by complete separation of biofilm and bulk medium in the Porous Substrate Bioreactors (PSBRs), which consists of a sheet-like micro-porous substrate in which microalgae are immobilized by self-adhesion, while culture medium circulates through an inner source layer. Nutrients reach the biomass

through the porous substrate by diffusion, but the pores should be small enough to prevent microalgae from crossing and to reduce contamination in biomass (Liu et al., 2013; Murphy et al., 2012; Naumann et al., 2013). The "Twin-Layer" was the first developed PSBR (Melkonian and Podola, 2007). Maximum biomass surface productivities in a PSBR were recently reported on the Twin-Layer by using high light: Biomass of *Halochlorella rubescens* increased with increasing light intensity, reaching a maximum of 31.2 g m^{-2} day^{-1} surface productivity at 1,000 µmol photons m^{-2} s^{-1} with supplementary CO_2. No evidence of photoinhibition was observed (Schultze et al., 2015). Moreover, footprint productivities as high as 80 g m^{-2} day^{-1} were obtained for *Scenedesmus obliquus*, when using multiple PSBRs organized in parallel (Liu et al., 2013).

PSBRs have been shown to support growth of different microalgal species (Benstein et al., 2014; Cheng et al., 2014; Ji et al., 2013; Liu et al., 2013; Naumann et al., 2013; Nowack et al., 2005; Schultze et al., 2015), including *H. pluvialis* (Nowack et al., 2005; Wan et al., 2014a; Yin et al., 2015; Zhang et al., 2014). The effect of cultivation parameters, such as inoculum density, temperature, light intensity and nutrient concentration in culture medium were investigated on the immobilized cultivation of *H. pluvialis*. However, research was limited to continuous light conditions with maximum irradiances of 230 µmol photons m^{-2} s^{-1}. Moreover, *H. pluvialis* immobilized cultivation has only been proposed for use in astaxanthin induction (stress phase), and not the entire process (Wan et al., 2014a; Yin et al., 2015; Zhang et al., 2016, 2014).

1.4 Aim of this study

The main aim of this study was to optimize *H. pluvialis* immobilized cultivation on a bench-scale Twin-Layer PSBR for astaxanthin production. In order to do so, different *H. pluvialis* strains were initially evaluated to verify their potential for biofilm cultivation and to identify attractive traits such as high biomass and astaxanthin

productivities and robustness. Optimization of the cultivation process in respect to light intensity and carbon dioxide was then conducted with one selected strain.

Astaxanthin production was further optimized by: (1) Investigation of the effect of stress factors (nutrient depletion and salinity); (2) comparison of different cultivation strategies (one vs. two-step). Moreover, for a better comprehension of the biofilm structure and dynamics, biofilm cross-sections were evaluated by microscopy and microsensor analysis for light and dissolved oxygen and were performed.

Material and Methods
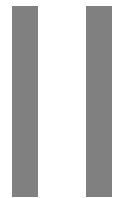
2.1. Microalgal strains and cultivation

2.1.1 Strains and culture maintenance

A total of 26 strains of *H. pluvialis* were obtained from different culture collections worldwide: Culture Collection of Algae at the University of Cologne, Cologne, Germany (CCAC); Coimbra Collection of Algae (ACOI), Coimbra, Portugal; Culture Collection of Algae and Protozoa (CCAP), Oban, Scotland; National Institute for Environmental Studies Microbial Culture Collection (NIES), Tsukuba, Japan and Culture Collection of Algae at the University of Göttingen (SAG), Göttingen, Germany. The strains are listed on Table 2.1, together with available information on its isolation.

All strains were obtained axenic and were maintained in this condition, in 100 mL Erlenmeyer flasks, with 50mL of culture medium and transferred every 3 - 4 weeks. Stock cultures were grown in 16 $^{\circ}$C culture chambers, at around 30 µmol photons m^{-2} s^{-1} provided by fluorescent lamps (L36W/640i energy saver cool white and L58W/956 BioLux fluorescent lamps; Osram, Munich, Germany), using a 14/10 hours light/dark cycle.

For experiments on the Twin-Layer PBR, cultures were expanded to 2 or 5 L Erlenmeyer flasks and placed in a 23 $^{\circ}$C culture chamber, with same lamps and light/dark cycle. Flasks were placed in order to be exposed to 50 - 60 µmol photons m^{-2} s^{-1} light intensity and were aerated with 0.5% additional CO_2, at a flow rate of 0.5 mL min^{-1}. Culture medium was refreshed accordingly and microalgae were collected from logarithmic growth phase.

Table 2.1. Strains of *Haematococcus pluvialis*

Strain ID	Origin	Isolator
CCAC 0526	n.a.	n.a.
CCAC 0528	n.a.	n.a.
CCAC 0529	n.a.	n.a.
CCAC 0055	Germany, Lohmar near Cologne. Rainwater reservoir.	Powalowski (1990)
CCAC 0868	Russia; Moscow, Biology Institute of the State University.	Sineshchekov
CCAC 0869	Russia; Moscow, Biology Institute of the State University.	Sineshchekov
CCAC 1023	n.a.	n.a.
CCAC 2072B	Germany, Cologne, Botany Department of the University	Podola (2000)
CCAC 0125	Germany, Asbach-Oberplag / Westerwald.	Naumann (2004)
CCAC 0129	Germany, Lohmar near Cologne	B. Melkonian (2004)
CCAC 3305	Germany, Cologne, Wahner Heide, Fuchskaule. Freshwater.	M. Melkonian (2010)
CCAC 3319	Switzerland, Rylle. Freshwater.	M. Melkonian (2010)
CCAC 3323	Switzerland, Rylle. Freshwater.	M. Melkonian (2010)
M1024	Switzerland; Zürich. Stoup at Sihlfeld cemitery.	Zehnder (1953)
ACOI - 276	Portugal, Serra da Estrela. Pond near Lagoa Comprida.	M. F. Santos (1987)
CCAP 34/13	USA, Ferrum, Virginia. bird bath.	Ott (1959)
CCAP 34/14	USA, Cattonsville, Maryland. Cement urn,	Ott (1989)
CCCryo 096-99	Australia, Tilba-Tilba, NSW. Dried out concrete bird bath.	T. Leya (1999)
NIES-144	Japan, Sapporo Sapporo, Hokkaido.	Ichimura (1964)
SAG 34-1a	Sweden, Aneboda.	Pringsheim (before 1970)
SAG 34-1b	Former Czechoslavakia.	Mainx (probably 1931)
SAG 34-1f	Svalbard. From a stone.	Pringsheim (1932)
SAG 34-1h	Finland, Tvärminne. Supralittoral rock pool.	Droop (1951)
SAG 34-1 l	Switzerland, Zürich. Stoup at Sihlfeld cemitery.	Zehnder (1953)
SAG 34-1n	Switzerland, Graubünden. Little "blood pond" near Samnun	Zehnder (1953)
SAG 44.96	South Africa, Cape Town. Soil from Cape Flats "De Klip"; leg. M. A. Pocock, 1967	Schlösser (1969)

n.a. information not available

2.1.2. Culture media

Modified BG11-H medium was used for *H. pluvialis* cultivation in both suspension and immobilized conditions. Stock solutions were prepared as described in Table 2.2, and stored at 4 °C. For the preparation of final medium, 40 mL of main nutrients and 1 mL of each trace elements, Fe-EDTA, vitamins and buffer stock solutions were added to double distilled water (Milli-Q water, TKA-X-CAD, Germany) and were then completed to 1 L. Once prepared, pH was corrected to 7.3 - 7.4 with NaOH and media bottles were immediately autoclaved.

For astaxanthin induction purposes, the following adaptations of the modified BG11-H medium were applied: N zero, P zero, NP zero, NaCl, and N zero + NaCl. N zero, P zero and NP zero media were prepared by leaving out from the main nutrients stock solution the $NaNO_3$, $K_2HPO_4 \cdot 3H_2O$ and both compounds, respectively. For the NaCl, 8 g L^{-1} of NaCl were added to the final BG11-H medium, yielding a concentration of 0.8 %. These compositions will be referred to as stress media.

2.2. Twin-Layer PSBR

2.2.1 Inoculation: Immobilization of *H. pluvialis*

H. pluvialis immobilization was always performed on polycarbonate membranes (PC40, 0.4 µm pore size, 25 mm diameter, Whatman, Dassel, Germany), that have a weight of 4.44 ± 0.01 mg. The inoculated area on the filter was 2.5447 cm^2.

Inoculum quality is of great importance for the development of the experiment and its results, therefore, they were always prepared following the same protocol: Suspension cultures were transferred one week and refreshed two days before inoculation. This way, cells in logarithmic growth phase were collected and concentrated by centrifugation (800 x g for 5 minutes). Under these conditions, no damage was observed to flagellate cells. Concentrated culture density was then determined by filtering 1mL of the suspension onto a polycarbonate membrane,

which was then dried in compartment drier (WTB Binder, Germany) at 105 °C for two hours.

Table 2.2. Composition of modified BG11-H culture medium.

Compound	Stock solution (L^{-1})	Molarity in final medium
Main nutrients (40 ml per liter medium)		
$NaNO_3$	37.500 g	17.650 mM
$K_2HPO_4 \cdot 3H_2O$	1.312 g	0.230 mM
$MgSO_4 \cdot 7H_2O$	1.875 g	0.300 mM
$CaCl_2 \cdot 2H_2O$	1.620 g	0.440 mM
Na_2CO_3	0.500 g	0.190 mM
Trace elements (1 ml per liter medium)		
H_3BO_3	2.860 g	46.260 µM
$MnCl_2 \cdot 4H_2O$	1.810 g	9.150 µM
$ZnSO_4 \cdot 7H_2O$	0.220 g	0.770 µM
$Na_2MoO_4 \cdot 2H_2O$	0.390 g	1.600 µM
$CuSO_4 \cdot 5H_2O$	79.000 mg	0.320 µM
$Co(NO_3)_2 \cdot 6H_2O$	49.400 mg	0.170 µM
Fe-EDTA (1 ml per liter medium)		
EDTA (Titriplex II)	5.220 g	17.860 µM
$FeSO_4 \cdot 7H_2O$	4.980 g	17.910 µM
KOH	54.000 ml 1N KOH	54 µM
Vitamins (1 ml per liter medium)		
Vitamin B_{12}	0.200 mg	0.150 nM
Biotin	1.000 mg	4.000 nM
Thiamine-HCl	0.100 g	0.300 nM
Niacinamide	0.100 mg	0.800 nM
Buffer (1 ml per liter medium)		
HEPES	238.310 g	1.000 mM

All chemicals were manufactured by Merck (Germany), with the exception of H_3BO_3 (Roth, Germany) and $MnCl_2 \cdot 4H_2O$ (Sigma-Aldrich, Germany). .

After cooling down to room temperature in desiccator, the weight of membrane and biomass were determined gravimetrically and culture density was calculated as follows:

$$D = Wt - Wm$$ *Equation 01*

Where D is the density of the culture in mg mL^{-1}; Wt and Wm are the total (biomass + membrane) and membrane weight, both in mg.

It was then possible to calculate the volume that should be used, in order to achieve a density of 5 g m^{-2} (unless otherwise stated) in the inoculation area. Volumes of 0.8 to 1.5 mL were usually used. If necessary, inoculum culture was further concentrated or diluted. Once ready, the suspension culture was placed on a magnetic stirrer, to maintain homogeneity during the entire inoculation process.

Immobilization of *H. pluvialis* followed the protocol described by Naumann et al. (2013). Custom made polyvinylchloride (PVC) blocks were used for inoculation, each of which containing six holes (Ø 18 mm) that determined the inoculation area. Polycarbonate membranes were soaked in double distilled water and placed individually on the top of each hole. The block and filters were then covered with a wet highly absorbent paper (Gel-Blotting-Paper GB002; Schleicher & Schuell, Dassel, Germany), and turned upside down on a pile of dry paper towels. The previously determined volume of the suspension culture was pipetted into these holes, the culture medium was filtered through the paper and cells were immobilized on the membrane, as illustrated in Figure 2.1. Inoculated filters were maintained moist on glass fibre soaked in culture medium, until placement on the Twin-Layer PSBR. Both suspension cultures used as inoculum and immobilized algae were frequently monitored under the microscope. Cell morphology, colour, life stage and possible contamination were observed.
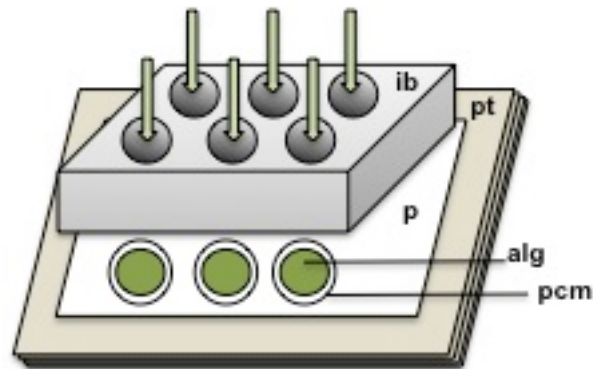
Figure 2.1. Immobilization of microalgae for inoculation on the bench-scale Twin-Layer PSBR. lb – inoculation block, pt – paper towel, p – highly absorbent paper, alg – algae, pcm – polycarbonate membranes

2.2.2 Bench-scale Twin-Layer PSBRs setup

The bench scale Twin-Layer PSBRs used in the present work were described by Schultze et al. (2015), based on the design by Shi et al. (2007) and is showed in Figure 2.2. The system consisted of a transparent acrylic tube (50 cm long, 12 cm diameter) on a PVC support box. A glass fibre mat (50 x 10 cm – 80 g/m²; Isola AS, Eidanger, Norway) was used as a source layer, hanging vertically from the lid inside the tube.

A reservoir bottle containing 1 L of culture medium was placed under the acrylic tube, inside the PVC support. Medium circulated from the bottle to the top of the glass fibre through PVC (Rauclair, Germany) and pump tubes (Spetec, Erding, Germany) at a flow rate of 4.5 - 5.5 mL min^{-1}. Once applied at the top, it spread down with gravity, soaking the glass fibre and returning to the reservoir bottle by means of an opening in the support box. Culture medium was exchanged every 2 - 3 days to avoid nutrient limitation for algal growth, even when applying stress media with nutrient deficiencies. Evaporated water was replaced whenever found necessary. Inoculated polycarbonate membranes were easily adhered to the wet glass fibre due to the hydrophilic properties of both materials.

Sodium discharge lamps (SON-T AGRO 400W, Philips, Hamburg, Germany) were used as light source, following a 14/10 hour light/dark cycle that was controlled by timers (Theben Timer 26, Theben, Haigerloch, Germany). Different irradiances were obtained according to the distance from PSBR tubes to the lamps and/or by the use of filters capable of reducing light intensity in 50 and 75% (Filter types 209 and 210, LEE, Germany). Irradiances were measured with a photometer (LI-250A, LI-COR, Lincoln, NE, USA).

Aeration was supplied directly inside the PMMA tube, through a second opening in the support box. Compressed air and CO_2, were applied together in concentrations from 0 to 10% CO_2, at a flow rate of 1 L min^{-1}. In some cases, aeration with no additional CO_2 was performed by aquarium pumps (Schego Prima, Schemel & Goetz GmbH & Co KG, Offenbach am Main, Germany).

A few hours prior to inoculation, the system started running with culture medium, so to ensure glass fibre mats would be soaked with nutrients when receiving the algae.
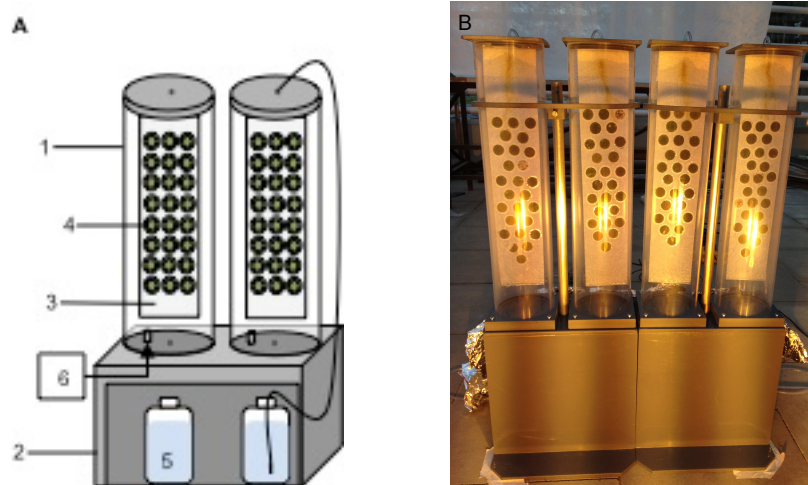
Figure 2.2. Bench scale Twin-layer PSBR tubes. **A** Schematic drawing of one system containing 2 acrylic tubes (1) on a PVC support (2). Glass fibre (3) hangs inside the tubes, where the polycarbonate membranes, containing the biomass (4) are placed. A reservoir supplies culture medium to circulate on the system (5) and aeration is provided directly inside the tubes (6). **B** Front image of four PBRs.

2.2.3 Harvest

Harvests were usually performed every 2 - 3 days, but could be more spaced in longer experiments. They consisted of removing at least 3 membranes from different positions of the glass fibre, in the PSBR. This way, possible spatial variations would be included in the analysis. To ensure that only biomass in the inoculated area would be accounted for, surplus biomass was scraped off with the aid of an 18 mm diameter tube. Membrane and remaining biomass were lyophilized for two hours and subsequently weighed in an analytical balance (Sartorius, Bovenden, Germany). Biomass per area was determined according to Equation 02, and the samples were then stored at -20 $^\circ$C until pigment analysis.

$$B = \frac{Wt - Wm}{a} \qquad\qquad Equation\ 02$$

Where B is the biomass in g m^{-2}; Wt and Wm are the total (biomass + membrane) and membrane weight, both in mg, and a is the inoculation area in m^2.

2.3. Pigment analysis

Lyophilized biomass samples were removed from polycarbonate membranes and mixed to disperse clumps, until a homogeneous powder was obtained. A small amount of 1 - 2 mg of this powder was weighed in a high precision balance and separated for pigment extraction. All the following extraction and measurement process was carried out in darkness.

2.3.1 Astaxanthin

A calibration curve was prepared from a commercial astaxanthin standard (98.6% purity, Dr. Ehrenstorfer GmbH, Augsburg, Germany). An initial master solution was performed in DMSO, followed by 12 dilutions in the same solvent. Samples were plated in triplicates in 96-well plates (200 µL well^{-1}) and the OD was measured at 530 nm (Infinite M200 plate reader, Tecan, Männedorf, Switzerland). From the linear correlation between OD and astaxanthin concentration (Figure 2.3), equation 03 was obtained.

Astaxanthin was then determined spectrophotometrically as described by Li et al. (2012). Freeze dried biomass samples were extracted with Dimethyl sulfoxide (DMSO; Merck, Germany), incubated in water bath at 70°C for 5 minutes with intervals for vortexing, then centrifuged at 4,000 g for 5 minutes. Extraction was repeated until a colourless pellet was obtained and supernatants were collected together. When necessary for complete extraction, cells were broken by grinding with sea sand (AppliChem, Germany).

$$Y = 0.665x + 0.008236 \qquad\qquad \textit{Equation 03}$$
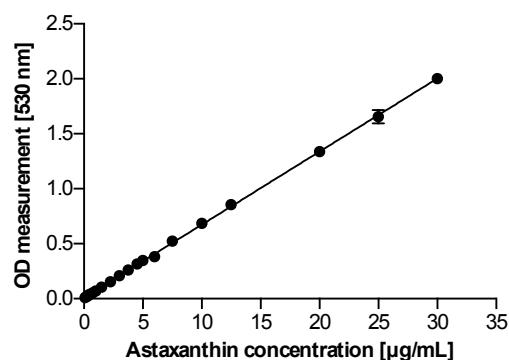
Figure 2.3. Astaxanthin standard calibration curve for spectrophotometry.

Supernatants were plated in triplicates onto flat-bottom 96-well plates (200 µL well^{-1}) and the OD was measured at 530 nm. Pure DMSO was used as a blank and, when necessary, 1:2 dilutions were performed with the solvent. Absorbance measurements were then used to determine astaxanthin concentration in the wells with equation 03 and the value was multiplied by the DMSO dilution used for extraction and plating. From these results, astaxanthin content in extracted biomass was calculated in percentage, with subsequent estimation of total astaxanthin production per biofilm surface (in g m^{-2}).

2.3.2 Chlorophyll

Since no alkali treatment was performed during astaxanthin extraction, the same supernatants could be used for chlorophyll analysis. The OD of the plated samples was also measured at 664 and 647 nm, and chlorophyll quantification (mg L^{-1}) was conducted according to equations 4 and 5 (Jefferey and Humphrey, 1975). These equations were created using 90% acetone as solvent, but the absorption spectra of chlorophylls a and b are identical in and DMSO (Shoaf and Lium, 1976).

$$Chl\ a = 11.93\ Abs_{664} - 1.93\ Abs_{647} \qquad\qquad Equation\ 4$$

$$Chl\ b = 20.36\ Abs_{647} - 5.5\ Abs_{664} \qquad\qquad Equation\ 5$$

Since Equations 2 and 3 are based on measurements in cuvettes (light path of 1 cm), OD measurements were corrected for the light path in the 96-well plate, i.e. 0.6217 cm. This value was calculated from the height of the 200 µL DMSO column in a well of 6.4 mm diameter. Total chlorophyll was calculated as the sum of chlorophylls a and b.

2.4. Cryosectioning of biofilm

To gain insight into the microalgal biofilm structure, pieces of around 3 mm x 3 mm were cut from fresh membranes in strategic time points. Biofilm borders were always avoided and careful handling with forceps and sharp blades helped to preserve the original structure. Cut pieces were placed in plastic supports containing a thin layer of Tissue-Tek O.C.T compound (Sakura Finetek USA Inc., Torrance, CA, USA) and then completely embedded by the product, removing bubbles that might have been formed. The supports containing samples were immediately placed inside liquid nitrogen containers, exposed to the vapour but not immersed in the liquid. Once frozen, samples were individually wrapped in accordingly labelled tin foil and stored at -35 °C. 90 μm transversal sections were cut in a cryostat microtome (HM500, Microm International, Walldorf, Germany), using the cutting temperature of -16 °C. Sections were immediately placed on glass slides, observed under a light microscope and photographed.

Biofilm thickness and layers were measured from the micrographs using Image J software (ImageJ, U. S. National Institutes of Health, Bethesda, Maryland, USA).

2.5. Experimental designs

2.5.1 Screening of *H. pluvialis* strains

Screening experiments were performed to select among the 26 *H. pluvialis* strains listed on table 2.1, which were capable of biofilm growth on the Twin-Layer PSBR. Strains were immobilized separately onto polycarbonate membranes at densities of 2 - 3 g m^{-2}, but placed sorted in the Twin-Layers. Thus, each PBR tube accommodated one sample from each strain.

A two-step cultivation approach was employed, where full BG11-H medium was supplied for eight days ("growth phase"), followed by six days under nitrogen starvation conditions (N zero medium - "stress phase"). Applied light intensity was

203 µmol photons m^{-2} s^{-1}, provided by white fluorescent lamps, with a light/dark cycle of 14/10 hours. PBRs were aerated at a flow rate of 0.5 L min $^{-1}$ with 0.5% additional CO_2 and the temperature was 23°C. Four samples per strain were harvested at the end of each phase for dry weight and astaxanthin measurements.

A screening experiment was also performed in secondary wastewater to evaluate robustness of the *H. pluvialis* strains. Municipal wastewater was obtained from the Erftverband facility, in Frechen, Germany. A large sample was collected in September 2013 from the secondary settlement tank after biological treatment (prior to discharge). It was left to settle for two hours to remove suspended particles and was then stored in 5 L flasks at -21 $^{\circ}$C. One day before use, flasks were left at room temperature to thaw and were later separated to 1 L bottles to be applied in the Twin-Layers. Cultivation was conducted for one week, with daily wastewater exchange. Tubes were exposed to 200 µmol photons m^{-2} s^{-1}, provided by sodium discharge lamps at a 14/10 hour light/dark cycle. Meanwhile, aeration was performed by means of aquarium pumps, with no additional CO_2. At the end of the experiment, all of the biofilms were harvested and exceptionally dried at 105 $^{\circ}$C for two hours, followed by 20 minutes in desiccator to reach room temperature. Final dry weight was determined gravimetrically.

2.5.2 The effect of light intensity and CO_2 supplementation on biomass and astaxanthin production

Strain CCAC 0125 was chosen as one of the most astaxanthin productive from the screening test and was therefore used in all further experiments for the optimization of immobilized cultivation of *H. pluvialis*. For all of these experiments, inoculation density was 5 g m^{-2} and around 90% of cells in inoculum were flagellates. Full BG11-H culture medium was used throughout the experimental period with replacements every two to three days. Hence, nutrients were always available in sufficient amounts.

The effect of light intensity on growth and astaxanthin production was the first to be investigated. Initially, a common two-step approach was used: Twin-Layers were

irradiated with 90 μmol photons m^{-2} s^{-1} for eight days and then moved to 1,000 μmol photons m^{-2} s^{-1} for another period of eight days, adding up to a total of 16 days. Aeration was supplemented with 5% CO_2.

Light and was further investigated in the system, this time in a one-step process, in which the same irradiance was maintained throughout the cultivation period. 10 different light intensities in the range 20 to 1,015 μmol photons m^{-2} s^{-1} were evaluated under two aeration conditions, either only ambient air or ambient air supplemented with 5% CO_2. Due to the heat emitted by the lamps, the temperature on the glass fibre increased as a function of the light intensity. Temperature control was attempted by reducing room temperature, opening lids and aerating tubes. Nevertheless, the variation could be reduced but not avoided, as described on Table 2.3. Experiments with CO_2 supplementation were conducted for 16 days while those with only ambient air ran for 31 days.

Table 2.3. Light intensity and glass fibre temperatures in PSBRs for irradiance experiments with and without supplementary CO_2.

Light intensity [μmol photons m^{-2} s^{-1}]	Temperature [°C]	
	Ambient air	5% CO2 supplementation
20	18.6	18.6
44	21.5	19.3
89	20	22
211	20	22.2
329	24.5	24.5
440	24.2	24
535	28.1	24.5
644	23.4	24.5
789	23.6	24.7
1,015	28.3	28.6

This initial investigation showed maximum growth and astaxanthin production at high light intensities. Thus, the aim of the following experiment was to identify the

appropriate CO_2 concentration to support high growth rates at 1,000 µmol photons m^{-2} s^{-1}. In order to do so, aeration was conducted with mixtures of air and CO_2 at concentrations of 1; 2.5; 5; 7.5 and 10%. Glass fibre temperatures in all five tubes were 27 ± 0.5 $^{\circ}$C. To evaluate the effect of the CO_2 concentrations in the culture medium, pH was measured after the exchange.

2.5.3 Astaxanthin induction with stress media

Numerous conditions are considered to trigger astaxanthin accumulation besides high light. Aiming at further increasing astaxanthin production, nutrient starvation and salinity stress were coupled to the high irradiances, in a series of experiments. A growth phase of three days with full BG11-H medium preceded the onset of stress with P zero, N zero, NP zero, N zero + NaCl and NaCl culture medium.

At first, all the stress media were applied at 800 µmol photons m^{-2} s^{-1}. In a following experiment, NP zero and NaCl were evaluated under a range of irradiances from 345 to 805 µmol photons m^{-2} s^{-1}. The light intensity was maintained the same throughout the experimental period and aeration was supplemented with 1% CO_2.

2.6. Determination of light and oxygen profiles in the biofilm using microsensors

In the attempt to better understand *H. pluvialis* biofilm structure and growth in the different environmental conditions, depth profiles of light and oxygen were acquired with microsensors. Three types of biofilms were analysed: LL -grown at low light intensity; LL/HL - grown at low light, then transferred to high light intensity and HL/Nzero - grown exclusively at high light and transferred to N zero culture medium.

2.6.1. Biofilm preparation

All the membranes were inoculated with strain CCAC 0125 at a biomass density of 5.6 g m^{-2}, and cultivated with 2% supplementary CO_2 for a total of 28 days. Initial growth was conducted for 18 days, at light intensities of 130 µmol photons m^{-2} s^{-1} for LL and LL/HL groups and 1,000 µmol photons m^{-2} s^{-1} for the HL/Nzero. Full BG11-H culture medium was supplied to all three groups during this growth phase and was replaced every 3 days to avoid nutrient limitation. At day 18, biofilms were transferred to the same culture conditions that were used at the microsensor analysis, for 10 days of acclimation. LL biofilms were placed at 20 µmol photons m^{-2} s^{-1} and LL/HL biofilms, at 1,000 µmol photons m^{-2} s^{-1}, but both groups were maintained with full BG11-H. HL/Nzero biofilms continued at the same light intensity (1,000 µmol photons m^{-2} s^{-1}), but culture medium was switched to BG11 N zero.

Irradiance distribution and dissolved oxygen concentration ([DO]) profile were determined from two biofilms for every culture condition. Once measurements were completed, samples were prepared for cryosectioning. Furthermore, three extra biofilms from each group were lyophilized for dry weight calculation.

2.6.2 Microsensor measurements

Microsensor measurements were performed as described by Li et al. (2015a, 2015b), based on works of Gieseke and de Beer (2004). Biofilms grown under the above mentioned conditions were removed from the Twin-Layer PSBRs and placed on a glass fibre mat inside a measurement chamber. Glass fibre was maintained wet by circulating 50 mL culture medium (BG11-H or BG11-H N zero) through the system with a peristaltic pump, at a flow rate of 3 mL min^{-1}. In order to avoid light and gas exchange in the remaining glass fibre around the biofilm, it was covered with a black plastic foil. The chamber was partially closed with a transparent plastic cover, to maintain a stable environment, leaving only the biofilm exposed. Compressed air containing 2% CO_2 was continuously introduced from the right and left sides of the chamber at a flow rate of 1 mL min^{-1}. All the measurements were performed at room

temperature of 23 °C and carried out with 40 μm resolutions. The movement of the sensor was controlled by a computer-driven micromanipulator (Pollux Drive, PI miCos, Eschbach, Germany).

Microsensors, amplifiers, micromanipulator and data acquiring software were kindly provided by Dr Dirk de Beer, Max Planck Institute for Marine Microbiology, Bremen. His group constructed microsensors with tip diameters < 10 μm and a response time ≤ 0.5 s used for the determination of [DO]. For this analysis, two-point linear calibration was performed using culture medium saturated with nitrogen gas or compressed air (zero and 0.274 mM of [DO]). The signals were amplified and converted into digital data (DAQpad 6015 and 6009, National Instruments, Munich, Germany), sent to a custom-made software (Microprofiler).

Light profiles in the biofilms were measured with a fibre optic microsensor with a spheric tip (Ø 80 μm), connected to a portable spectrometer (USB 4000,Ocean optics, Dunedin,USA). The acquired data was integrated and values for total photosynthetically active radiation (PAR; 400 - 700 nm) and specific colour bands: red (400 - 500 nm), green (500 – 600 nm) and blue (600 - 700 nm) irradiation intensities were estimated.

2.7. Data analysis

Growth rates were calculated according to the biomass data. For longer time periods, growth rates were calculated for individual points by first orders derivatives of a second order polynomial function. When growth was linear, in shorter time periods, a single growth rate was calculated as the slope of a linear regression. Astaxanthin productivities were only calculated as the slope of a linear regression in limited cultivation periods. For all the analyses, three or more replicates were used per data point and only fits with $R^2 > 0.90$ were considered.

When normal distribution could be verified, comparisons between data points were performed with one- and two-way anova, followed by Holm Sidak's or Turkey's

multiple comparison tests, respectively. When n was insufficient for normality tests, the Kruskal-Wallis test was carried out. Results were considered significantly different when $p \leq 0.05$. To compare curves, area under curve (AUC) was calculated.

Biomass growth rate dependency on irradiance was plotted using the Photosynthesis-irradiance (PI) model proposed by Platt et al. (1980):

$$PB = PBs\left(1 - e^{-\alpha I/Ps}\right) e^{-\beta I/PBs} \qquad\qquad Equation\ 6$$

Where PB is the biomass-specific rate of photosynthesis, Ps is the maximum theoretical photosynthetic rate in the absence of photoinhibition, α the slope of the line at low light (initial portion of the curve), β the photoinhibition constant, and I is the irradiance. Growth rates were also used to calculate photosynthetic efficiency, i.e. the biomass (in g) produced per unit of irradiance (μmol photons m^{-2} s^{-1}), in one day.

Values shown in figures are expressed as mean ± SD of at least 3 replicates. All data was organized in Microsoft Excel sheets and analysis was performed using GraphPad Prism v5.04 statistical software (GraphPad Software Inc., La Jolla, USA).

Results

3.1. Screening of *H. pluvialis* strains

Screening of 26 strains of *H. pluvialis* was performed in order to select the best performing in respect to growth and astaxanthin production on a Twin-Layer PSBR. Successful growth of *H. pluvialis* strains was observed in all strains when cultivated with BG11-H culture medium and supplementary CO_2 (Figure 3.1A). Biomass yield ranged from 35.12 g m^{-2} (CCCryo 096-99) to 64.7 g m^{-2} (CCAP 34/13) after the 8 day green phase and increased significantly during the astaxanthin induction period. CCAP 34/13 showed maximum biomass production after 14 days (112 g m^{-2}), whereas the lowest biomass was 73 g m^{-2}, observed in strain SAG 34-1l. For some strains, astaxanthin production was already induced by the 203 µmol photons m^{-2} s^{-1} light intensity. Thus, after the first 8 days, CCAC 0526 had an astaxanthin content of 0.83% of dry weight, the highest observed at this period. Nevertheless, all the strains responded to nitrogen starvation with an increase in astaxanthin content. 22 of them accumulated over 1% astaxanthin per dry weight and strains SAG 34-1l, CCAC 0125, SAG 44.96 and NIES-144 reached even more than 1.5%. The maximum astaxanthin yield obtained after the 14 days was 1.6 g m^{-2} and no significant difference in total astaxanthin was found between the four best performing strains: SAG 44.96, CCAP 34/13, CCAC 0125, NIES-144 (Figure 3.1B).

For further evaluation of the strains' robustness, they were grown in secondary wastewater from the Erftverband municipal treatment plant. Biomass yields after the 7 days cultivation period are shown in Figure 3.2. With the exception of strain ACOI-276, all others presented good and similar growth under these conditions. Maximum final standing crop was 56.63 g m^{-2} dry weight, observed on strain CCAC 0526, but it was not significantly different from the other 24 strains with exception of ACOI-276 (19.1 g m^{-2}).

Results
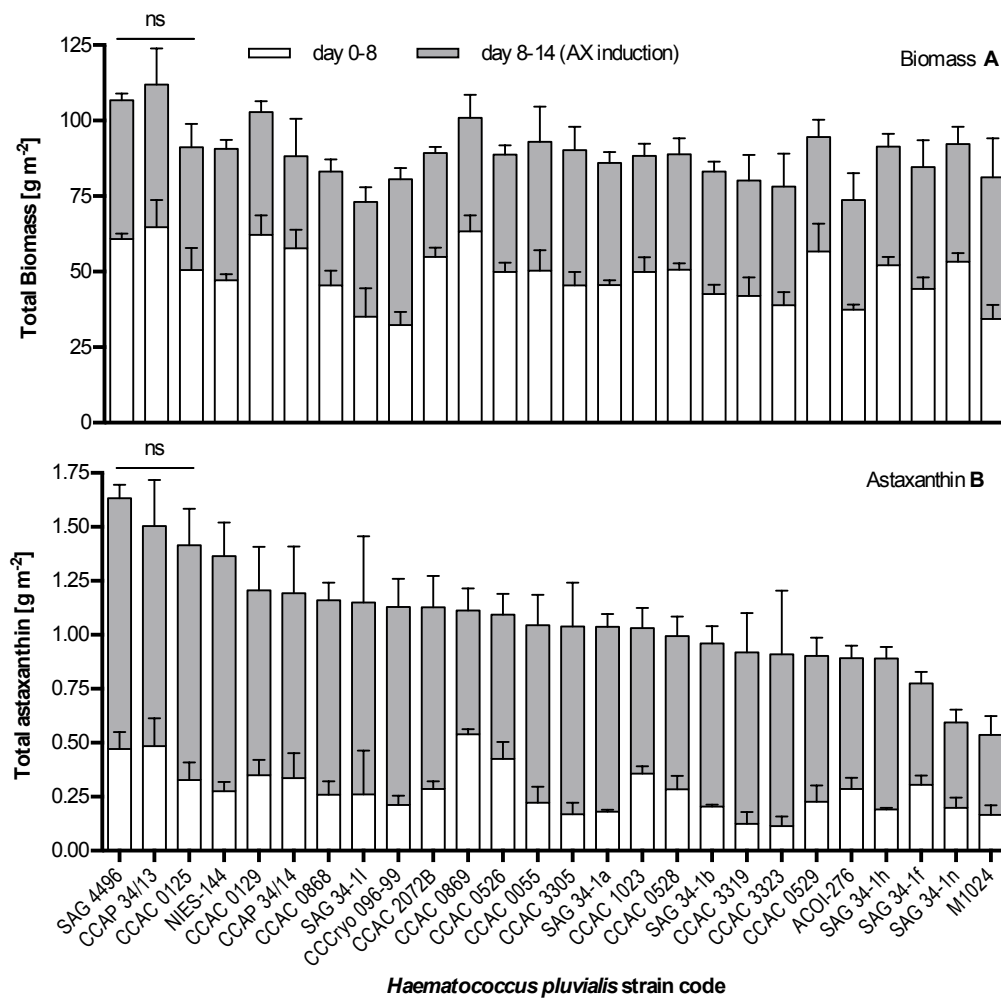
Figure 3.1. Total biomass **(A)** in g dry matter m^{-2} ± SD (n=4) and total astaxanthin **(B)** in g m^{-2} ± SD (n=4) of 26 strains of *H. pluvialis* during 14 days of cultivation in a Twin-Layer PSBR. White bars represent amounts after cultivation using BG11 culture medium until day 8, whereas grey bars indicate produced biomass/astaxanthin from day 8-14 during stress phase using nitrogen-depleted BG11. Light intensity was 203 µmol photons m^{-2} s^{-1} and aeration was supplied with 0.5% CO_2. ns: no significant differences were found between data sets (Kruskal-Wallis test; p=0.05)

In order to compare the performance on wastewater and BG11-H, biomass productivity was calculated by dividing the difference between initial and final biomass by the number of days. Only the growth phase (8 days with full BG11-H) was considered for the biofilms that received culture medium.   Results are summarized on Figure 3.3. Most of the strains exhibited higher growth rates when cultivated with BG11-H and supplementary CO_2. Strains CCAC 0526, 0868, 3305, 3319 and 3323 had similar productivities in both treatments, as did SAG 34-1l and 3-1b. Meanwhile, M1024 and CCCryo 096-99 seemed to grow better on wastewater.
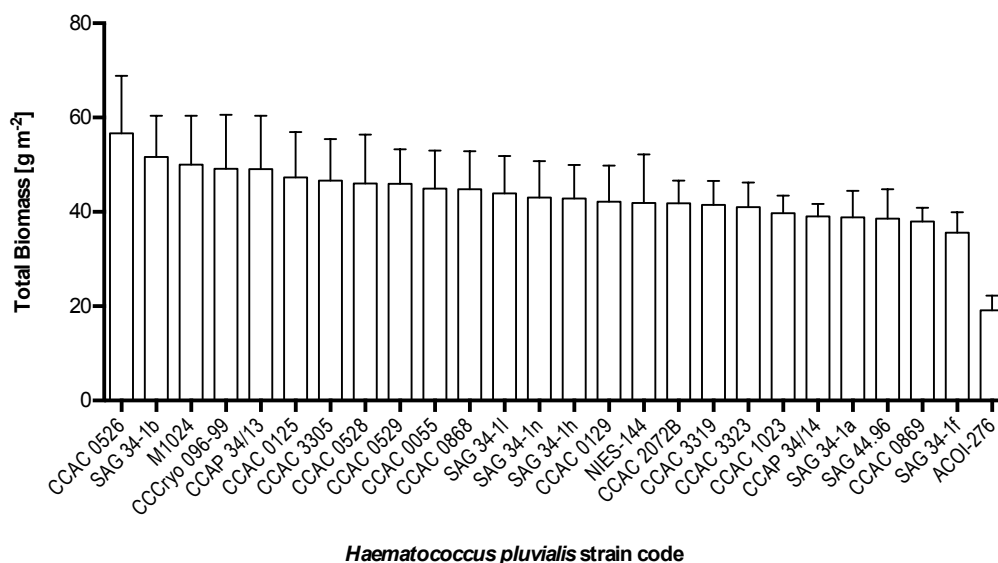
Figure 3.2. Total biomass in g dry weight m^{-2} ± SD (*n*=4) of 26 strains of *H. pluvialis* during seven days of cultivation in a Twin-Layer PSBR with secondary municipal wastewater. Light intensity was 200 μmol photons m^{-2} s^{-1} and aeration was performed only with ambient air.

Despite of the similar performance on immobilized biomass and astaxanthin production of most of the strains, some differences were observed during cultivation. Slight colour variations were naturally present, however diversity of biofilm surface and growth orientation was surprising. Extremely irregular, with elevations and depressions as shown in Figures 3.4A left and 3.4B and smooth surfaces (Figure 3.4C) were observed, as were levels in between (Figure 3.4A right). Most of the irregular surface strains also exhibited growth to the sides, frequently taking over the whole polycarbonate membrane, whereas smooth surface strains' growth was more constrained. No conclusive correlation could be drawn, but the most biomass productive strains seemed to have a rough surface, with the exception of strains CCAC 0869 and SAG 44.96.
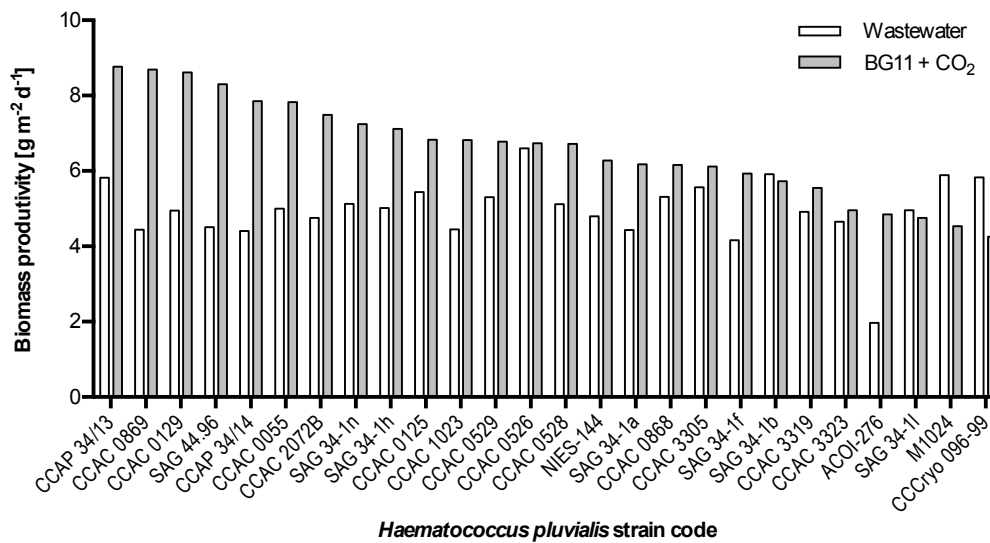
Figure 3.3. Estimated biomass productivity for eight days of growth with secondary municipal wastewater and aeration with no additional CO_2 and for seven days of growth with BG11-H and 2% CO_2. In both conditions, light intensity was 200 µmol photons m^{-2} s^{-1}.
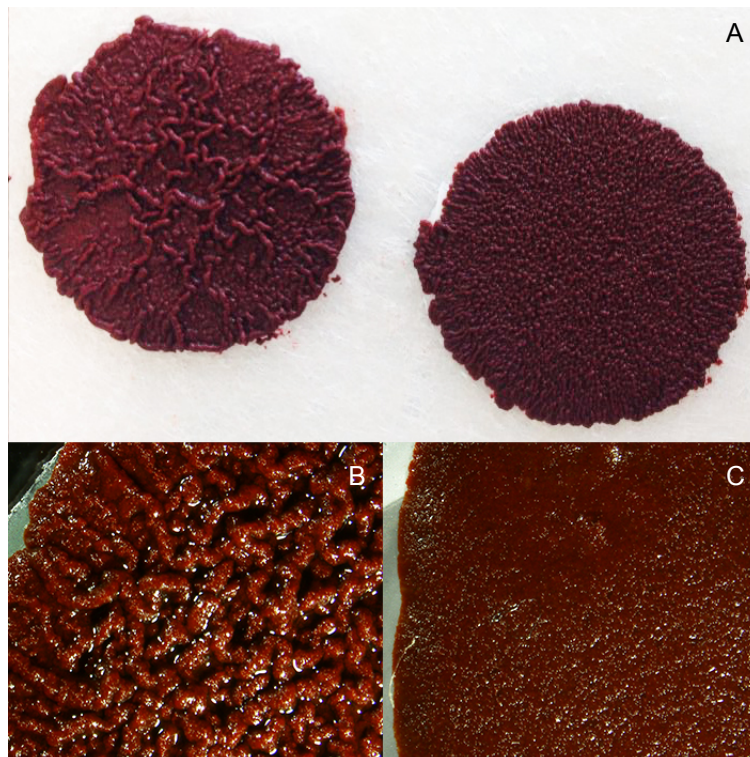
Figure 3.4. Biofilm surfaces of different strains of *H. pluvialis* cultivated for 14 days in a Twin-Layer PBR at 203 µmol photons m^{-2} s^{-1}. **A:** Polycarbonate membranes completely covered by biofilms with different levels of rough surfaces On the left, strain CCAC 0125 and right, CCAC 0869. **B:** binocular image of a rough surface biofilm from strain CCAC 0125 and **C** smooth surface, from SAG 44.96. Full BG11-H medium was supplied for the first 7 days of growth and N-depleted BG11-H, for days 8-14. Aeration was supplemented with 5% CO_2.

Considering the good and comparable performance of most of the strains, CCAC 0125 was selected for further studies in optimization of the immobilized cultivation of *H. pluvialis*, based on the high astaxanthin yield obtained. On BG11 culture medium, this strain reached final astaxanthin and biomass values of 1.4 and 91.2 g m^{-2} and an astaxanthin content of 1.5% of the dry weight. Furthermore, it can be considered robust, capable of growth on secondary wastewater.

3.2. The effect of light intensity and CO_2 supplementation on biomass and astaxanthin production

3.2.1 Two-step cultivation with high light

Light intensity plays a major role on both biomass and astaxanthin production and is usually applied in two different conditions: initially low irradiances are used to favour biomass growth and high irradiances are then introduced for astaxanthin accumulation. This classical two-step approach was simulated for the Twin-Layer, when cultures were exposed to 90 µmol photons m^{-2} s^{-1} for eight days (growth phase), then transferred to 1,000 µmol photons m^{-2} s^{-1} for the same period (stress phase).

Biomass increased linearly in each stage of cultivation, but with very different growth rates (Figure 3.5A). A growth rate of 5.4 g m^{-2} d^{-1} was observed at low light, yielding a biomass of 48.2 g m^{-2} after 8 days of cultivation. When switched to high light, growth rate increased to 17.2 g m^{-2} d^{-1} and a final standing crop of 177.1 g m^{-2} was obtained. Astaxanthin production was restricted to the high light phase, in which a rate of 0.36 g m^{-2} d^{-1} was observed, leading to a final yield of 2.8 g m^{-2} (Figure 3.5B). This was confirmed by the astaxanthin content in the biomass that increased from 0.16% to 1.6% during the first four days of exposure to 1,000 µmol photons m^{-2} s^{-1} and was then stable until the end of the experiment.

Figure 3.6 depicts cross-sections of the biofilms at the end of each cultivation phase. At day eight, biofilm was almost completely green, with a very thin red layer emerging

on the top. Surface was mostly smooth, though some elevations could be observed. After exposure to high light, the biofilm increased in thickness and was composed by two very distinct layers of similar depths. The outermost, formed by big red akinetes while the inner layer showed small green cells.
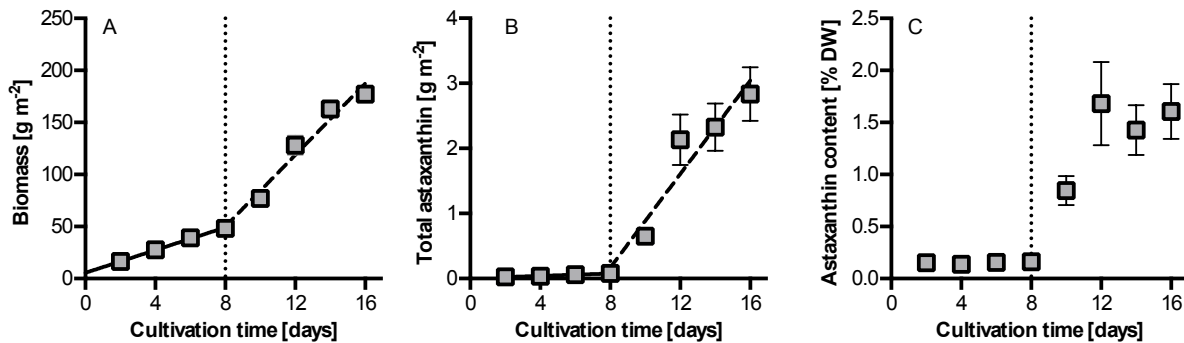
Figure 3.5. Biomass and astaxanthin kinetics of a two-step cultivation of *H. pluvialis* using only high light as a stress factor. **A** Biomass production (g m^{-2} ± SD, n=3); **B** Total astaxanthin (g m^{-2} ± SD, n=3) and **C** Astaxanthin content in biomass (% ± SD, n=3). Biofilms were grown for eight days at 90 µmol photons m^{-2} s^{-1} (growth phase) then transferred to 1,000 µmol photons m^{-2} s^{-1} for another eight days (stress phase), as indicated by the vertical dotted line. Culture medium was full BG11-H and aeration was supplemented with 5% CO$_2$. Biomass and astaxanthin productivities were calculated from the linear regressions showed in the graphs.
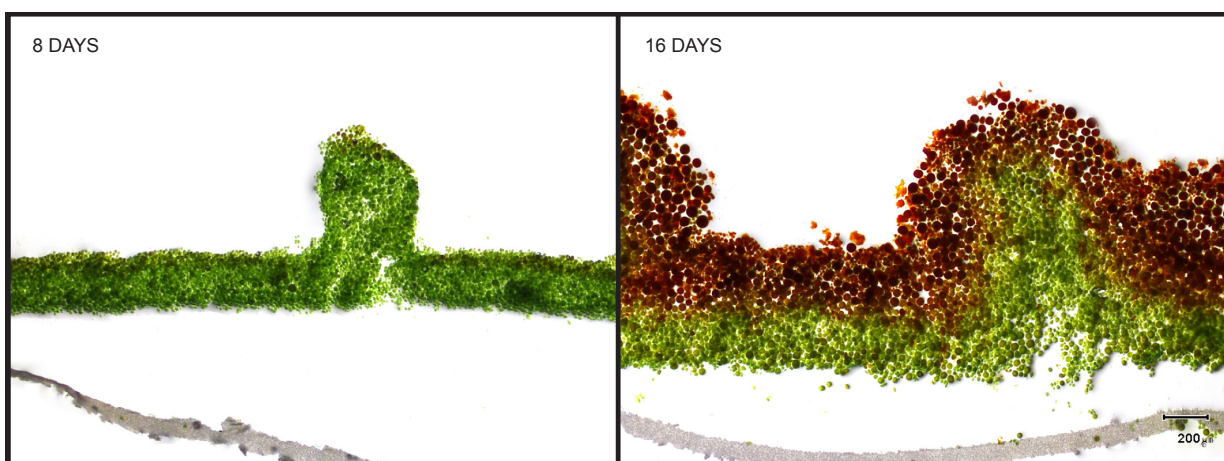
Figure 3.6. Cross-sections of *H. pluvialis* biofilms at the end of the growth (8 days) and stress (16 days) phases. Light intensity was 90 µmol photons m^{-2} s^{-1} for the first and increased to 1,00 µmol photons m^{-2} s^{-1} for the latter. Full BG11-H culture medium and aeration with 5% CO$_2$ were supplied throughout the cultivation period. Scale bar corresponds to 200 µm and applies for both images.

During the stress phase, high light supported biomass and astaxanthin productivities, raising the interest on the effect of light intensity on the *H. pluvialis* biofilm, which was further investigated.

3.2.2 Light intensities and CO_2 supplementation

Ten different irradiances, ranging from 20 to 1,015 µmol photons m^{-2} s^{-1} were evaluated for its effect on biomass and astaxanthin production, under two aeration conditions: ambient air and 5% supplementary CO_2. Light conditions were maintained constant throughout the cultivation period.

Biomass growth

Biomass production in terms of dry matter per m^2 increased with increasing light and this effect was more pronounced when additional CO_2 was supplied (Figure 3.7). Hence, lowest biomass growth occurred at 20 µmol photons m^{-2} s^{-1} and highest at 1,015 µmol photons m^{-2} s^{-1} for both aeration conditions. When only ambient air was applied, biomass yield at 16 days was 33.8 g m^{-2} (20 µmol photons m^{-2} s^{-1}) and 103.2 g m^{-2} (1,015 µmol photons m^{-2} s^{-1}), whereas at 31 days it reached 60.00 and 153.5 g m^{-2}. Meanwhile minimum and maximum final standing crop after 16 days of cultivation with supplementary CO_2 was 34.3 g m^{-2} and 213.5 g m^{-2}. Indeed, area under curve analysis indicated that CO_2 supplementation increased growth by only 12.3% at the lowest light intensity, whereas this effect was about 11.5 times higher (141.8%) at the highest irradiance.

When no CO_2 was supplemented, biomass increased linearly throughout the 31 days at light intensities ≤ 89 µmol photons m^{-2} s^{-1}. At higher irradiances, a gradual saturation in growth was observed. A similar trend was observed in the groups that received additional CO_2, but saturation was much stronger at 644, 789 and 1015 µmol photons m^{-2} s^{-1} and final biomass yields were not significantly different in these groups (Figure 3.7).
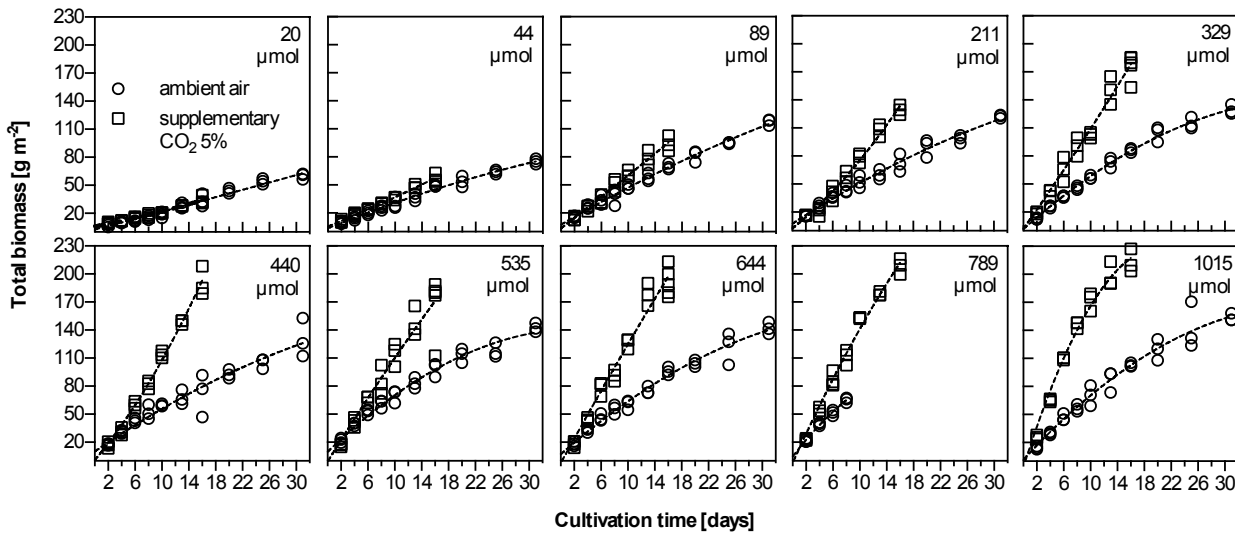
Figure 3.7 Total dry biomass of *H. pluvialis* grown in a Twin-Layer biofilm (g m^{-2} ± SD, *n*=3) over a maximal growth period of 31 days for different light intensities ranging from 20 to 1,015 µmol photons m^{-2} s^{-1}. Experiments were conducted with ambient air (open circles) or ambient air supplemented with 5% CO_2 (open squares) using BG11 culture medium.

Daily biomass productivities (growth rates) were calculated and helped to recognize this saturation effect. Figure 3.8 depicts plotted values with the PI-model fit. Growth rates from tubes aerated with ambient air designed a curve with two parts: an initial sharp increase in productivity until 89 µmol photons m^{-2} s^{-1}, after which the steepness of the slope is eased. Values in this flattened part of the curve did decrease over time, however, full saturation was not reached. 1,015 µmol photons m^{-2} s^{-1} registered the highest growth rates, ranging from 7.6 (day 2) to 4.9 g m^{-2} d^{-1} (day 31) without supplementary CO_2.

The effect of CO_2 supplementation was evident on the growth rates at high irradiances. In fact, the maximum growth rate of 19.4 g m^{-2} d^{-1} was observed on day 2, at 1,015 µmol photons m^{-2} s^{-2} (Figure 3.8). However, the biomass growth saturation was also higher and saturation was reached at day 10 for light intensities over 440 µmol photons m^{-2} s^{-1}. At day 16, three parts could be identified in the biomass-irradiance curve: an initial light dependent increase in biomass production (0 – 329 µmol photons m^{-2} s^{-1}); a small plateau, where growth rates don't seem to be affected by the irradiance (329 - 535 µmol photons m^{-2} s^{-1}) and a light dependent decrease of the growth rates (535 – 1,015 µmol photons m^{-2} s^{-1}). These results

indicate that biomass grows faster at very high light intensities but it tends to saturate earlier. Thus, similar amounts of biomass can be reached after longer cultivation periods with intermediate irradiances.
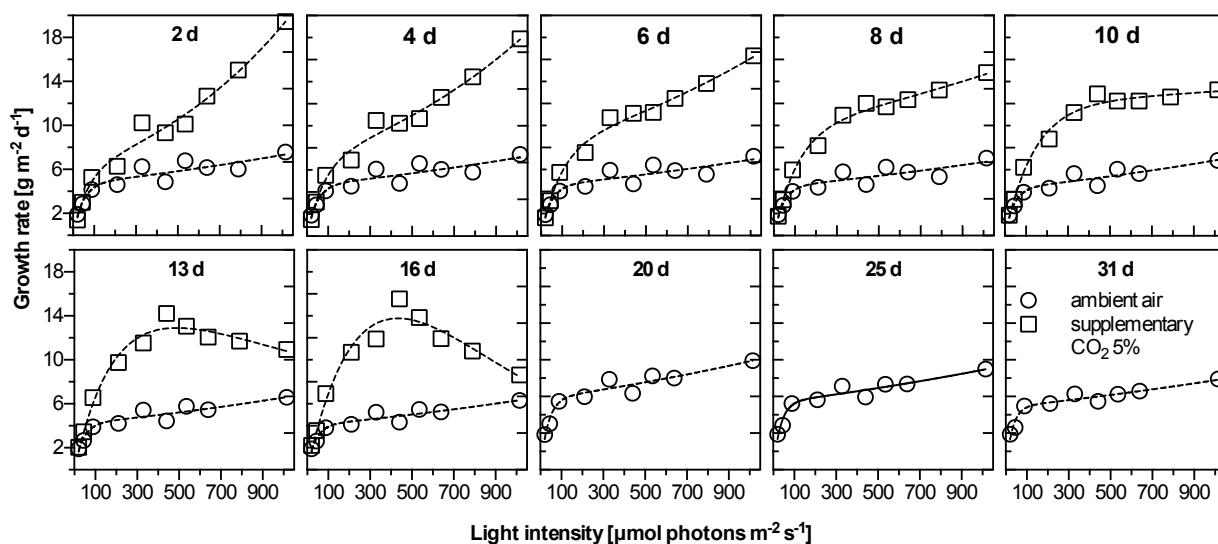
Figure 3.8. Biomass productivity on *a* Twin-Layer (g m^{-2} d^{-1}) during 16 and 31 days of cultivation in dependence of light intensity from 20 to 1,015 µmol photons m^{-2} s^{-1}. Aeration was performed only with ambient air (open circles) or ambient air supplemented with 5% CO_2 (open squares) and BG11 culture medium was applied. Values were calculated from the first derivative of a second order polynomial fit of biomass growth (n=3).

While biomass productivities increased with irradiance, efficiency of light energy use reduced drastically (Figure 3.9). Highest values of 1.29 g biomass per mol light were observed at 20 µmol photons m^{-2} s^{-1}. The more pronounced reduction occurred from 20 to 211 µmol photons m^{-2} s^{-1} and the trend was similar throughout the experimental period, both with or without CO_2 supplementation.
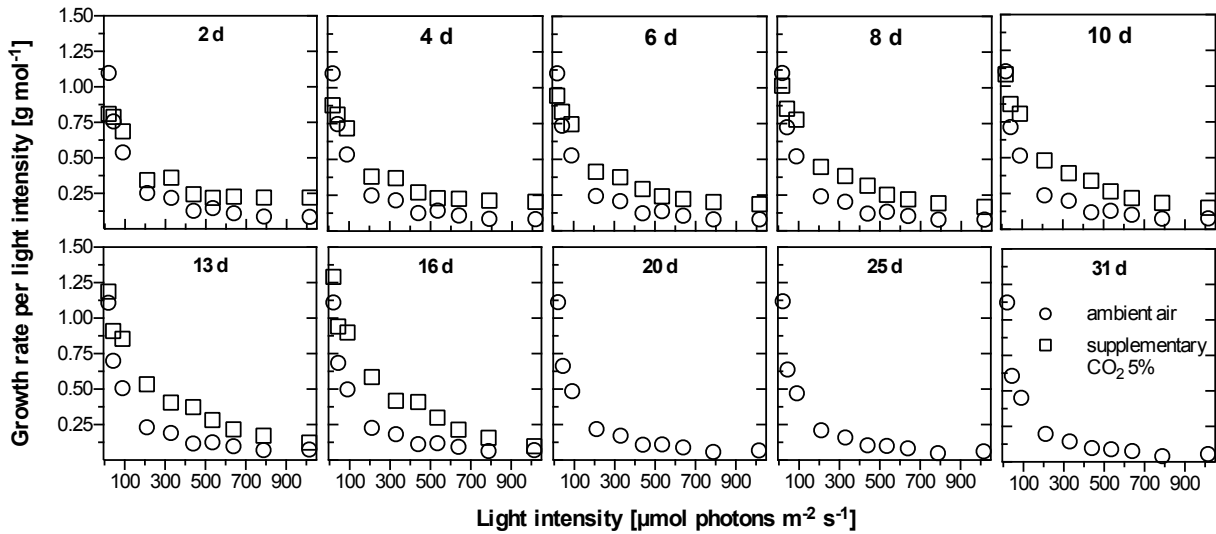
Figure 3.9. Biomass productivity of *H. pluvialis* per mol light intensity on *a* Twin-Layer PSBR (g mol) during 31 days of cultivation in dependence of light intensity from 20 to 1,015 µmol photons m^{-2} s^{-1}. Aeration was performed only with ambient air (open circles) or ambient air supplemented with 5% CO_2 (open squares) and BG11 culture medium was applied.

Astaxanthin production

Similar to biomass, total astaxanthin production and content per dry weight showed a light dependent increase. Astaxanthin analyses in tubes aerated only with ambient air were conducted at days 6, 16 and 31 and results are shown in Figure 3.10. Highest astaxanthin contents were observed at day 6, in the range of 0.4 (20 µmol photons m^{-2} s^{-1}) to 2.3% (1,015 µmol photons m^{-2} s^{-1}). However, it reduced over time and after 31 days, astaxanthin contents varied from 0.2 to 1.5%, still showing a light-dependency trend. Regardless of this reduction, biomass increase over time led to an increase of total astaxanthin production. Astaxanthin productivities were not calculated due to too few time points for an appropriate kinetic analysis.
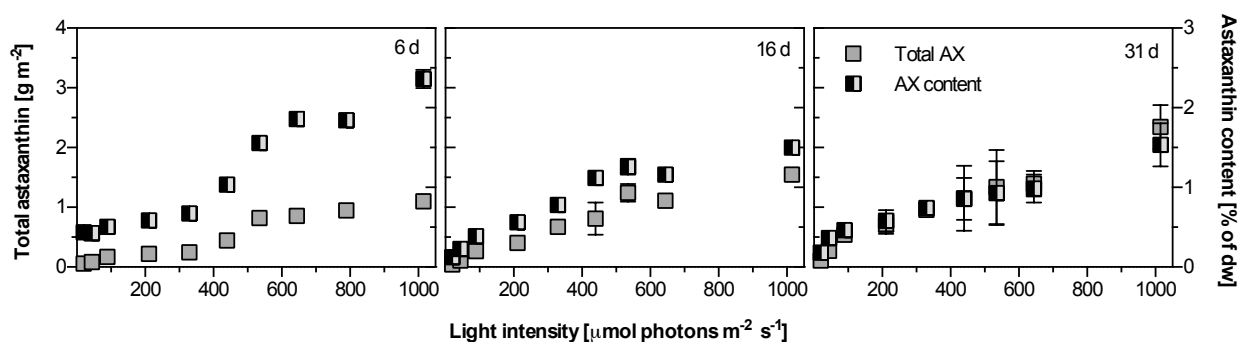
Figure 3.10. Total astaxanthin (g m^{-2} ± SD, *n*=3, grey squares) and astaxanthin content (% of dry biomass ± SD, *n*=3, black/grey squares) of *H. pluvialis* grown in a Twin-Layer at light intensities from 20 to 1,015 μmol photons m^{-2} s^{-1}, with BG11-H culture medium and no supplementary CO_2. Measurements were performed at 6, 16 and 31 days of cultivation.

Supplementary CO_2 did not affect astaxanthin content per dry matter when compared to aeration with ambient air, but increased the total astaxanthin production per area by increasing the total standing crop on the reactor surface. Figure 3.11 shows the astaxanthin kinetics during the 16-day experimental period with supplementary CO_2. Astaxanthin induction by light began at very low levels in a later stage of cultivation at 89 μmol photons m^{-2} s^{-1} and increased at higher irradiances (Figure 3.11). When light was ≥ 440 μmol photons m^{-2} s^{-1}, contents of 1.5 - 2 % astaxanthin were already observed in early cultivation stages (days 2 and 4) and highest values of around 2.5% astaxanthin per dry weight were reached at 789 μmol photons m^{-2} s^{-1}. Total astaxanthin increased linearly for around 10 - 13 days and then started to saturate at irradiances over 200 μmol photons m^{-2} s^{-1}, following the trend of biomass production. Astaxanthin productivities were calculated for the linear phases depicted in Figure 3.11 and confirmed dependency on light intensity (figure 3.12). Cultivation of *H. pluvialis* at 789 μmol photons m^{-2} s^{-1} resulted in the highest astaxanthin productivity (0.39 g m^{-2} d^{-1}) and total astaxanthin yield in the experimental period (3.4 g m^{-2}). Maximum yields, however, were not significantly different at 644, 789 and 1,015 μmol photons m^{-2} s^{-1}.
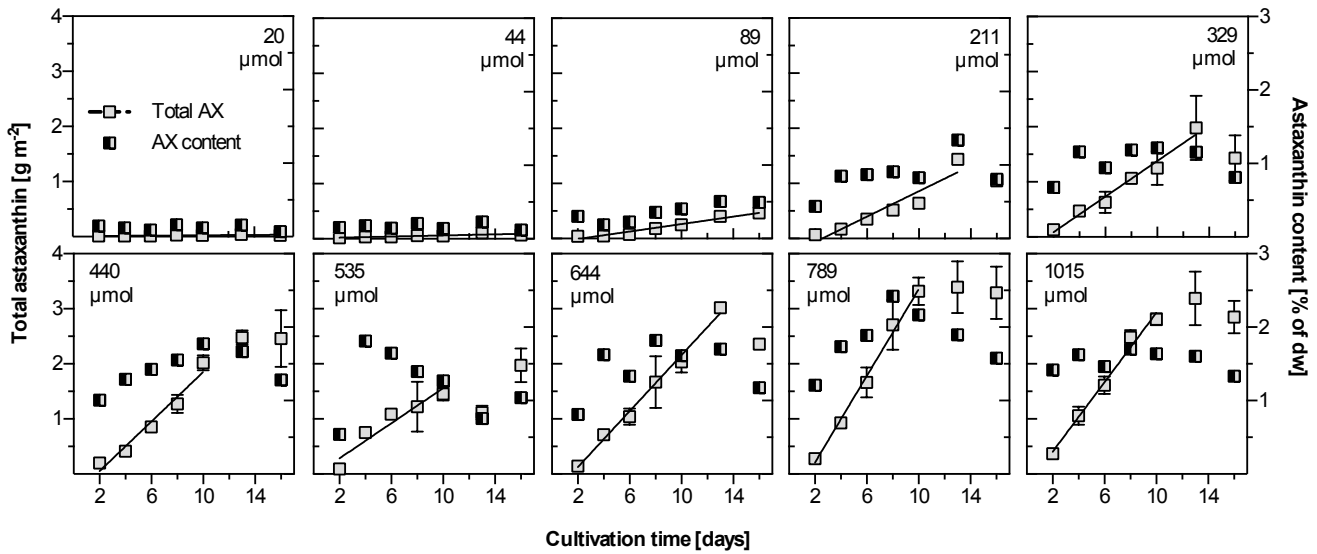
Figure 3.11. Total astaxanthin (g m^{-2} ± SD, n=3, grey squares) and astaxanthin content (% of dry biomass ± SD, n=3, black/grey squares) over a growth period of 16 days for different light intensities ranging from 20 to 1,015 µmol photons m^{-2} s^{-1}. Experiments were conducted with ambient air supplemented with 5% CO_2 and BG11-H culture medium. A linear increase of total astaxanthin over time prior to saturation is indicated by the solid line.
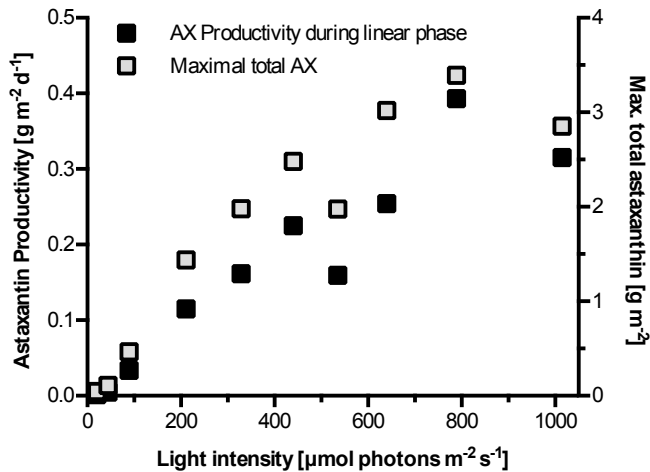
Figure 3.12. Light-induced astaxanthin productivity by *H. pluvialis* in terms of productivity during the linear phase (g m^{-2} d^{-1} ± SD, n=3; for linear phase refer to fig. 4) and maximal total astaxanthin (g m^{-2} ± SD, n=3) in dependence of PAR light intensity from 20 to 1,015 µmol photons m^{-2} s^{-1}. Experiments were conducted with ambient air supplemented with 5% CO_2 and BG11 culture medium.

Biofilm appearance and structure

The described effect of light intensity on biomass and astaxanthin was visible on the biofilms (Figure 3.13). The very low astaxanthin production at 89 µmol photons m^{-2} s^{-1} starts to change the colour of the biofilm surface, but it becomes evident at 211 µmol photons m^{-2} s^{-1}, when it is already red. The irregular surface of the biofilm formed by strain CCAC 0125 is also visible in the images, increasing at higher light intensities, when there was more biomass production.
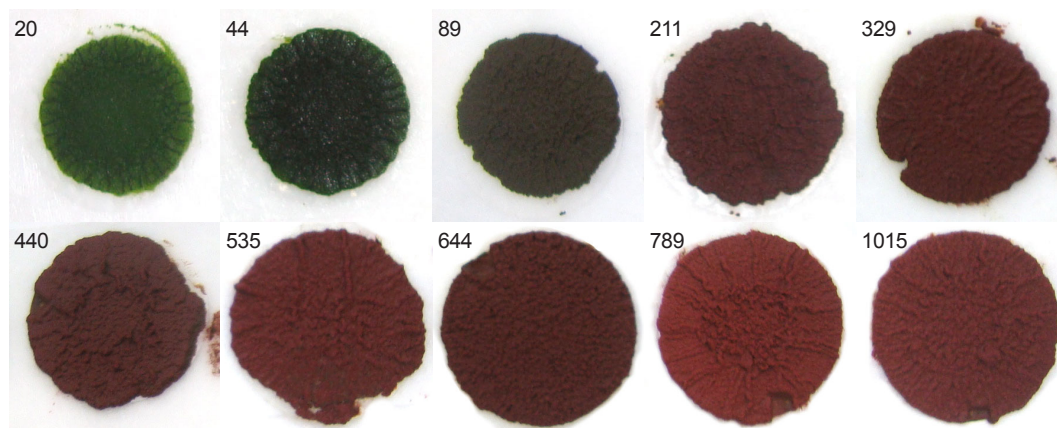
Figure 3.13. *H. pluvialis* biofilms on polycarbonate membranes after 16 days of cultivation at different light intensities and aerated with 5% additional CO_2.

Cryosectioning of *H. pluvialis* biofilms (Figure 3.14) grown at different irradiances with 5% CO_2 was conducted at the end of the experiment. The images support biomass and astaxanthin results, showing increased biomass thickness and presence of red akinetes at higher irradiances. Astaxanthin accumulation occurred mainly in the outermost layer of the biofilms, exposed to the light source. The thickness of this red layer formed by akinetes depended on the irradiance available, as did the size and colour of the cells in its composition. Sectioning confirmed almost completely green biofilms at 20 and 44 µmol photons m^{-2} s^{-1} and a very thin red layer at 89 µmol photons m^{-2} s^{-1}, which increased in thickness and akinete size at high light intensities.
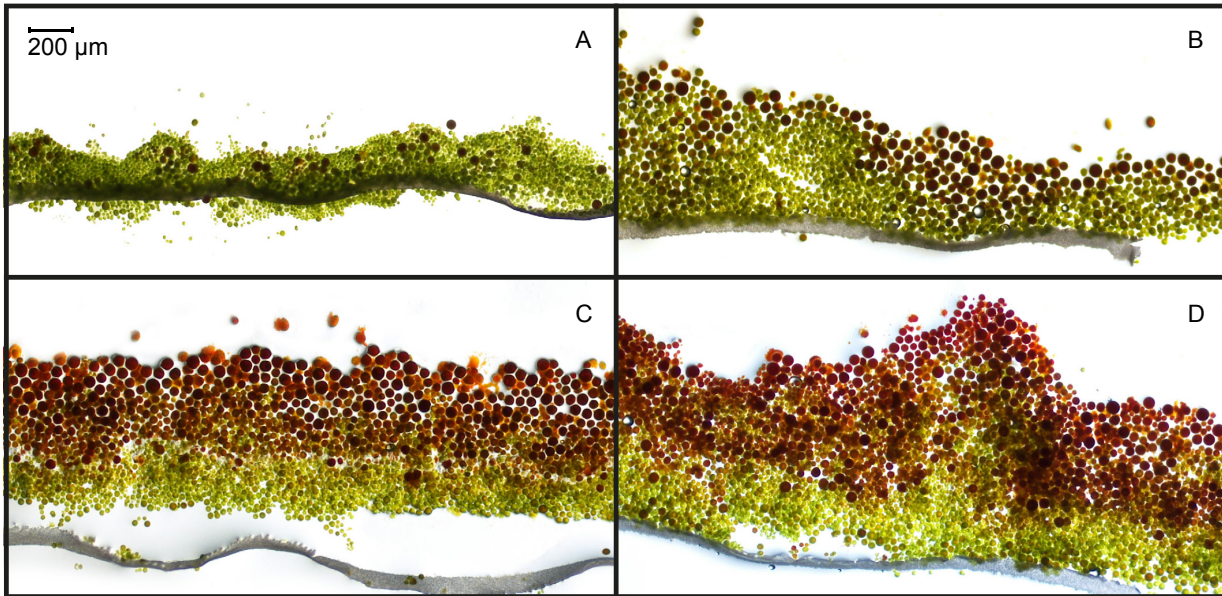
Figure 3.14. Micrographs of biofilm sections after 16 days cultivation at: **A** 20 µmol photons m^{-2} s^{-1}, **B** 89 µmol photons m^{-2} s^{-1}, **C** 329 µmol photons m^{-2} s^{-1} and **D** 1,015 µmol photons m^{-2} s^{-1}. Experiments were conducted with ambient air supplemented with 5% CO_2 and BG11-H culture medium.

3.2.3 Cultivation at high light: one versus two-step strategy

The effect of high light boosting both biomass and astaxanthin production observed in the classic two-step approach was confirmed while investigating the range of irradiances. The results for cultivation at 1,000 µmol photons m^{-2} s^{-1} were then compared to elucidate the need of a growth phase with low light. In this comparison, results obtained from cultivation at 1,000 µmol photons m^{-2} s^{-1} for the entire 16 days are referred to as one-step.

Biomass growth rates were very similar for the first eight days cultivation at high light, namely 17.2 g m^{-2} d^{-1} and 18.3 g m^{-2} d^{-1} for two and one-step strategies. Since it was preceded by a low light period, standing crop was 48.2 g m^{-2} in the first, compared to 146 g m^{-2} in the latter after 8 days of cultivation (Figure 3.15A). Nevertheless, due to the previously described biomass growth saturation, the final yield was only 20% higher in the one-step process (213.5 g m^{-2} vs. 177.1 g m^{-2}).

Similar trends were observed when analysing total astaxanthin data. Accumulation in the two-step was restricted to the high light phase, but in a similar rate to that observed for the first eight days of the one-step: 0.34 and 0.36 g m^{-2} d^{-1}, respectively

(Figure 3.15B). At day 8, astaxanthin yield was 2.5 g m^{-2} at 1,000 µmol photons m^{-2} s^{-1} and 0.08 g m^{-2} at 90 µmol photons m^{-2} s^{-1}, a 32-fold increase when applying one-step cultivation. Nevertheless, this difference was abolished after the exposure to high light and astaxanthin production reached 2.8 g m^{-2} at day 16 in both approaches. While astaxanthin content in biomass was ca. 1.5% already after 2 days of cultivation at 1,000 µmol photons m^{-2} s^{-1}, 12 days were necessary to reach this value when using a two-step approach (Figure 3.15C).

Biofilm cross-sections support these findings. After 16 days of cultivation, the biofilm grown in a two-step process was thinner but resembled the one exposed to 1,000 µmol photons m^{-2} s^{-1} during the entire cultivation period (Figures 3.6 and 3.14D).

High light boosted both growth and astaxanthin production on a *H. pluvialis* biofilm and its effect was independent of the beginning of the exposure. That is, cultivation could be entirely conducted at high irradiances and the use of a low light growth phase only hindered the high productivities, but similar values were reached when considering a total of 16 days cultivation period.
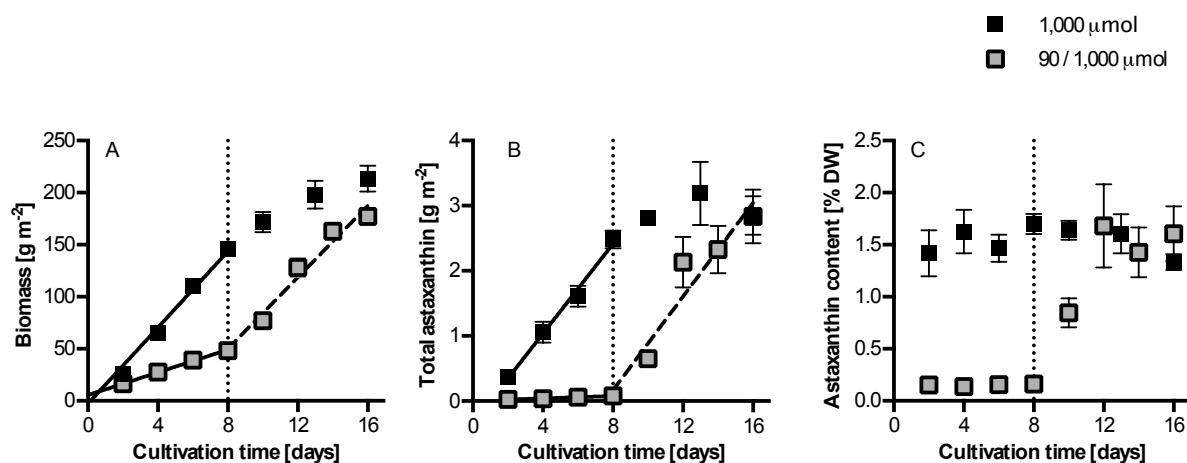
Figure 3.15. Biomass and astaxanthin kinetics of one versus two-step cultivation of *H. pluvialis* using only high light as a stress factor. **A** Biomass production (g m^{-2} ± SD, n=3); **B** Total astaxanthin (g m^{-2} ± SD, n=3) and **C** Astaxanthin content in biomass (% ± SD, n=3). One-step approach consisted of exposure to 1,000 µmol photons m^{-2} s^{-1} for 16 days (black squares), whereas two-step consisted of 8 days pre-cultivation at 90 µmol photons m^{-2} s^{-1} and 8 days at 1,000 µmol photons m^{-2} s^{-1} (grey squares). Vertical dotted line indicates when light intensity was switched for the two-step approach. Biomass and astaxanthin productivities were calculated from the linear regressions showed in the graphs.

3.2.4 CO_2 optimization at high light

In light of the increase in biomass productivities at high irradiances, the required CO_2 concentration to sustain or further boost *H. pluvialis* growth in these conditions was investigated. Five different concentrations were tested (1, 2.5, 5, 7.5 and 10 %) at 1,015 µmol photons m^{-2} s^{-1} for 16 days.

Biomass growth was similar among all groups and to the previous experiment. Growth rate calculations show slightly higher values at 5% and lower at 10% CO_2 during the first 6 days of growth (Figure 3.16A). However, as previously observed, higher early growth rates tend to have a more pronounced decrease over time. Therefore, all CO_2 concentrations yielded a final standing crop of around 213 g m^{-2}, with no significant differences (Figure 3.16B). Total astaxanthin yields at day 16 were also similar, approximately 3 g m^{-2} (Figure 3.16C), while contents in biomass were 1.5% of dry weight.

High concentrations of CO_2 could have led to acidification of the culture medium, inhibiting biomass growth. However, when measured at media exchange, the lowest pH values were 6.72, at 10% CO_2. When 1% CO2 was supplied, the pH was almost stable and a value of 7.2 was measured.
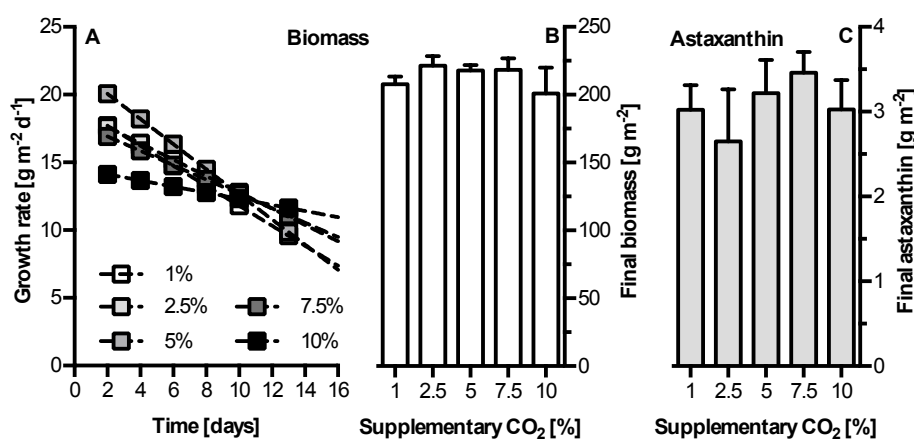
Figure 3.16. Effect of supplementary CO_2 on biomass and astaxanthin of *H. pluvialis*: **A** Growth rate (g m^{-2}) over time within the 16 d of cultivation. **B** Total biomass (g m^{-2} ± SD, *n*=3) and. **C** Maximal total astaxanthin produced within the 16 days of cultivation (g m^{-2} d^{-1} ± SD, *n*=3). All experiments were conducted at light intensity of 1,000 µmol photons m^{-2} s^{-1} using BG11-H culture medium.

Thus, at 1,015 µmol photons m^{-2} s^{-1} and feeding BG11-H medium, aeration with 1% CO_2 is enough to avoid carbon limitation and support maximum growth and astaxanthin production. It was therefore maintained as the standard CO_2 concentration for the following experiments

3.3. Astaxanthin induction with stress media

Previous results indicated that high irradiances could be applied throughout the immobilized cultivation of *H. pluvialis* in biofilms, increasing astaxanthin accumulation not only without compromising biomass production, but even boosting it. High light was then applied in combination with culture medium stress factors in an attempt to further improve astaxanthin production.

3.3.1 The effect of culture media stress factors coupled to high light

Initially, nutrient depletion (nitrogen and/or phosphorous), salinity and nitrogen depletion together with salinity were applied after a growth phase of 3 days with full BG11-H medium. Light intensity was 800 µmol m^{-2} s^{-1} throughout the experiment and one tube was maintained as a control, with full medium. The experiment was conducted for a total of 17 days: 3 days with full BG11-H medium and 14 days with the different stress media.

Biomass production was similar among all groups for the first 4 days of stress. At day 10, significant differences began to emerge, with the full BG11 (control) and P zero maintaining higher values when compared to the others (Figure 3.17). At day 17, biomass yields were highest in control (210.3 ± 7.3 g m^{-2}) and P zero (186.9 ± 11.4 g m^{-2}), with no significant difference among them. Other stress treatments lead to a reduction from 31% (NP zero) to 44% (NaCl) in final biomass, as depicted in figure 3.18.
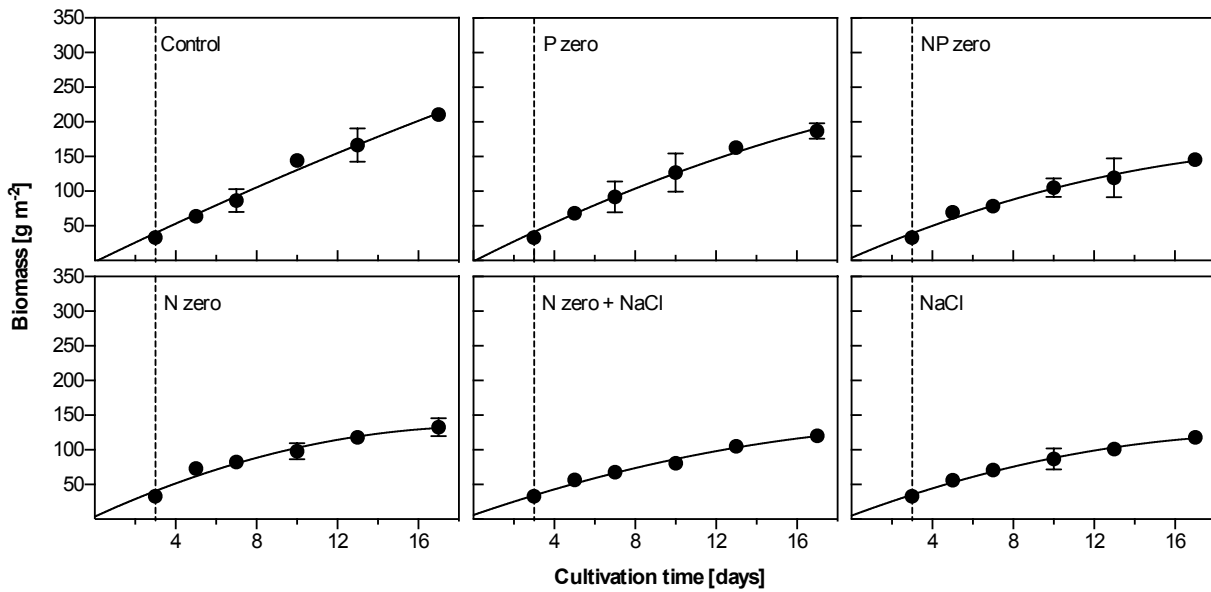
Figure 3.17. Biomass production (g m^{-2} ± SD, n≥3) during cultivation with different culture media. Vertical dashed line indicates transition from full BG11-H to different stress media: P zero, NP zero, N zero, N zero+ NaCl and NaCl. Light intensity was 800 µmol photons m^{-2} s^{-1} and aeration was performed with additional 1% CO_2.
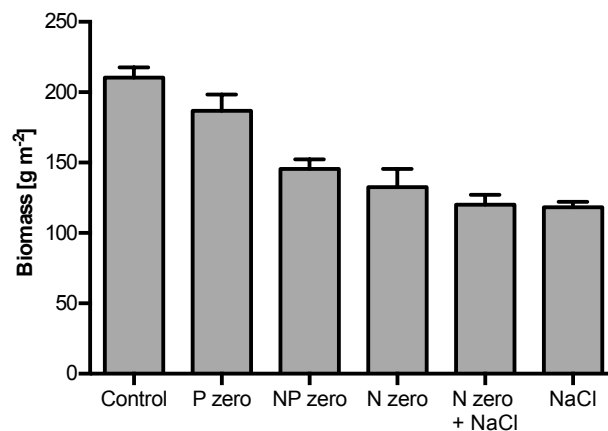
Figure 3.18. Final biomass yield in the different media treatments (g m^{-2} ± SD, n≥3). Biofilms were grown with full BG11-H (control) culture medium for 3 days and for the following 14 days with one of the stress media: P zero, NP zero, N zero, N zero + NaCl and NaCl. Light intensity was maintained at 800 µmol photons m^{-2} s^{-1} and additional 1% CO_2 was supplied in aeration.

Astaxanthin production and content in biomass for the control and different stress treatments are shown in Figures 3.19 and 3.20. At day 3, all groups contained 1.2 ± 0.2 % astaxanthin of dry matter and immediately after the onset of stress, a steep

increase was observed in the tubes fed with N zero, NP zero, N zero + NaCl and NaCl. A maximum content of 2.8 and 2.9 % was reached in N zero and N zero + NaCl biofilms, significantly higher than the control. More gradual astaxanthin accumulation in biomass occurred when full BG11 and P zero media were applied, resulting in lower contents of 1.7 and 2.2 % (Figures 3.19 and 3.20).
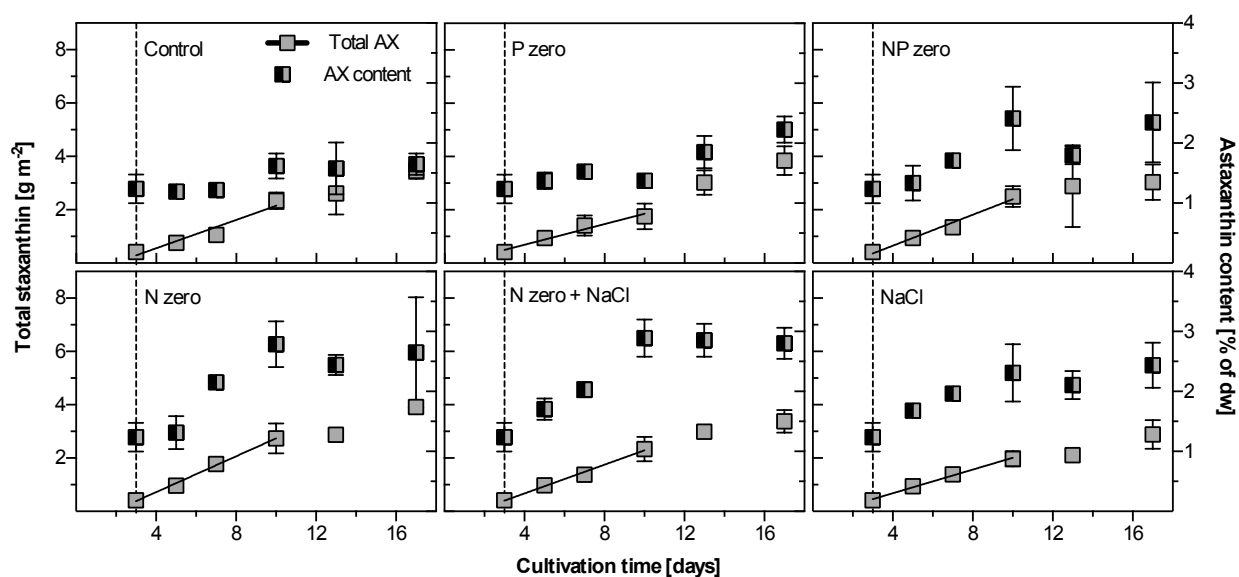
Figure 3.19. Total astaxanthin (g m^{-2} ± SD, $n\geq3$, grey squares) and astaxanthin content (% of dry biomass ± SD, $n\geq3$, black/grey squares) for biofilms cultivated for 3 days with full BG11-H culture medium and subsequent 17 days with stress media. Vertical lines indicate beginning of stress phase. Light intensity was 800 μmol photons m^{-2} s^{-1} and aeration was supplemented with 1% CO_2.

Astaxanthin productivities were calculated for the period of 3 to 10 days, when increase was linear among all experimental conditions (Figure 3.20A). N zero showed the highest productivity of 0.336 g m^{-2} d^{-1}, whereas the lowest was observed in P zero (0.194 g m^{-2} d^{-1}). Extreme values were significantly different from each other, but when comparing all stress factors with the control, no statistical difference was found.

Since higher biomass production was associated to lower astaxanthin contents, total production of the carotenoid was not significantly different among the tested culture

media. At day 17, values ranged from 2.9 g m^{-2} in NaCl to 3.8 g m^{-2} in P zero (Figure 3.20C).
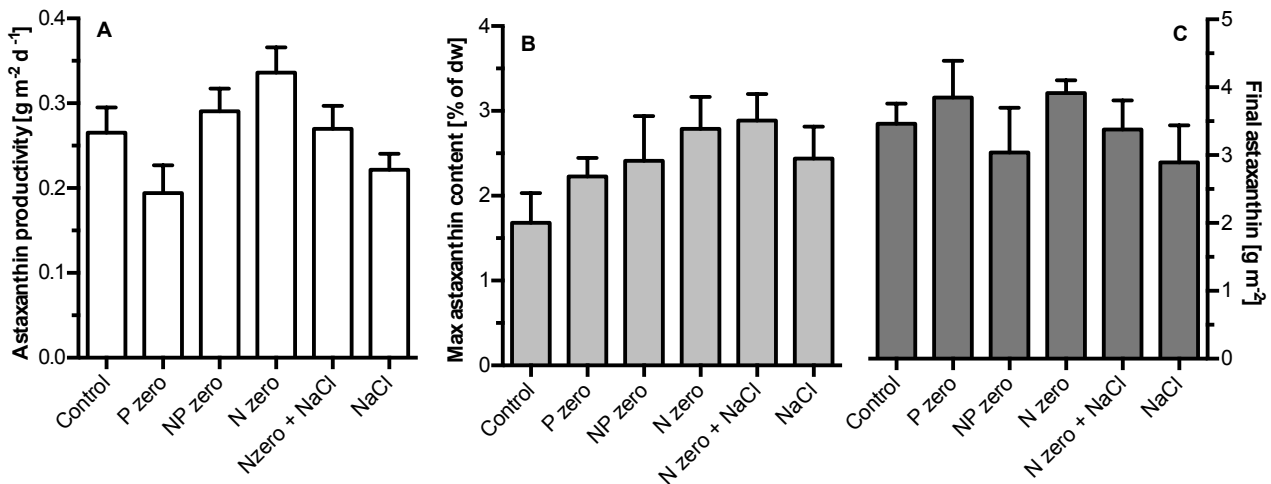
Figure 3.20. Astaxanthin productivity, maximum content in biomass and final yield of *H. pluvialis* biofilms under different stress conditions. **A** Astaxanthin productivity calculated from linear regression of days 3-10 g m^{-2} d^{-1} ± SD, *n*≥3). **B** Maximum reached astaxanthin content in biomass during the stress phase (% of dw ± SD, *n*≥3). **C** Final yield after 17 days of cultivation (g m^{-2} ± SD, *n*≥4). Light intensity was 800 µmol photons m^{-2} s^{-1} and aerated with 1% CO_2 supplementation for the entire experiment.

In order to better understand the effect of the different stress factors, total chlorophyll was also analysed in the biofilms. Data are organized in Figures 3.21 and 3.22. Total chlorophyll values increased over time in the control, following the biomass trend. Biofilms fed with P zero medium showed a similar rise until day 10, i.e. 7 days of stress, followed by a decrease. For the other stress factors, total chlorophyll was stable or showed a very discrete increment (Figure 3.21). As a consequence, final yield in the control was 2.7 g m^{-2}, whereas maximum value in stress media was 1.1 g m^{-2} in P zero. There were no significant differences between yields at day 17 among the different stress factors, however lowest values seemed to be associated to nitrogen deficiency (Figure 3.22A).

Prior to stress, chlorophyll content was 0.9% of dry weight in all groups. In the control, there was a modest increase over time and the final value was 1.3%. On the

other hand, it decreased in all of the stress treatments. In the presence of salt, decrease was already observed at day 7, meanwhile, in nutrient deficiency, chlorophyll content decrease was delayed to days 10 or 13 (Figure 3.21). Final contents showed the same trend as total chlorophyll: maximum values were found in the control and minimum, in the nitrogen deprived groups (Figure 3.22B).
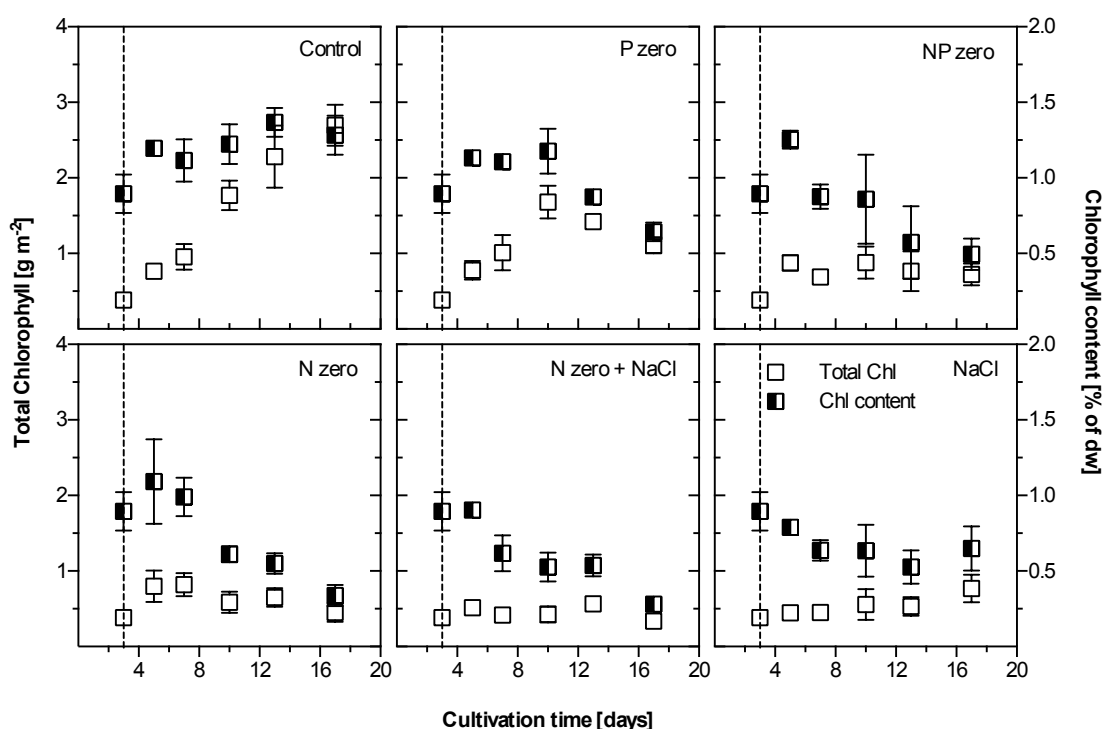
Figure 3.21. Total chlorophyll production (g m^{-2} ± SD, $n≥3$, empty squares) and content in biomass (% of dw ± SD, $n≥3$, black and white squares) in the different stress conditions. Vertical dashed line indicates the onset of the stress media. Light intensity was 800 µmol photons m^{-2} s^{-1} and aerated with 1% CO_2 supplementation for the 17 days.

The carotenoid / chlorophyll ratio is frequently used for an insight into the physiological state of microalgae. Here, astaxanthin / chlorophyll ratios were calculated at day 17 for this purpose. Significantly higher ratios were observed in N zero and N zero + NaCl groups, with values of 11.5 and 10, indicating greater stress. As expected, biofilms grown only on full BG11-H culture medium showed the lowest astaxanthin / chlorophyll ratio of 1.3 (Figure 3.23).
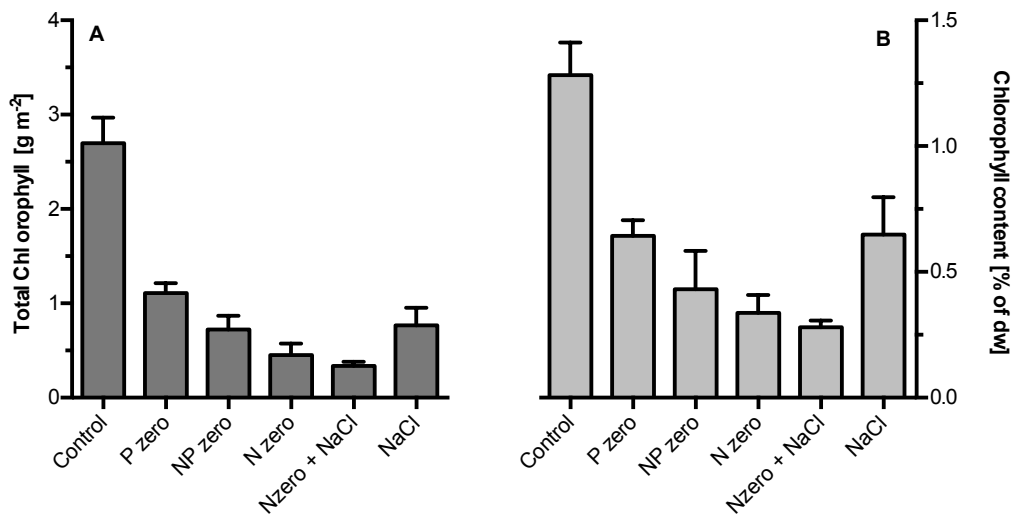
Figure 3.22. Final chlorophyll values in: **A** total production (g m^{-2} ± SD, $n≥3$) and **B** content in biomass (% ± SD, $n≥3$). Values from 17th day, after 3 days of cultivation with full BG11-H culture medium, followed by 14 days of feeding with the different stress media. Light intensity was 800 µmol photons m^{-2} s^{-1} and aerated with 1% CO_2 supplementation for the entire experiment.
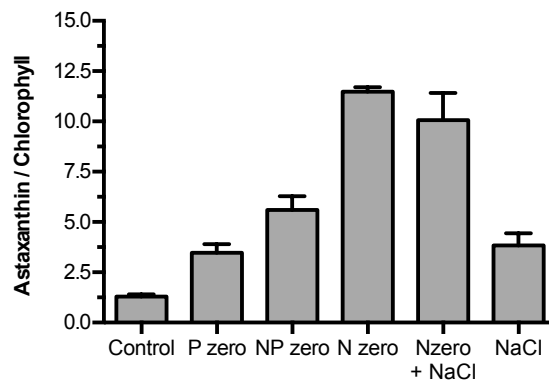
Figure 3.23. Final astaxanthin / chlorophyll ratios of biofilms cultivated for 3 days with full BG11-H culture medium, followed by 14 days with the stress media (± SD, $n≥3$). All groups were exposed to 800 µmol photons m^{-2} s^{-1} and aerated with 1% CO_2 supplementation.

Day 3 was chosen for the onset of the induction with stress media because the biofilm should be thin enough for the light to completely penetrate it. Indeed, when measured, thickness was around 150 µm, thus completely illuminated (see section 3.4). Nevertheless, astaxanthin accumulation was mainly concentrated in the top cell layers (Figure 3.24). The effects of the different stress factors at day 17 are shown in Figures 3.25 B-G. Apart from the control and P zero, astaxanthin accumulation could

be observed in the inner part of the biofilm, but still in a lower degree than the outermost cell layers. This is related to the thinner biofilms and the inner green cells are more frequent in the thicker areas, under the elevations.

Differences in thickness and cell composition could also be observed in the biofilm sections. In agreement with biomass growth results, thickest biofilms occurred in control and P zero conditions. Salt stress resulted in bigger cells in the entire biofilm (Figure 3.24F and G). On the other hand, nitrogen deficiency resulted smaller cells with a brighter red colour, probably due to different pigment composition, hence the high astaxanthin / chlorophyll ratio (Figure 3.24 D-F).
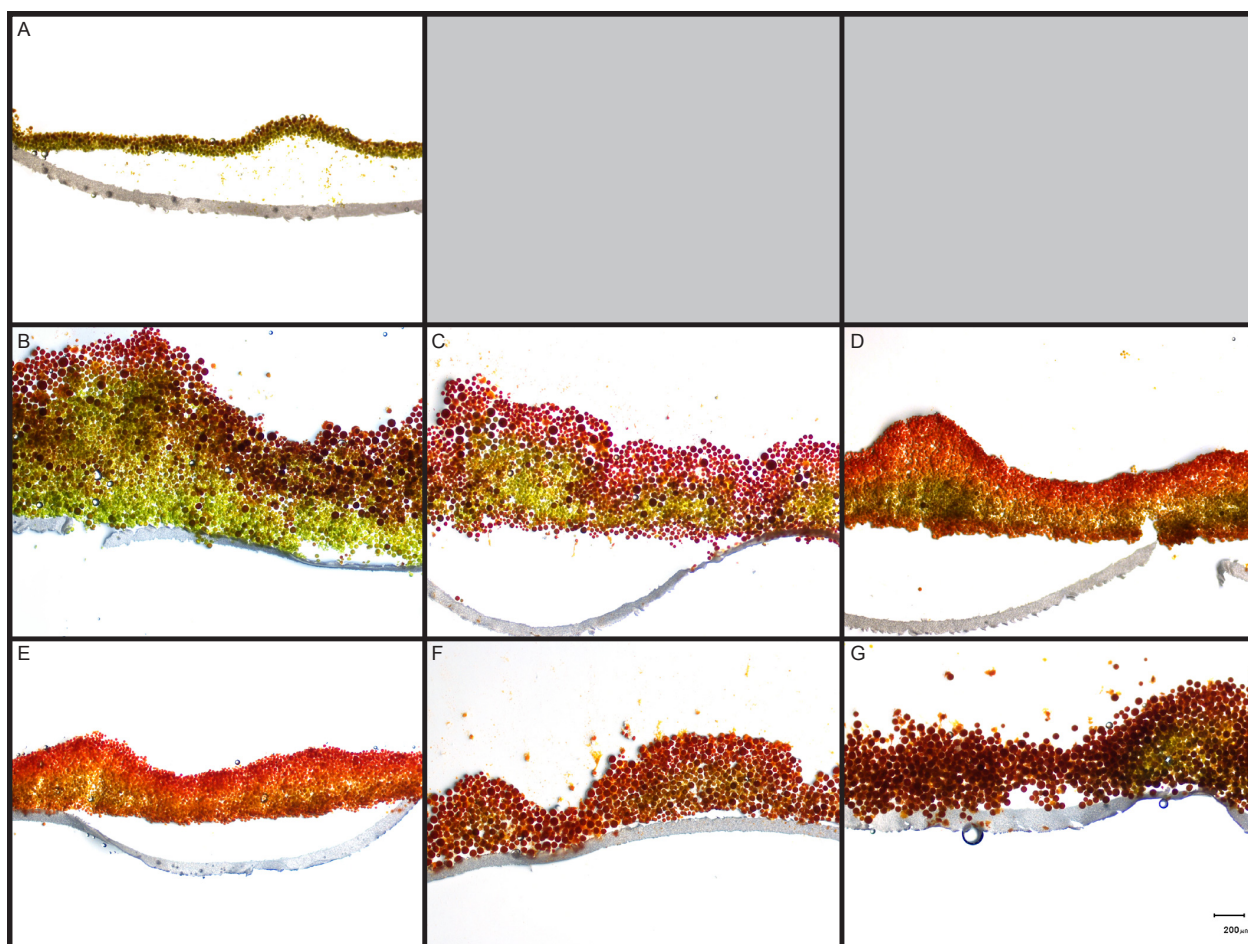
Figure 3.24. Biofilm cross sections before and after astaxanthin induction. **A** At day 3, prior to application of stress. **B-G** At day 17: **B** full BG11-H (control); **C** P zero; **D** NP zero; **E** N zero; **F** N zero + NaCl; **G** NaCl. Scale bar represents 200 μm and is applicable to all the micrographs. Light intensity was 800 μmol photons $m^{-2} s^{-1}$ and aerated with 1% CO_2 supplementation for the entire experiment.

3.3.2 The effect of stress culture media at a range of high irradiances

Additional stress factors originated from the culture medium were not capable of increasing total astaxanthin production at 800 µmol photons $m^{-2} s^{-1}$ but did increase astaxanthin content in biomass. Another experiment was conducted to investigate if similar yields could be obtained applying nutrient starvation and salinity at irradiances between 340 and 800 µmol photons $m^{-2} s^{-1}$. The use of low light was discarded due to previous findings that light intensities below this range compromise both biomass and astaxanthin production, even in the presence of other stress factors (unpublished observations). This was also observed in the screening (see Section 3.1), where maximum astaxanthin contents were 1.5% in N deprived conditions at 200 µmol photons $m^{-2} s^{-1}$.

In this setup, biofilms were grown for 3 days on full BG11-H medium, and for a subsequent period of 7 days with NP zero or NaCl media. A shorter cultivation period was applied because both biomass and astaxanthin trends were already visible at 10 days in the previous experiments. Controls were maintained on full BG11-H medium for the entire experimental period at the following irradiances: 485, 655 and 805 µmol photons $m^{-2} s^{-1}$.

Biomass production in the different conditions is shown in Figure 3.25. During the 7 days of stress media, biomass growth was linear and growth rates could be calculated from the regression. As previously observed when applying full BG11-H, growth rates in 10 days increased with increasing light intensity, with values of 11.4, 13.9 and 15.6 g $m^{-2} d^{-1}$ at 485, 655 and 805 µmol photons $m^{-2} s^{-1}$, respectively. When stress was induced from the culture medium, this correlation was not visible and biomass productivity was stable in the irradiance range here investigated. Indeed, no significant differences were found for each stress factor and all the growth rates were lower than those observed for the controls (Figure 3.26). Thus, final biomass yield after 10 days of cultivation was also highest in biofilms fed with full BG11-H medium, ca. 145 g m^{-2} at both 655 and 805 µmol photons $m^{-2} s^{-1}$ (Figures 3.25 and 3.26).
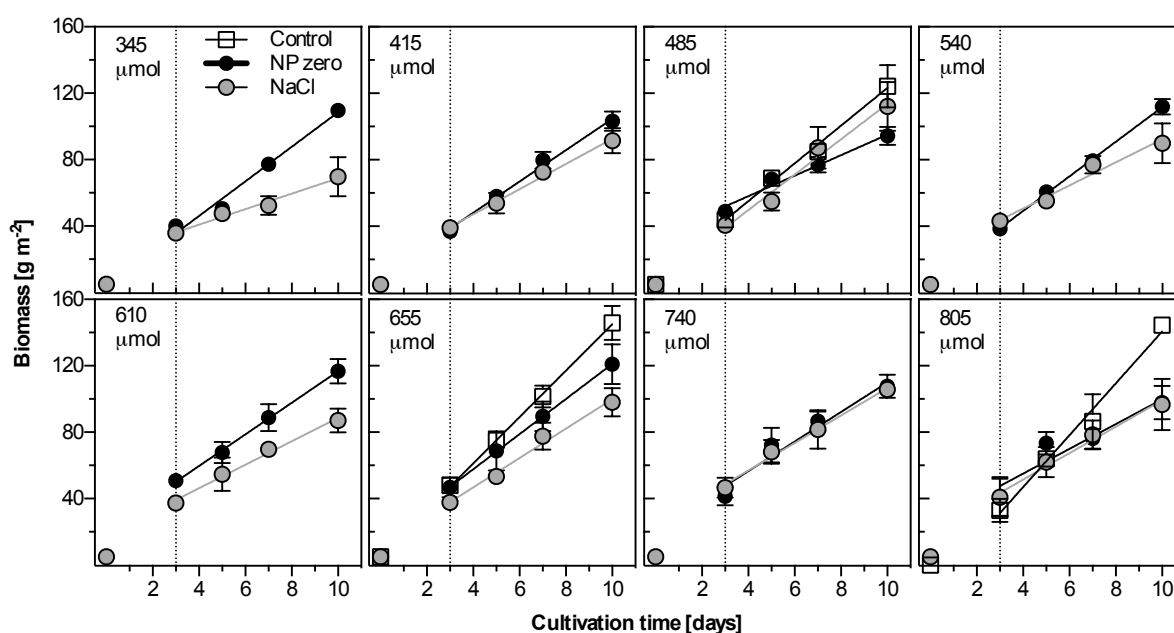
Figure 3.25. Biomass production in 10 days cultivation when applying different stress media at the range of irradiance from 345 to 805 µmol photons $m^{-2} s^{-1}$. Astaxanthin induction was conducted from day 3 to 10 and the onset is indicated by the vertical dashed line. Applied culture media were: NP zero (g m^{-2} ± SD, $n \geq 3$; black circles) and NaCl (g m^{-2} ± SD, $n \geq 3$; grey circles). At light intensities of 485, 655 and 805 µmol photons $m^{-2} s^{-1}$ a control group was included, maintained in full BG11-H for the entire period of 10 days. All groups were aerated with 1% supplementary CO_2.
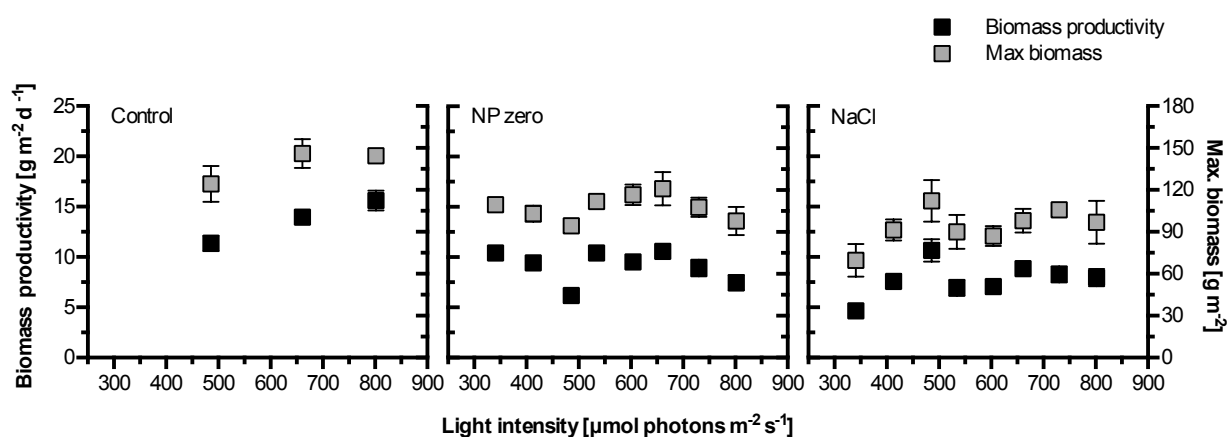
Figure 3.26. Biomass productivities (black squares; g m^{-2} d^{-1} ± SD, $n \geq 3$) and maximum yield (grey squares; g m^{-2} ± SD, $n \geq 3$) at irradiances in the range 345 - 805 µmol photons $m^{-2} s^{-1}$, when applying different stress media – NP zero and NaCl. Productivities were calculated from linear regression of days 3 to 10. At light intensities of 485, 655 and 805 µmol photons $m^{-2} s^{-1}$ a control group was included, maintained in full BG11-H. All groups were aerated with 1% supplementary CO_2.

Kinetics of astaxanthin content in all tested irradiances were comparable to previously observed results at 800 µmol photons $m^{-2} s^{-1}$: an increase was reported in the controls during the first three days, after which values were stable, whereas astaxanthin content continued to increase after the onset of stress in NP zero and NaCl groups (Figure 3.27). Both stress media increased astaxanthin content in the biomass already from day 5, when compared to the control at 655 and 805 µmol photons $m^{-2} s^{-1}$. At 485 µmol photons $m^{-2} s^{-1}$ such increase was only visible at day 10, mainly in the NP zero group. Nutrient deficiency resulted in higher astaxanthin contents than salinity in all light intensities. Nevertheless, in the presence of stress media, final values were all superior to 2% of astaxanthin per dry weight. At day 10, lowest astaxanthin content was 1.6% in biofilms grown at 805 µmol photons $m^{-2} s^{-1}$ with full BG11-H medium, whereas maximum values of 3.6 and 3.5% were observed in NP zero at 655 and 740 µmol photons $m^{-2} s^{-1}$, respectively.
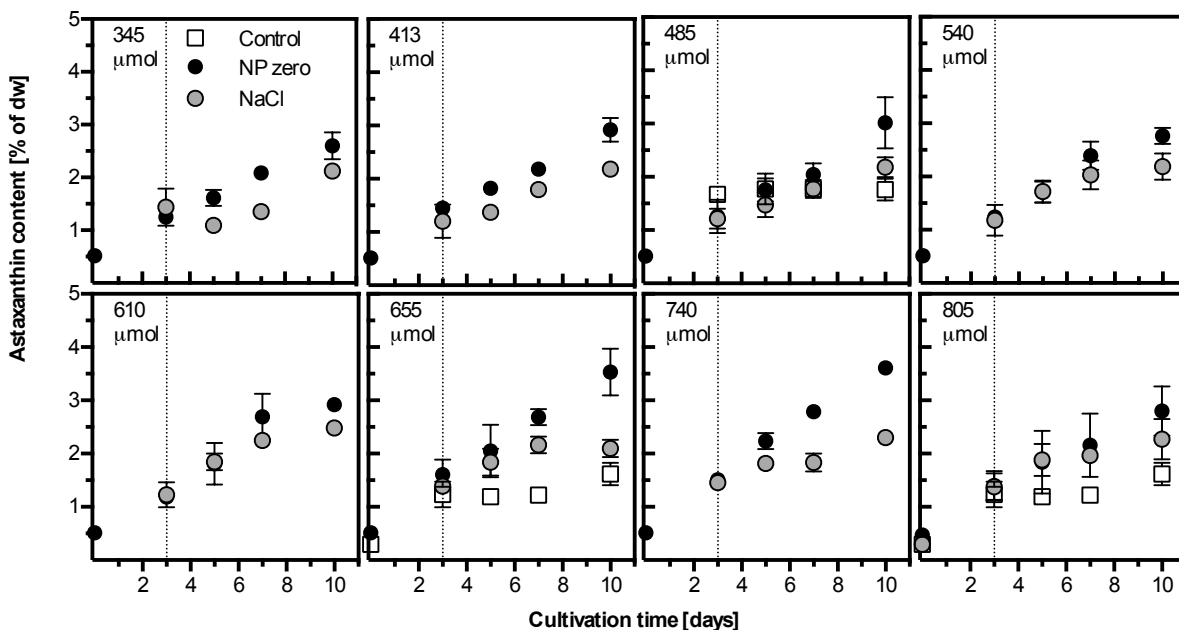
Figure 3.27. Astaxanthin contents in biomass (% of dw, ± SD, $n \geq 3$) of *H. pluvialis* cultivated with different medium at irradiances from 345 to 805 µmol photons $m^{-2} s^{-1}$. Stress media were NP zero (black circles) and NaCl (grey circles), applied from day 3, as indicated by the dotted line. A control group was fed with full BG11-H for the 10 days (white squares) at specific light intensities. Aeration with additional 1% CO2 was supplied to all of the groups.

Very much like biomass, astaxanthin production also followed a linear trend at days 3-10 (Figure 3.28). Due to the increased astaxanthin contents, total astaxanthin was also higher under nutrient starvation at all tested irradiances, when compared to control and salinity. A maximum total astaxanthin of 4.2 g m^{-2} was obtained at day 10 of cultivation with NP zero medium and 655 µmol photons m^{-2} s^{-1} irradiance, whereas minimum final yield was 1.5 g m^{-2} at NaCl and 348 µmol photons m^{-2} s^{-1} conditions (Figures 3.28 and 3.29). Calculated astaxanthin productivities in relation to light intensity are shown in Figure 3.29 and different trends can be observed according to the culture medium applied.

Astaxanthin productivity and final yield in cultivation with full BG11-H and NaCl media show a very similar trend of that observed for biomass (Figure 3.26 and 3.29). The isolated effect of irradiance has already been described, with an increase of astaxanthin production until saturation at light intensities over 600 µmol photons m^{-2} s^{-1} conditions (Figures 3.11 and 3.12). The three control points of this experiment fit these previous results, but due to limited data, it is not possible to describe the trend. In NaCl biofilms, a slight increment of astaxanthin production was observed with increasing irradiance until 485 µmol photons m^{-2} s^{-1}, where the maximum values of 0.29 g m^{-2} d^{-1} for productivity and 2.45 g m^{-2} for final yield were reached. Higher irradiances had no effect on astaxanthin production when cultivation was performed with this medium (Figure 3.29). The most interesting finding, however, was in the NP zero biofilms, in which a peak of astaxanthin production was observed at 655 µmol photons m^{-2} s^{-1}. With an astaxanthin productivity of 0.51 g m^{-2} d^{-1}, this was the most efficient condition for the pigment production among all of the experimental setups here described. Maximum yields and productivities for biomass and astaxanthin for the induction with stress media experiments are synthesized in the Appendix (Table 7.1).
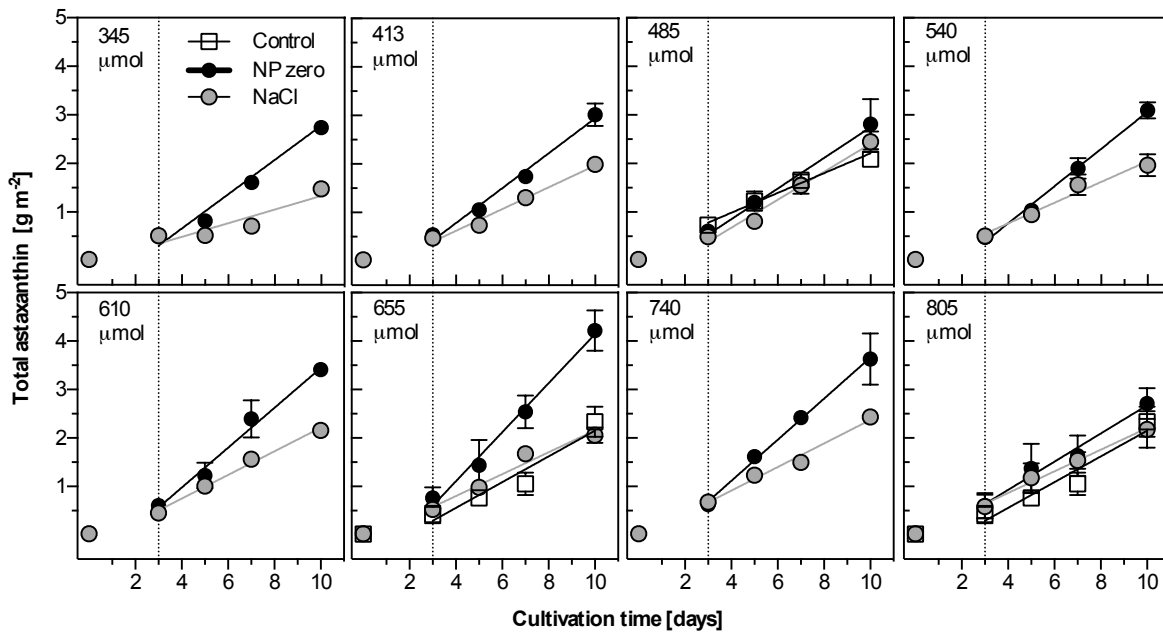
Figure 3.28. Astaxanthin production at light intensities from 345 to 805 µmol photons $m^{-2} s^{-1}$, during 10 days of cultivation (g m^{-2} ± SD, $n \geq 3$). Full BG-11 medium was applied for 3 days, followed by induction with NP zero (black circles) or NaCl medium (grey circles). Vertical lines indicate this transition. At 485, 655 and 805 µmol photons $m^{-2} s^{-1}$ a control group was also included, maintained with full BG11-H culture medium for the whole 10 days of experimental period. Aeration was performed with 1% CO_2.
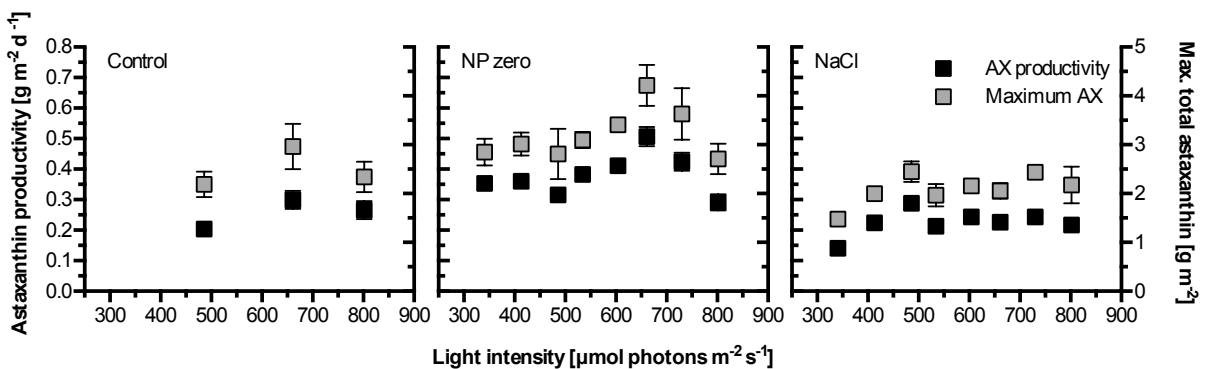
Figure 3.29. Astaxanthin productivity (g $m^{-2} d^{-1}$ ± SD, $n \geq 3$) and maximum yield (g m^{-2} ± SD, $n \geq 3$) according to irradiance, in controls and stress media. Productivities were calculated from red phase of seven days with NP zero or NaCl culture media and full BG11-H for control.

Since it was the best performing condition for astaxanthin production, a longer experiment was conducted with a 3 days of full BG11-H, followed by 20 days of astaxanthin induction with NP zero medium, all at 655 µmol photons $m^{-2} s^{-1}$ light

intensity. The aim was to verify if astaxanthin content continued increasing after the first week of stress, which was not observed. Astaxanthin content saturated after 10 days of cultivation but total astaxanthin production continued to increase due to biomass growth, even after 20 days of nutrient starvation (Figure 3.30). The biofilm cross-sections show very red cell layers, in accordance with the high astaxanthin contents observed, however an inner green zone is still present (Figure 3.31).
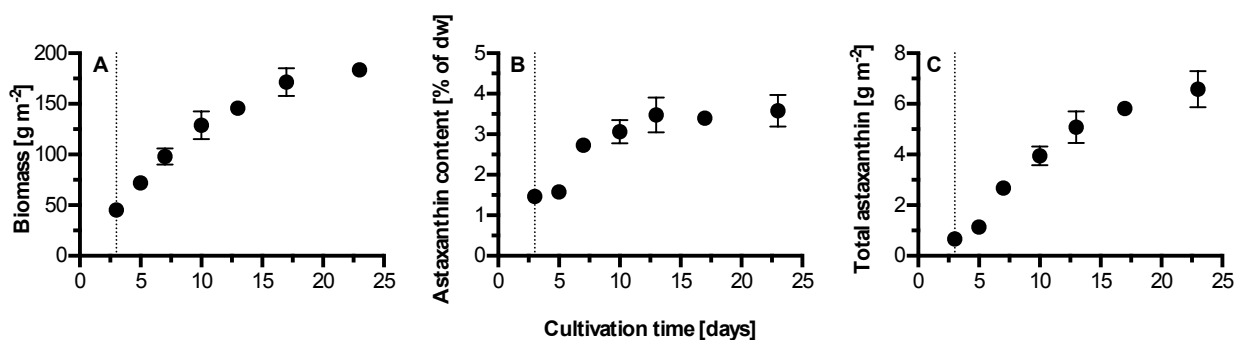
Figure 3.30. Biofilm cultivation of *H. pluvialis* at 650 µmol photons m^{-2} s^{-1} with nutrient starvation from day 3 (dotted line). **A** Biomass production (g m^{-2} ± SD; n *n*≥3); **B** astaxanthin content in the biomass (% of dry weight ± SD; n *n*≥3) and **C** total astaxanthin production per cultivation area (g m^{-2} ± SD; n *n*≥3). Aeration was supplemented with 1% CO_2.
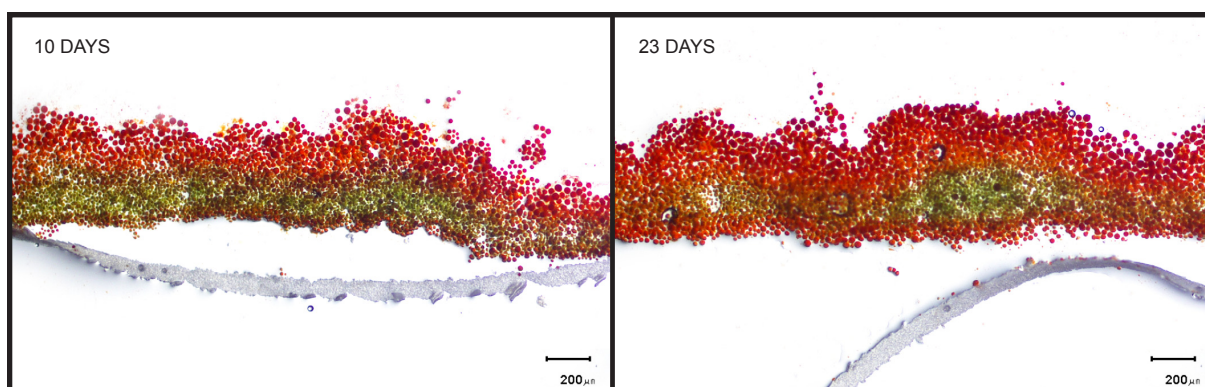
Figure 3.31. Cross-section of biofilm grown at 650 µmol photons m^{-2} s^{-1} for 3 days with full BG11-H medium and 20 days under nutrient depleted conditions. Micrographs show biofilms at days 10 (left) and 23 (right). 1% supplementary CO_2 was supplied in aeration.

3.4. Light and oxygen profiles of the biofilms

For better comprehension of processes in *H. pluvialis* biofilms, depth profiles were acquired with microsensors for both light intensity and dissolved oxygen concentration. Obtained data were then correlated to the biofilm structure and cell distribution. Biofilms were cultivated and measured at low light conditions (LL); pre-cultivated at low light and transferred to high light (LL/HL) and pre-cultivated at high light with full culture medium before cultivation at the same irradiance with N zero medium (HL/Nzero). Measurements were performed at either 20 (LL) or 1,000 µmol photons m^{-2} s^{-1} (LL/HL and HL/Nzero).

Figure 3.32 depicts the different biofilms that were analysed and their cross-sections. Cell distribution as a result of the cultivation conditions were in agreement with previous findings. LL biofilms were pre-cultivated at 130 µmol photons m^{-2} s^{-1} before acclimation at 20 µmol photons m^{-2} s^{-1}, hence the presence of a rather diffuse red akinete layer. Nevertheless, akinetes were smaller and more tightly packed than those observed at HL and the biofilm was mostly green (Figure 3.32B). LL/HL showed the two very distinct zones: an outermost layer of approximately 350 µm composed of large red akinetes and a green inner layer (Figure 3.32C). An additional bright red layer (± 310 µm) was observed at/near the surface of the biofilm, over the dark red cells (± 310 – 700 µm depth) when cultivated under the HL/Nzero condition (Figure 3.32D).

Light profiles exhibited very similar trends in the three investigated biofilms, independent of the irradiance on the surface (Figures 3.33A, C and E). A steep decrease in light intensity was observed in the first 300 µm depth, a reduction of 90% of the total PAR at high light and 80% at low light. This was followed by a more gradual decrease, which was not evident in the biofilms exposed to 20 µmol photons m^{-2} s^{-1} due to the very low irradiances. In fact, at 200 µm depth, light intensity was already <10 µmol photons m^{-2} s^{-1} in LL biofilms, (Figure 3.33A). A similar irradiance was only reached at 480 µm depth, when biofilm surface was exposed to 1,000 µmol photons m^{-2} s^{-1} (Figures 3.33 C and E). Red and green light follow the same trend as

total PAR, whereas blue light is very low already at the surface, being the first to be fully absorbed inside the biofilm.
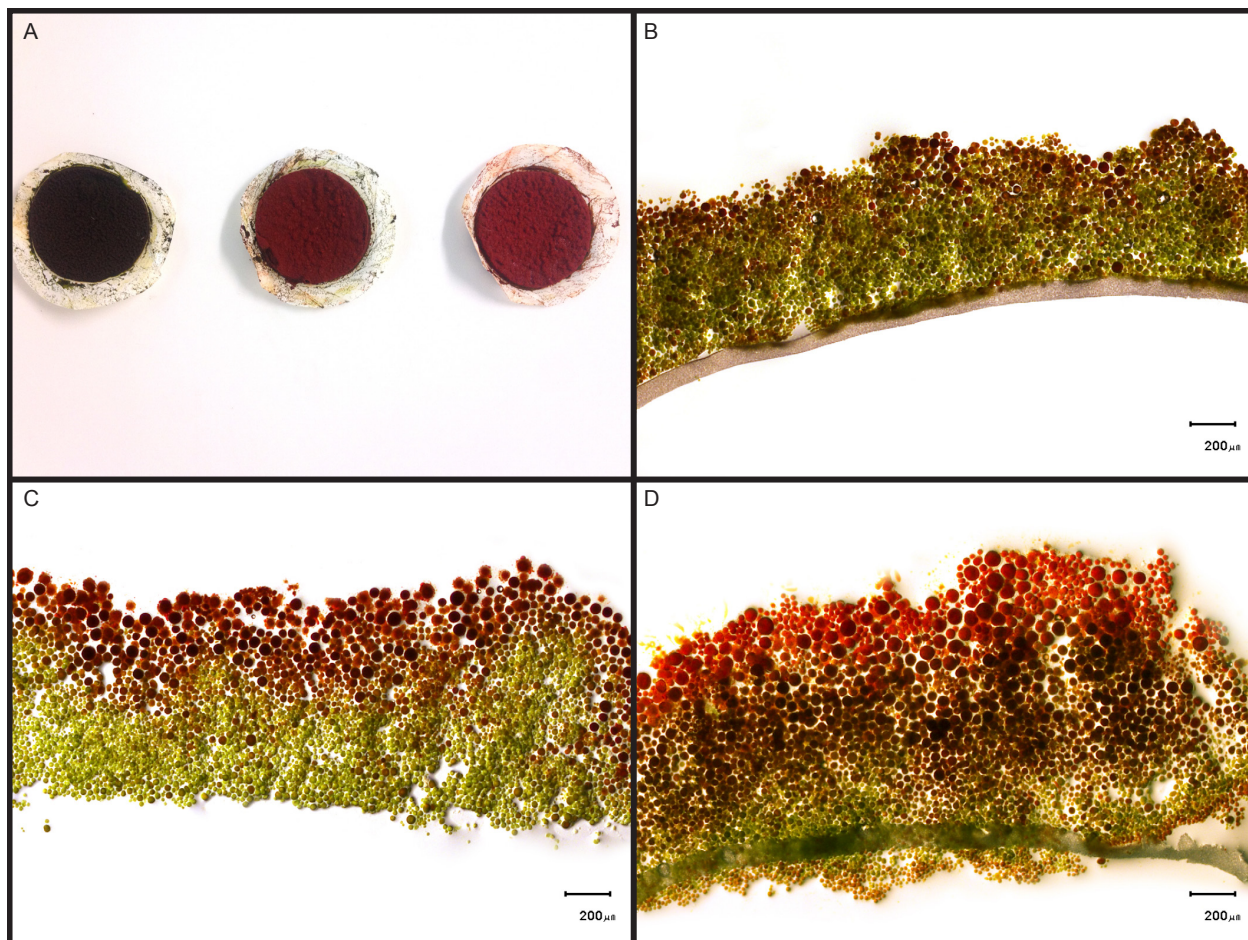
Figure 3.32. Biofilms used in microsensor measurement. **A** Polycarbonate membranes with biofilm and **B-D** cross- sections of biofilms cultivated and measured at low light - LL (B), pre-cultivated at low light, then acclimated and measured at high light - LL/HL and (C) cultivated at high light for the entire period, but acclimated and measured with N zero culture medium - HL/Nzero (D). Low and high light for measurements were 20 and 1,000 µmol photons m^{-2} s^{-1}, respectively.

The difference in light intensities resulted in a big disparity in the [DO] in biofilms (Figure 3.33 B, D and F). In biofilms illuminated with 20 µmol photons m^{-2} s^{-1}, [DO] reduced to a value below that of saturated culture medium (0.274 mM), indicating a higher consumption than production rate under these conditions (Figure 3.33B). On the other hand, when data was acquired from biofilm exposed to 1,000 µmol photons m^{-2} s^{-1}, [DO] increased in the outermost cell layers, reaching a peak of around 0.9 mM and then decreased in deeper layers. Minimum values at 1,000 µm depth were similar to those observed in O$_2$ saturated BG11-H. Coupling high light and N

deficiency resulted in a larger peak area of [DO], but with the same maximum value (0.9 mM). Area under curve analysis confirmed an increase of 11% in the [DO] at HL/Nzero biofilms (Figure 3.33F), when compared to LL/HL (Figure 3.33D).
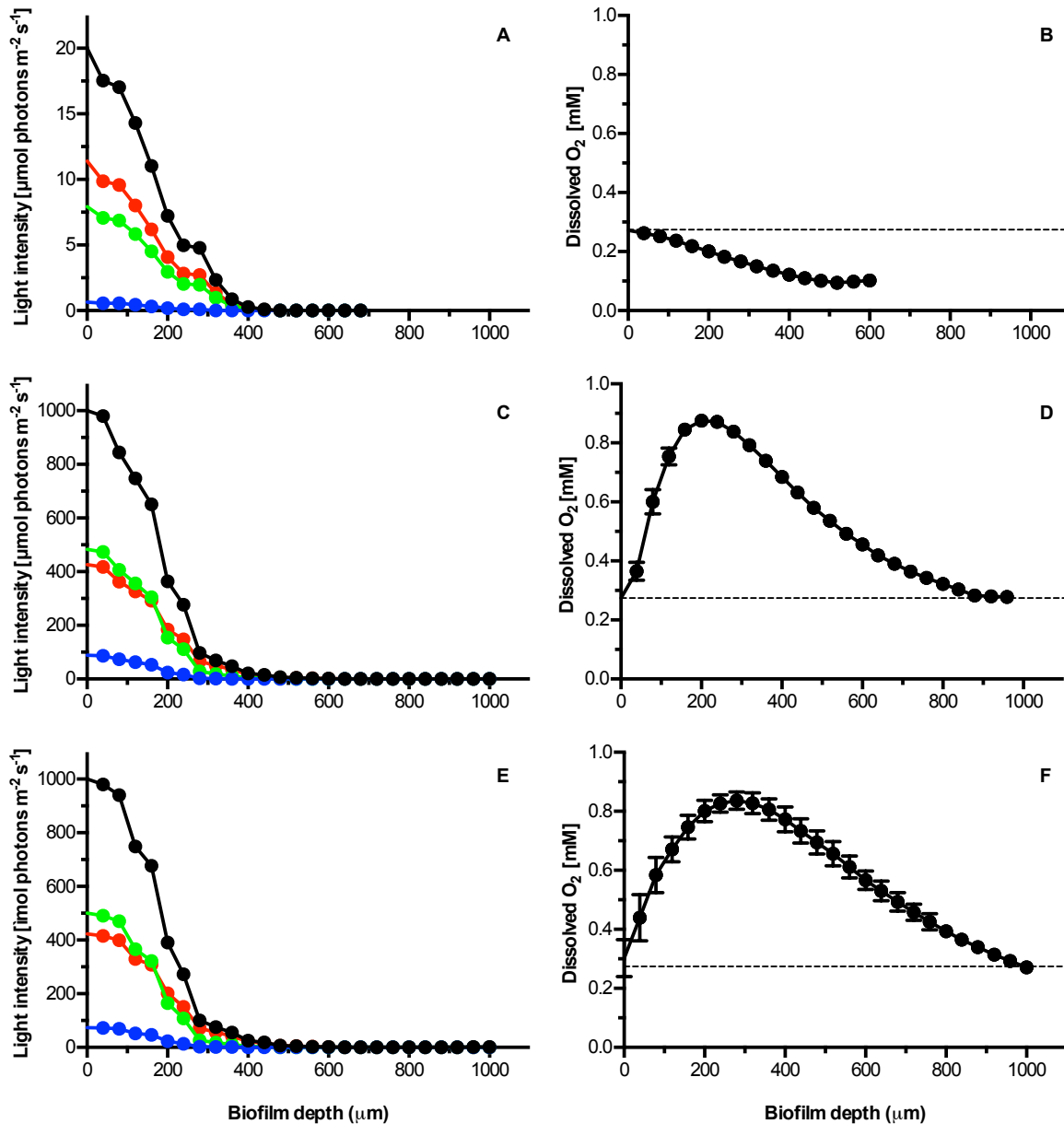
Figure 3.33. Biofilm depth profiles of light intensity (µmol photons m^{-2} s^{-1}; A, C, E) and dissolved O$_2$ concentration (mM; B, D, F). In the first row (A and B) are shown the results for LL group, in which measurements were performed at a surface irradiance of 20 µmol photons m^{-2} s^{-1}. LL/HL data are exhibited in the second row (C and D) and HL/Nzero, in the third (E and F). For both groups, measurements were taken under a light intensity of 1,000 µmol photons m^{-2} s^{-1}, but for HL/Nzero, nitrogen depleted medium was applied. Horizontal dashed line in the row on the right indicates the oxygen concentration in culture medium saturated with compressed air.

Discussion IV

4.1. Screening of *H. pluvialis* strains on a PSBR

Strain selection is a major step for the commercial cultivation of microalgae. Identifying more robust strains and traits such as enhanced biomass and carotenoid productivities could significantly reduce costs of large scale production of *H. pluvialis* and natural astaxanthin. There are many *H. pluvialis* strains available in culture collections worldwide, but most of the research is concentrated in only a few of these. In this work, screening of 26 *H. pluvialis* strains was performed, the first one in immobilized conditions.

All the tested strains were capable of biofilm growth on BG11-H culture medium and of astaxanthin accumulation under nitrogen starvation. Final biomass and astaxanthin values were in the range of 73 to 112 g m^{-2} and 0.53 to 1.6 g m^{-2}, respectively. The immobilized cultivation of *H. pluvialis* was first approached by Nowack et al (2005), using a 96-well Twin-Layer system for the successful growth and maintenance of a large number of different microalgal species. No additional study was published at the time of the beginning of this work, but with an increasing interest in PSBRs, *H. pluvialis* has been studied in more detail in recent years (Wan et al., 2014a; Yin et al., 2015; Zhang et al., 2016, 2014). Zhang et al (2014) used strain SAG 34-1b, that was included in this screening, and reported a biomass productivity of around 4 g m^{-2} day^{-1} for the strain at 100 μmol photons m^{-2} s^{-1} continuous light when inoculum density was similar to the one used in this work. A comparable result was observed here when growing on BG11-H: 5 g m^{-2} day^{-1} at 203 μmol photons m^{-2} s^{-1} with 14/10 light/dark cycle.

The 26 strains also underwent immobilized growth on secondary wastewater, indicating robustness. While one strain had a significantly lower performance, the others exhibited similar biomass production. Furthermore, nine of these strains showed similar or higher biomass productivities in wastewater than BG11-H culture medium. This might be explained by the presence of organic compounds in the wastewater, since *H. pluvialis* is capable of mixotrophic growth (Droop, 1955; Kobayashi et al., 1991). *H. pluvialis* growth on wastewater and nutrient uptake have

already been reported in suspension cultures, even for the NIES-144 strain that was also used here (Kang et al., 2006a; Wu et al., 2013),

Coupling *H. pluvialis* cultivation to wastewater treatment would represent an attractive option for the reduction of production costs and sewage treatment. However, there are a few drawbacks such as legal barriers for direct or indirect human consumption (by means of animal feed), as well as public acceptance resistance. Wastewater treatment and astaxanthin production also have completely different market sizes and values (Sprujit, 2015). If the focus is then on the wastewater treatment, regardless of astaxanthin production, other green algae are faster growing than *H. pluvialis*, thus with higher potential for nutrient recovery. For these reasons, research was followed up with BG11-H culture medium and its variations.

Taken together, the screening results clearly support the feasibility of immobilized cultivation of *H. pluvialis*. Furthermore, with the exception of ACOI-276 on wastewater, strains performances were not extremely different, especially when considering biomass production. Variations among most of the strains were usually lower than 50%. However, when considering extreme values, differences up to two-fold were observed for biomass and three-fold for astaxanthin production. Such variations are in accordance with that reported for different strains in previous works (Gao et al., 2014; Noroozi et al., 2012; Zhang et al., 2009). Genetic variability was also observed among *H. pluvialis* strains (Allewaert et al., 2015).

Since different strains can have different optimal conditions both for biomass and astaxanthin production, further screenings with other settings could give a more precise outlook for convenient strains and protocols for scale-up purposes. This can easily be done on the Twin-Layer PSBR, simplifying the screening process. Indeed, the successful use of a Twin-Layer as a screening platform had already been reported by Nowack et al (2005), on a 96-well plate system. In the present work, 26 different strains were immobilized in different polycarbonate membranes and cultivated in the same PBR without cross-contamination showing that the bench scale setup is also an adequate system for such a study.

4.2. The effect of light and CO$_2$ on immobilized cultivation of *H. pluvialis*

The use of natural sunlight is desirable for obvious economic and environmental reasons but it can reach up to 2,000 µmol photons m^{-2} s^{-1}, considered prohibitive for *H. pluvialis* biomass growth. This problem is commonly avoided by two-step cultivation, in which artificial light below 150 µmol photons m^{-2} s^{-1} is used for vegetative growth during the green phase and irradiances beyond that are applied for astaxanthin induction, frequently in association with other stress factors (Aflalo et al., 2007; Fábregas et al., 2003; Li et al., 2010; Suh et al., 2006; Yoo et al., 2012). However, even when restricted to the stress phase, high light can lead to photoinhibition and cell death (Li et al., 2010; Steinbrenner and Linden, 2003; Wang et al., 2013a; Zhang et al., 2009). In suspension cultures, damage can be reduced by using high density cultures due to the self-shading effect. Moreover, light dilution can be achieved by appropriate PBR design (Liu et al., 2013; Naumann et al., 2013; Posten, 2009).

Immobilized cultivation of *H. pluvialis* on the Twin-Layer allowed both biomass and astaxanthin production to increase together as a function of the light intensity. Maximum productivities reported for cultivation without culture medium stressors were 19.4 and 0.393 g m^{-2} d^{-1} at 1,015 and 789 µmol photons m^{-2} s^{-1}. These values are in the order of three and five-fold higher than previously reported for *H. pluvialis* in immobilized conditions when supplied full medium, under the maximum irradiance of 150 µmol photons m^{-2} s^{-1} (Zhang et al., 2014). Biomass productivities were close to those observed in *Halochlorella rubescens*, a much more robust and fast growing green alga, under similar conditions (Schultze et al., 2015). Moreover, final standing crop reached the impressive amount of 213 g dry matter m^{-2} (adequate to about 1 kg of fresh weight) in 16 days of cultivation.

Biomass productivity increased until 1,015 µmol photons m^{-2} s^{-1} with no evidence of photoinhibition. Saturation of growth was indeed observed at longer time periods mainly over 500 µmol photons m^{-2} s^{-1} and when supplementary CO$_2$ was added. This was probably associated to the thickness of the biofilms. Hence, thicker biofilms

exhibit larger dark zones, which result in a decrease of net photosynthesis, compromising biomass production (Li et al., 2015a). Nutrient limitation should not play a role, since it is not expected in the biofilm grown under these condition (Li et al., 2015c).

Successful cultivation at such high irradiances can be explained by the biofilm structure and the appropriate combination of environmental factors. Simultaneous growth and astaxanthin production at high light intensities in a one-step process is possible due to the biofilm organization, in which cells are immobilized and light is received solely from one direction. Outermost cell layers are exposed to full irradiance and transform into astaxanthin-rich akinetes that protect the inner layers, composed of mostly green cells. The pigment gradient formed inside the biofilm enables further light penetration (Li et al., 2015a) while protecting inner cells from harmful irradiances and wavelengths. Astaxanthin accumulation is then limited to the illuminated area of the biofilm, but biomass growth could possibly occur at two stages: cell division inside the biofilm and increased volume in akinete formation and maturation. The biofilm structure is fully discussed in Section 4.5.

This organization of red and green cells was used by Suh et al (2006) to develop a suspension PBR. In their system, green cells were grown in an inner cell core, with full culture medium and shielded by red akinetes, cultivated in an outer separate compartment with nitrogen limitation and exposed to high irradiances. Furthermore, higher resistance to light stress in *H. pluvialis* biofilm can result from the transformation into palmellas. Almost 100% of the cells shed the flagella during immobilization and enhanced acclimation to high light was associated to this stage (Wang et al., 2014).

After 16 days of cultivation at high light irradiances, the biofilm thickness reached 900 µm, which means that more than 50% of the biomass did not receive light and thus was not accumulating astaxanthin, as described in Section 4.5. Nevertheless, a total astaxanthin content up to 2.5% was obtained, which would already be appropriate for biomass commercialization (Lorenz and Cysewski, 2000). Such yields could possibly be increased when biofilms are exposed to natural sunlight, since blue and UV light are more efficient in inducing astaxanthin production (Katsuda et al., 2004;

Kobayashi et al., 1992a; Lababpour et al., 2004) and are low or absent in the spectrum of high pressure sodium lamps used as light source in the this work.

In respect to environmental conditions, irradiance, temperature, CO_2 and nutrient availability are inter-dependent factors for biomass production in both suspension and biofilm cultivation of microalgae (Schnurr and Allen, 2015). This is frequently ignored while evaluating productivities and the appropriate combination was essential for the high growth rates reported here. Temperatures over 30 °C can act as a stress factor in *H. pluvialis* cultures reducing cell division but maintaining growth through increase in cell volume and inducing astaxanthin production at light intensities below 130 µmol photons m^{-2} s^{-1} (Fan and Vonshak, 1995; Giannelli et al., 2015; Tjahjono et al., 1994). At 250 µmol photons m^{-2} s^{-1} without CO_2 supplementation, 28 °C was the optimal temperature for both growth and astaxanthin production, while 33 °C led to culture death (Wan et al., 2014b). High temperatures have shown to support algal growth at high irradiance (Dauta et al., 1990) and Wan et al reported higher temperature tolerance for *H. pluvialis* cultivation in biofilm, when compared to suspension (Wan et al., 2014a). In the experimental conditions reported here, higher irradiances were directly related to higher temperatures, reaching a maximum of 28.6 °C and the effect of light and temperature on growth and astaxanthin productivity cannot be distinguished. Nonetheless, in large-scale outdoor conditions, the parameters light and temperature are also closely related.

CO_2 supplementation can be easily controlled separately, but its effect is also dependent on light intensity. While it had little or no impact on biomass production when light was lower than 200 µmol photons m^{-2} s^{-1}, it significantly boosted growth at high irradiances, indicating that carbon was limiting in such conditions. These findings are in agreement with microsensor measurements in *Halochlorella rubescens* biofilms, where higher concentrations of CO_2 led to an increase in photosynthetic rate at high light intensities, while no difference was observed at lower irradiances. At 1,000 µmol photons m^{-2} s^{-1}, photosynthesis still increased with CO_2 supplementation up to 5% (Li et al., 2015a). These profiles were not performed in *H. pluvialis* biofilms, but 1% CO_2 was enough to sustain the high biomass and astaxanthin productivities at 1,000 µmol photons m^{-2} s^{-1} and increasing

supplementation did not improve yields. The same CO_2 range was identified as appropriate for immobilized cultivation of *H. pluvialis* under nitrogen limitation with irradiance of 100 µmol photons m^{-2} s^{-1} (Yin et al., 2015). Further optimization of the CO_2 supply should be focused on applying it in the culture medium, since at large scale, the Twin-Layer is essentially an open system that can be placed inside a greenhouse or simply under a transparent protection. In any case, CO_2 supplementation in the air is not feasible.

4.3. One vs. two-step cultivation with high light

Despite the higher productivities of a two-step approach when compared to the few one-step strategies reported in the literature (Aflalo et al., 2007), there are major drawbacks associated to this discontinuous cultivation. When considering astaxanthin as the target product, around 50% of the cultivation period, i.e. the growth phase, is non-productive (Aflalo et al., 2007; Suh et al., 2006). This is commonly disguised by overestimations of real productivities when values are reported separately for each phase (Aflalo et al., 2007). Another drawback is the higher technical effort required for the setup and maintenance of two separate and different systems, enhanced by the use of conventional suspension cultivation, which dominate *H. pluvialis* research and market.

In this context, the efficiency of the growth phase is essential, but is currently hindered by the use of low light. In order to simplify astaxanthin production from *H. pluvialis*, both growth and astaxanthin production should be conducted in the same cultivation system and using sunlight. Attempts have been made in this sense, and vegetative growth was reported at light intensities over 1,000 µmol photons m^{-2} s^{-1}, showing increase in biomass, however, astaxanthin was not produced unless nutrient stress was applied. Once nitrogen was depleted, astaxanthin accumulation was triggered and its accumulation rate was directly related to the calculated average irradiance per cell – that depends on both incident irradiance in the PBR and cell density (Del Río et al., 2008; García-Malea et al., 2009). This process can be

completely conducted in one PBR placed in natural sunlight. Indeed, high light intensities had not yet been shown to support alone simultaneous biomass growth and astaxanthin production.

In the present work, high biomass and astaxanthin production was obtained when *H. pluvialis* was cultivated directly at high irradiances, in a one-step process. Further, it was shown to be more effective than a two-step approach, consisting of pre-cultivation at low light (90 µmol photons m^{-2} s^{-1} – growth phase) and a stress phase in which light was the only stressor. Similar biomass and astaxanthin productivities were registered for 8 days of cultivation at 1,000 µmol photons m^{-2} s^{-1}, regardless of the beginning of exposure. However, the one-step process implicates on earlier exposure, thereby maximum yields were obtained in half of the cultivation period. Hence, the insertion of a low light green phase hindered the high productivities and is needless for a PSBR.

4.4. Astaxanthin induction with culture medium stress factors

Having shown that high irradiances can support biomass and astaxanthin productivities on the Twin-Layer, the additional effect of stress factors in the culture medium was investigated. Nutrient depletion and salinity can be easily manipulated in a Twin-Layer system, enabling a technically simplified two-step cultivation with none or very low additional costs. Indeed, the term "two-step" would only refer to the separation of maximum growth and astaxanthin production over time, with no implication whatsoever on modifying technical setups. Furthermore, nutrient depletion and salinity application in large scale cultures can also reduce risks of contamination, while creating extreme conditions. This is the case of open air cultivation of *Spirulina* in high pH (Vonshak and Richmond, 1988) and *Dunaliella salina* in very high salinity (Borowitzka and Borowitzka, 1990) for commercial purpose.

Different stress conditions have been thoroughly compared in *H. pluvialis* suspension cultures (Borowitzka et al., 1991; Boussiba and Vonshak, 1991; Droop, 1954;

Imamoglu et al., 2009). In immobilized cultivation, however, only nitrogen concentration and high light were approached for astaxanthin induction (Wan et al., 2014a; Zhang et al., 2014). In this work, the different stress factors were compared for the first time in *H. pluvialis* biofilms and at high irradiances. Hence, in this proposed cultivation strategy, the so-called growth phase refers to the initial cultivation period with control culture medium, but it is also astaxanthin productive due to the employment of high irradiances.

While high light increased astaxanthin and biomass production simultaneously, this was not the case when culture medium stress factors were added. At 800 µmol photons m^{-2} s^{-1}, biomass production was compromised in all of the stress conditions investigated, except P zero. On the other hand, astaxanthin content in biomass increased, but maximum values were only significantly higher than the control when N zero and N zero + NaCl culture medium was applied. As a result, similar final astaxanthin yields were observed in all groups.

Nitrogen starvation is the most commonly used stress factor for astaxanthin induction, along with high light. Here, N limitation was investigated alone and combined with phosphorous depletion or salinity, at high irradiances. Biomass continued to increase in N stressed cultures with yields similar to the control for at least four days, however reducing at longer cultivation periods. Increase in dry weight was also observed in all strains during nitrogen deprivation in the screening process. It is known that in the absence of nitrogen, protein synthesis in microalgae is compromised and by providing enough light, a shift to carbon metabolism is generally observed, resulting in production of carbohydrates, lipids and carotenoids (Boussiba and Vonshak, 1991; Lamers et al., 2012) Biomass growth is therefore more associated to an increase in cell volume during akinete formation and maturation rather than cell division (Scibilia et al., 2015; Wang et al., 2013b). Dry weight increase was shown here for up to 20 days under NP zero conditions. How long biomass growth can be sustained in the absence of nitrogen is still to be determined with further studies and kinetics, including cell count and cell size measurement.

The synergic effect of nitrogen depletion and light intensity on astaxanthin production observed here was already reported for suspension (Aflalo et al., 2007; Boussiba and

Vonshak, 1991; Fábregas et al., 1998; Scibilia et al., 2015) and immobilized cultures (Wan et al., 2014a). When comparing the different stress factors at 800 µmol photons m^{-2} s^{-1}, N starvation conditions resulted in the highest astaxanthin contents in the biofilm (almost 3% of dry weight) and productivity of 0.34 g m^{-2} d^{-1}. Astaxanthin accumulation was faster in nitrogen and salt stressed groups. Salinity also reduced significantly biomass growth and, according to by biofilm appearance, it seems to have disrupted cell division. This finding is in agreement with other authors and arrest in cell division was also observed at 0.8% NaCl (Boussiba and Vonshak, 1991). Meanwhile, Harker et al. (1996) reported that concentrations of 0.2 and 0.4% NaCl in culture medium inhibited cell division, while 0.6% led to cell death in suspension cultures. In any case, the remaining cells accumulated high levels of astaxanthin. Combination of N zero and NaCl stress evaluated here showed very similar results as when both conditions were applied separately. Cordero et al. (1996) reported a similar astaxanthin content in N zero + NaCl conditions at 140 µmol photons m^{-2} s^{-1} as observed here (3% of dry weight), but no data was shown regarding biomass and total astaxanthin production.

Diverging from the other stress factors, cultivation in phosphorus-depleted medium did not significantly impact biomass growth, when compared to the high light alone. Continued growth in the absence of phosphorus is enabled by the luxury uptake of the nutrient, known to occur in microalgae. It consists of taking up more P than needed for cell composition (usually around 1%) and storing it mostly as polyphosphate granules for internal reserve, used when the nutrient is limiting in the environment (Fogg, 1973; Ketchum, 1939; Mackereth, 1953). The effects of stress are then delayed, as observed in astaxanthin accumulation and chlorophyll degradation. Biomass growth was also observed for at least 15 days in suspension cultures under P depletion but different from what was shown here, it resulted in higher astaxanthin yields than N starvation (Harker et al., 1996). Considering that P zero did not significantly increase astaxanthin production, it is not surprising that the combination of N and P depletion did not have an additive outcome.

The effect of stress and astaxanthin accumulation on photosynthesis is not completely elucidated. A reduction of at least 50% in chlorophyll content in biomass

was observed in the biofilms exposed to all additional stress factors, when compared to the control. Nitrogen deprived cultures exhibited the most dramatic chlorophyll loss, since it is required for chlorophyll synthesis. This corresponds well to the bright red colour of the akinetes observed in biofilms grown with N zero medium. Chlorophyll reduction has also been associated to all of these stressors in suspension cultures of *H. pluvialis* (Boussiba and Vonshak, 1991; Boussiba et al., 1999; Fábregas et al., 1998; Han et al., 2012; Kim et al., 2011). Boussiba and Vonshak (1991) observed highest chlorophyll content of 1% at low light (85 µmol photons $m^{-2} s^{-1}$) and full medium while lowest content of 0.4% occurred at high light (170 µmol photons $m^{-2} s^{-1}$) and N limitation. Although irradiances are not comparable, similar values were obtained here at 800 µmol photons $m^{-2} s^{-1}$, i.e. 1.28% at full medium and 0.4% at N zero conditions. In spite of the chlorophyll loss, only a moderate decline in photosynthetic activity is usually observed in stressed *H. pluvialis* cultures (Torzillo et al., 2003; Wang et al., 2003; Zlotinik et al., 1993). Chen et al. (2012) reported that photosynthesis / respiration rates are reduced in the process of akinete maturation, whereas Rubisco activity is increased, explaining the continuous biomass accumulation. Furthermore, exposure of vegetative cells to high irradiance and nitrogen deprivation led to a decrease in chlorophyll biosynthesis and light harvesting complex related genes and activation of respiration-, lipid metabolism- and stress-related genes (Kim et al., 2011).

Molecular studies also indicate that stress factors can regulate the expression of different genes involved in astaxanthin production, at different time periods, which could result in additive effects in *H. pluvialis*, when applied in combination (Li et al., 2008; Vidhyavathi et al., 2008; Wang et al., 2004). In spite of the above mentioned differences, maximum astaxanthin accumulation per dry matter was not significantly different for the stress factors investigated. It is, however, important to consider that all the effects here described are already a combination of high light with a culture medium stressor. Furthermore, the quantification of biomass and pigments in the entire biofilm might have masked possible differences in the different cell layers.

When the same culture medium stressors are applied at irradiances $\leq$ 200 µmol photons $m^{-2} s^{-1}$, astaxanthin accumulation in biomass was slower (non published

observations), pointing to the major effect of high irradiances, in agreement with other authors (Choi et al., 2002; Harker et al., 1995). In fact, the same strain used in all the optimization experiments (CCAC 0125) accumulated only 1.5% of astaxanthin per dry weight at 200 µmol photons m^{-2} s^{-1} and under nitrogen starvation in the screening experiment. Furthermore, low biomass productivities that result from low light lead to much lower total astaxanthin yields.

A range of irradiances from 300 to 800 µmol photons m^{-2} s^{-1} was evaluated with nutrient depletion and salinity stressors. High astaxanthin productivities were supported at this light range. However, an optimum light intensity for astaxanthin production in NP zero medium was found to be around 655 µmol photons m^{-2} s^{-1}, where the maximum astaxanthin production on the Twin-Layer was reported: 0.507 g m^{-2} d^{-1}, with a content of 3.5% in biomass. An appropriate explanation for this has yet to be investigated with more detailed pigments and photosynthesis profiles inside the biofilm layers. Nonetheless, the effect of different stressors seems to vary according to the light intensity. A comparable phenomenon was reported by Imamoglu et al (2009): Astaxanthin production in distilled water, N zero and NP zero increased from 445 to 545 µmol photons m^{-2} s^{-1}, while P zero decreased. Values where anyhow lower than observed here, with a maximum of 3% astaxanthin content in the biomass.

4.5. Biofilm structure and profile

Microsensor and cryosectioning techniques were of great importance for the comprehension of biofilm structure and metabolism and thus, for better understanding of the results obtained. Analysis with microsensors has been used in naturally occurring biofilms for over 30 years (Revsbech and Jorgensen, 1983) but was only recently employed in an artificial unialgal biofilm by Li et al. (2015a). Meanwhile, cryosectioning was first described in 1905 and since then has become a widely used technique for examination of fresh tissues in biomedical sciences (Wilson, 1905). It has more recently been applied for analysis of bacterial biofilms,

also for fluorescence labelling and *in situ* hybridization (Wilmes et al., 2009; Yu et al., 1994). This is the first time it is used for microalgal biofilm on a PSBR.

Forward light scattering and formation of a pigment gradient increase light penetration into microalgal biofilms (Li et al., 2015a; Pringault and Garcia-Pichel, 2000). Light profile in *H. pluvialis* followed a very similar trend to that observed in *Halochlorella rubescens* biofilm, however with a slightly deeper penetration, up to 400 μm (Li et al., 2015a). This is probably a result of the enhanced pigment gradient observed in the *H. pluvialis* biofilm. Furthermore, the presence of large akinetes, which were are less tightly packed together, can also play a role. The illuminated area corresponded approximately to the red akinete layer, observed not only in the biofilms from which data were acquired, but in all biofilms grown at high light from different experiments.

Nitrogen depletion and salinity have negative effects on biomass production, resulting in thinner and almost completely red biofilms in the time periods analysed. The early onset of stress was of great importance for obtaining such red biomass. Later application of stress factors at high irradiances would not allow full penetration of light due to the thickness of the pre-grown biofilm and the inner cell layer would remain green. This was observed in the biofilm HL/Nzero, also used in microsensor measurements. It exhibited three distinct layers: an outermost bright red layer of ca. 300 μm; an intermediate composed of dark red akinetes (ca. 400 μm) and the inner green cells. Astaxanthin present in the middle zone was probably preserved from accumulation when it was exposed to light, but the dark production of astaxanthin under N zero conditions while unlikely, cannot be completely discarded at this point. Furthermore, a very thin red layer composed of small red cells was observed in the bottom (adjacent to polycarbonate membrane) of all biofilms that were stressed with nutrient deficiency and/or salinity. It results from very low light (< 10 μmol photons m^{-2} s^{-1}) penetration from the back of the glass fibre and polycarbonate membrane, because the posterior side of the Twin-Layer PBRs were not covered. Irradiances were too low to provoke independent astaxanthin accumulation but it was enough to enable production in otherwise stressed cells. This is in agreement with Boussiba

and Vonshak (1991), who observed that *H. pluvialis* only accumulated astaxanthin at low light when applying phosphorus or salt stress.

These results strongly support light dependency of astaxanthin production in the biofilms grown on inorganic culture medium. However, it is known that *H. pluvialis* is capable of heterotrophic growth and astaxanthin production when an organic carbon source is available (Droop, 1955; Kobayashi et al., 1992b). On the Twin-Layer, a very preliminary attempt of acetate supplementation for thick pre-grown biofilms did not significantly increase short-term astaxanthin production and it boosted bacterial growth in the biofilm (unpublished observations). Furthermore, acetate addition is not attractive for commercial cultivation as it increases costs and contamination risks.

Light penetration determines the photosynthetically active zone in the biofilm. Although photosynthetic performance was not analysed here, the acquired dissolved oxygen profiles can help to enlighten status of the biofilm. At high irradiance (1,000 μmol photons m^{-2} s^{-1}), [DO] increased while penetrating in the biofilm, reaching maximal values of 0.9 mM at ca. 200 μm depth, followed by a reduction while entering the dark zone. The same trend was observed in a *Halochlorella* biofilm but with a 2-3 fold higher peak value (Li et al., 2015a). This can be a result of different O_2 production/consumption ratio or just an effect of higher diffusion rates, related to higher porosity due to the presence or large akinetes.

Nitrogen deprivation led to an increase of 11% in [DO] peak area. Scibilia et al. (2015) suggest that the combined exposure to high light and nitrogen starvation can induce a more rapid acclimation of photosynthetic apparatus to stress. A reduction of functional PSII antenna size and increase in astaxanthin production would therefore, improve the resistance of cells to photo-oxidation. However, here cells were exposed to high light long before nitrogen depletion. If this is the case or if the increase in [DO] is only associated to biofilm structure (thicker akinete layer), is still to be explained. Photosynthesis microsensor measurements and pigment analysis for each cell layer would help to elucidate this issue. Regardless of these slight differences associated with nitrogen starvation, the oxygen profiles acquired at biofilms exposed to 1,000 μmol photons m^{-2} s^{-1}, showed a clear surplus in the overall production/consumption balance, suggesting that akinetes were photosynthetically active under these culture

conditions, since light did not seem to reach the green cells. Moreover, high dissolved O_2 concentrations can induce astaxanthin accumulation (Lee and Ding, 1995; Li et al., 2008) and could therefore, play an important role in the biofilm.

In an opposite scenario, 20 μmol photons m^{-2} s^{-1} irradiance was not enough to maintain the positive oxygen balance and its concentration decreased while penetrating the biofilm. In this scenario, biomass growth should be restricted to the first 50 μm, since [DO] is similar to that of saturated medium, and the interior of the biofilm should be losing biomass as a result of respiration > photosynthesis. It is important to consider that the biofilm used in the microsensor measurements was initially grown at 130 μmol photons m^{-2} s^{-1} and these results reflect a thick biofilm exposed to 20 μmol photons m^{-2} s^{-1}. For this situation, there is no kinetics available to evaluate biomass loss in long cultivation periods. However, in another experiment where cultivation was performed only at 20 μmol photons m^{-2} s^{-1}, linear growth was here reported for 31 days without CO_2 supplementation and for 16 days with 5% CO_2.

A detailed analysis of cell types and pigment composition of the above defined biofilm layers will allow better correlations and more conclusive findings. This was not performed here due to the irregular surface growth of strain the CCAC 0125. Hence, differences in thickness of almost 1 mm were observed in the same biofilm. Since light plays a major role in the structure, such variations reflected inside the biofilm, precluding the appropriate separation of cell layers by sectioning parallel to the surface. Therefore, pigment quantification was carried out for the entire biomass, representing an average that can mask important differences seen in the cryosections.

Furthermore, astaxanthin quantification was performed by spectrophotometry. It is a cheap and simple method that is widely employed in research, however it can overestimate real astaxanthin values, due to overlapping with other carotenoids. In order to reduce such interference, 530 nm was chosen for measurements (Li et al., 2012). Furthermore, under nitrogen deprivation and nutrient deprivation + high light conditions, astaxanthin esters have been shown to account for over 90% of the total carotenoids. When under salinity stress or phosphorous starvation, astaxanthin was

80-90% and when just exposed high light, 75-80% (Aflalo et al., 2007; Ranga et al., 2009). Hence, slight variations in carotenoid composition might have been overseen during the akinete maturation process.

4.6. Immobilized *H. pluvialis* cultivation: research and upscale

In spite of the long commercial interest in *H. pluvialis* and astaxanthin, its cultivation in immobilized systems is a recent topic in the microalgal biotechnology scenario. It represents a very different approach from that of suspension cultures, making it difficult to compare efficiencies. A large variety of systems, environmental conditions, cultivation periods and stress factors are employed in the experimental setups. Furthermore, data are frequently analysed in different manners and are presented in different ways. Another major barrier is the concealment of methods due to the commercial value of astaxanthin.

To have an insight into the real potential of the Twin-Layer PSBR for *H. pluvialis* cultivation, productivities per surface area were recalculated for other cultivation systems from literature data, which are usually provided in volumetric units. Papers that offered sufficient information for these are listed in table 4.1. The aim of this comparison was to place the results presented in this work in the research and commercial scenario. Therefore, when a publication investigated different conditions, the most productive option was selected and compared to the highest productivities described in this work. Biomass values are also considered, but it is focused on astaxanthin production, i.e. stress phases, since growth phases are frequently not addressed in detail in the literature. For bubble columns and tubular systems, the surface was calculated to be the rectangular cross-section of the PBR while open ponds were evaluated by their footprint areas. Naturally, vertical systems (tubular PBRs and bubble columns) can have a much lower footprint area than the cultivation surface when placing parallel modules and this must be taken into account.

Discussion

These calculations confirmed that astaxanthin productivity of 0.507 g m^{-2} d^{-1} described here for NP zero at 655 µmol photons m^{-2} s^{-1} is among the highest found in the literature. In fact, the strategy of using nutrient depletion at light intensities from 300 to 800 µmol photons m^{-2} s^{-1} only yielded astaxanthin productivities above 0.3 g m^{-2} d^{-1}. This is also true for the one-step cultivation at 800 and 1,000 µmol photons m^{-2} s^{-1}, with no additional stressor. Such results contradict Zhang et al. (2016), who concluded that biofilm cultivation of *H. pluvialis* is appropriate for biomass growth but not for astaxanthin production. Their experimental data were not collected from optimized conditions and the model seems to neglect spatial differences in the biofilm, considering different cell layers and types as similar.

Biomass productivity on the Twin-Layer at high light was also among the highest observed both in the presence or absence of additional stressors. Chaumont and Thépenier (1995) reported 13.2 g m^{-2} d^{-1} in one day of cultivation in a raceway pond with nutrient-rich medium, i.e. high irradiances from natural sunlight were the only stress factors employed. The same productivities were reported for stable large scale cultivation in tubular PBRs, however, a maximum productivity of 19 g m^{-2} d^{-1} and standing crop of 90 - 100 g m^{-2} were observed (Olaizola, 2000). While biomass productivity values correspond nicely to those observed here for cultivation in full medium, much higher standing crop capacities were supported by the Twin-Layer. Cultivation for 16 days at 1,000 µmol photons m^{-2} s^{-1} with 5% supplementary CO$_2$ gave a final yield of 230 g m^{-2}. Higher values have also been observed in longer periods, hence 263.4 g m^{-2} in the biofilm used for the microsensor and values of 300 g m^{-2}, when cultivating it longer.

Results presented here increase significantly the potential of biofilm cultivation of *H. pluvialis* for astaxanthin production. Productivities were much more attractive than previously reported for this approach, even if using a light/dark cycle when all other work was done with continuous illumination (Wan et al., 2014a; Yin et al., 2015; Zhang et al., 2016, 2014), known to almost double biomass and astaxanthin production (Wan et al., 2014b). Moreover, all these papers used at least 10 g m^{-2} inoculum densities because it was seen to increase performance (Wan et al., 2014a; Zhang et al., 2014). This is still to be optimized on the Twin-Layer, however large

Table 4.1 Surface productivities comparison of different *H. pluvialis* cultivation systems.

Cultivation system	Strain	Culture medium	Temperature [°C]	CO_2 [%]	Light conditions [µmol photons m^{-2} s^{-1}]	Stress factors	Cultivation period [days]	Astaxanthin content [% of dw]	Astaxanthin productivity [g m^{-2} d^{-1}]	Biomass productivity [g m^{-2} d^{-1}]	Reference
Tubular Outdoors	own isolate	BG11	25	sparged for pH control	sunlight 400 - 1600	HL	4	4.4	0.327[a]	3.8[a]	Torzillo et al., 2013
Open pond Outdoors	ZY-18	NIES -N	28	no	sunlight max 1,000	HL + N zero	20	1.7	0.06	2.34[a]	Wan et al., 2014b
Tubular loop Outdoors	NIVA-CHL 9	Enriched Bristol	25-28	sparged for pH control	sunlight max 1,000	HL	1	1.4[a]	0.140[a]	13.2[a]	Chaumont and Thépenier, 1995
Open pond Indoors	26	BG11	20	sparged for pH control	20 - 350 14/10 h	HL	12	2.79	0.06[a]	2.2[a]	Zhang et al., 2009
Bubble column Indoors	ZY-18	NIES -N	28	no	250 continuous	HL + Nzero	12	3.6	0.296[a]	6.6[a]	Wan et al., 2014b
Bubble column Indoors	K-0084	modified BG11	25	1.5	350 continuous	HL + N zero	5	4.1[a]	0.623[a]	13.2[a]	Aflalo et al., 2007
Biofilm Indoors	NIES-144	NIES-N	25	no	150 continuous	N zero	12	1.3	0.065	3.7	Wan et al., 2014a
Biofilm Indoors	SAG 34-1b	BG11	25	1.5	100 continuous	Low N until depletion	7	2.2	0.181	6.5	Zhang et al., 2014
Biofilm Indoors	CCAC 0125	modified BG11	26	1.0	650 14/10 h	HL + NP zero	7	3.5	0.507	10.6	This study

[a] recalculated values

inoculum also demands higher energy and labour inputs and this should be accounted for at a larger technical scale. Nevertheless, the effect of the inoculum density is of particular interest because the scale up of the Twin-Layer and harvesting strategies, so it should be evaluated.

Implications for upscale

Cultivation in open systems can significantly reduce production costs when compared to closed PBRs. Estimations for the Twin-Layer in large scale plants have not yet been concluded and finding surface material with appropriate quality and attractive price is of great importance in this context. Anyhow, the cultivation strategy reported here aims at a cost-effective scale up process. The use of such a simple PBR, with lower energy and water requirements (Naumann et al., 2013) is already one step in this direction. Furthermore, the exclusive use of sunlight, enabled by the successful cultivation at high light, represents a major economic advantage. This was confirmed by life cycle analysis that appointed electricity requirements as one of the major economic and environmental burdens of astaxanthin production from *H. pluvialis*. Cultivation in closed PBR has a high energy demand, out of which 19.5% represents light use for green phase and 58.5% for red phase (Pérez-López et al., 2014). Furthermore, the irradiances applied here represented not only cost reduction but also higher surface productivities.

PSBRs such as the Twin-Layer can be arranged in vertical modules that support biomass growth on both sides. Distribution of such modules determines the surface to footprint ratio and, consequently, the light dilution rate (Liu et al., 2013; Schultze et al., 2015). PBR design typically aims at high light dilution for higher photosynthetic efficiencies and Schultze et al (2015) estimated maximum footprint productivities at high light dilution rates despite the impressive surface productivities obtained at high irradiances. However, the costs for construction, maintenance and harvest are directly related to the surface area used for cultivation, thus, increasing the number of modules for light dilution comes at a cost (Richmond, 1996). Furthermore, the use of high light reported here was not only aiming on biomass yield but also for astaxanthin

production, and, since astaxanthin is the commercial target, production costs should be calculated based on the latter. In this context, setups with surface irradiances as low as 300 µmol photons m^{-2} s^{-1} can yield high astaxanthin productivities when under nutrient depletion. According to measurements taken during a sunny summer day in Cologne, Germany, an average of 330 µmol photons m^{-2} s^{-1} can be reached in 3 m^2 surface panels spaced 1 m from each other, with a surface to footprint ratio of 3/1 (Dr Björn Podola, oral communication). Hence, astaxanthin productivities footprint area would reach 1.06 g m^{-2} d^{-1} in a vertical PSBR system under this setup.

The use of a horizontal Twin-Layer can also be considered for cost reduction, simplifying the system and reducing energy requirements for pumping. In such a system, surface and footprint area are the same and areal productivities should then be similar to that reported here. Naturally, light intensities can be considerably higher, reaching 2,000 µmol photons m^{-2} s^{-1}.

Variation of sunlight during the day was not approached in the present work, however in other algal species, total light quantity determined biomass production (Schultze et al., 2015; Toro, 1989). Thus, extrapolation of irradiances applied here to average sunlight is possible but should be cautious and experimental comparison is still recommended. Nevertheless, since high astaxanthin productivities were observed at a range of high irradiances, light variations will likely sustain such values.

Further optimizing large scale cultivation, harvesting periods have to be carefully analysed. Biomass and total astaxanthin were shown to increase in much faster rates at very high light intensities but productivities tend to reduce over time, thus reducing differences in longer cultivation periods. In order to take maximum advantage of the high irradiances, more frequent harvests should be considered. From the results reported here, a total cultivation period of 10 days, 7 of them under nutrient limitation, is suggested. Frequent harvests and such stress medium would also significantly reduce risks of contamination. However, it requires higher efforts and increases costs.

Conclusions and Outlook V
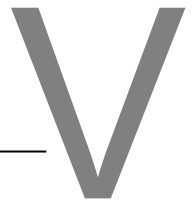
In the present work, immobilized cultivation on a Twin-Layer PSBR was approached for *H. pluvialis* cultivation and astaxanthin production, reporting the feasibility of the process and further optimization. Aside from the technical advantages of cultivation of microalgae on a PSBR, other specific positive features could be associated to *H. pluvialis:* Coupling high biomass and astaxanthin productivities under high light intensities was possible due to the biofilm organization and can represent a breakthrough in the commercial production of in *H. pluvialis*.

Taken together, the results presented here support astaxanthin production by simplified process with several advantages to the two-step currently employed. Firstly, the use of high irradiances ensures an astaxanthin productive growth phase and discards the need for two separate reactors or setups. It also raises the possibility of surface cost reduction by making use of low light dilution rates, possibly in a horizontal system. Finally, further astaxanthin induction can be naturally developed with nutrient depletion and was here shown to yield impressive astaxanthin productivities, among the highest found in the literature.

Microscopic analysis of the biofilm structure and microsensor measurements of light and dissolved oxygen helped to understand the organization and physiology of the biofilm. They indicated that astaxanthin accumulation was light dependent, under the experimental conditions tested in this work, and could give insights into biomass growth behaviour. Enhancing the knowledge on the biofilm dynamics in response to different stressors can help further optimization of the system. Microscopic and microsensor analyses will be of great importance in this context, helping to elucidate unanswered questions, such as if there really is cell division in the green layers and if so, understand how it occurs. It could also help to understand why astaxanthin production is highest at 655 µmol photons m^{-2} s^{-1} in nutrient deprived conditions.

Moreover, a pilot scale test with natural sunlight is essential to confirm the high productivities reported for the bench-scale Twin-Layer PSBR. Together with the upscale, appropriate selection of material and estimation of costs will allow the identification of the most cost-efficient setup for astaxanthin production from *H. pluvialis*.

References VI

Acién Fernández, F.G., Fernández Sevilla, J.M., Molina Grima, E., 2013. Photobioreactors for the production of microalgae. Rev. Environ. Sci. Biotechnol. 12, 131–151. doi:10.1007/s11157-012-9307-6

Aflalo, C., Meshulam, Y., Zarka, A., Boussiba, S., 2007. On the Relative Efficiency of Two- vs. One-stage Production of Astaxanthin by the Green Alga *Haematococcus pluvialis.* Biotechnol. Bioeng. 98, 300–305. doi:10.1002/bit.21391

Allewaert, C.C., Vanormelingen, P., Proeschold, T., Gomez, P.I., Gonzalez, M.A., Bilcke, G., D'Hondt, S., Vyverman, W., 2015. Species diversity in European *Haematococcus pluvialis*. Phycologia 54, 583–598. doi:10.2216/15-55.1

Ambati, R.R., Moi, P.S., Ravi, S., Aswathanarayana, R.G., 2014. Astaxanthin: Sources, extraction, stability, biological activities and its commercial applications - A review. Mar. Drugs 12, 128–152. doi:10.3390/md12010128

Andrewes, A.G., Borch, G., Liaaen-Jensen, S., Snatzke, G., 1974. Animal Carotenoids. 9. On the absolute configuration of astaxanthin and actinioerythrin. Acta Chem. Scandivavica B 28, 730–736.

Andrewes, A.G., Phaff, H.J., Starr, M.P., 1976. Carotenoids of *Phaffia Rhodozyma*, a red-pigmented fermenting yeast. Phytochemistry 15, 1003–1007. doi:10.1016/S0031-9422(00)84390-3

Andrewes, A.G., Starr, M.P., 1976. (3R,3R)- Astaxanthin from the yeast *Phaffia rhodozyma*. Phytochemistry 15, 1009–1011. doi:10.1016/S0031-9422(00)84391-5

Baker, B.R., Saling, P., 2003. Comparing natural with chemical additive production. Feed Mix 11, 12–14.

BCC Research, 2015. Boom in Astaxanthin Supplements Boosting Global Carotenoid Market [WWW Document]. URL http://www.bccresearch.com/market-research/food-and-beverage/carotenoids-global-market-report-fod025e.html (accessed 2.10.16).

Benstein, R.M., Çebi, Z., Podola, B., Melkonian, M., 2014. Immobilized Growth of the Peridinin-Producing Marine Dinoflagellate *Symbiodinium* in a Simple Biofilm Photobioreactor. Mar. Biotechnol. 621–628. doi:10.1007/s10126-014-9581-0

Berner, F., Heimann, K., Sheehan, M., 2014. Microalgal biofilms for biomass production. J. Appl. Phycol. doi:10.1007/s10811-014-0489-x

Blanken, W., Janssen, M., Cuaresma, M., Libor, Z., Bhaiji, T., Wijffels, R.H., 2014. Biofilm growth of *Chlorella sorokiniana* in a rotating biological contactor based photobioreactor. Biotechnol. Bioeng. 111, 2436–2445. doi:10.1002/bit.25301

Borowitzka, L.J., Borowitzka, M.A.., 1990. Commercial Production of β-carotene by *Dunaliella salina* in open ponds. Bull. Mar. Sci. 47, 244–252.

References

Borowitzka, M. a., Huisman, J.M., Osborn, A., 1991. Culture of the astaxanthin-producing green alga *Haematococcus pluvialis* 1. Effects of nutrients on growth and cell type. J. Appl. Phycol. 3, 295–304. doi:10.1007/BF02392882

Boussiba, S., Bing, W., Yuan, J.P., Zarka, A., Chen, F., 1999. Changes in pigments profile in the green alga *Haeamtococcus pluvialis* exposed to environmental stresses. Biotechnol. Lett. 21, 601–604. doi:10.1023/A:1005507514694

Boussiba, S., Vonshak, A., 1991. Astaxanthin Accumulation in the Green Alga *Haematococcus pluvialis*. Plant Cell Physiol. 32, 1077–1082. doi:10.1111/j.1744-7909.2007.00468.x

Brennan, L., Owende, P., 2010. Biofuels from microalgae - A review of technologies for production, processing, and extractions of biofuels and co-products. Renew. Sustain. Energy Rev. 14, 557–577. doi:10.1016/j.rser.2009.10.009

Chaumont, D., Thépenier, C., 1995. Carotenoid content in growing cells of Haematococcus pluvialis during a sunlight cycle. J. Appl. Phycol. 7, 529–537. doi:10.1007/BF00003939

Chen, Z., Wang, G., Niu, J., 2012. Variation in Rubisco and other photosynthetic parameters in the life cycle of *Haematococcus pluvialis*. Chinese J. Oceanol. Limnol. 30, 136–145. doi:10.1007/s00343-012-1060-8

Cheng, P., Wang, J., Liu, T., 2014. Effects of nitrogen source and nitrogen supply model on the growth and hydrocarbon accumulation of immobilized biofilm cultivation of *B. braunii*. Bioresour. Technol. 166, 527–533. doi:10.1016/j.biortech.2014.05.045

Chien, Y.H., Jeng, S.C., 1992. Pigmentation of kuruma prawn, *Penaeus japonicus* Bate, by various pigment sources and levels and feeding regimes. Aquaculture 102, 333–346. doi:10.1016/0044-8486(92)90186-O

Choi, Y., Yun, Y., Park, J., 2002. Evaluation of factors promoting astaxanthin production by a unicellular green alga, *Haematococcus pluvialis*, with fractional factorial design. Biotechnol. Prog. 18, 1170–1175. doi:10.1021/bp025549b

Christenson, L.B., Sims, R.C., 2012. Rotating algal biofilm reactor and spool harvester for wastewater treatment with biofuels by-products. Biotechnol. Bioeng. 109, 1674–1684. doi:10.1002/bit.24451

Christiansen, R., Lie, O., Torrissen, O.J., 1994. Effect of astaxanthin and vitamin A on growth and survival during first feeding of Atlantic salmon, *Salmo salar* L. Aquacult. Fish. Manag. 25, 903–914.

Cordero, B., Otero, A., Patiño, M., Arredondo, B.O., Fabregas, J., 1996. Astaxanthin production from the green alga *Haematococcus pluvialis* with different stress conditions. Biotechnol. Lett. 18, 213–218. doi:10.1007/BF00128682

Dauta, a, Devaux, J., Piquemal, F., Boumnich, L., 1990. Growth rate of four freshwater algae in relation to light and temperature. Hydrobiologia 207, 221–226. doi:10.1088/0957-4484/22/26/265707

Del Río, E., Acién, F.G., García-Malea, M.C., Rivas, J., Molina-Grima, E., Guerrero, M.G., 2008. Efficiency Assessment of the One-Step Production of Astaxanthin by the Microalga *Haematococcus pluvialis*. Biotechnol. Bioeng. 100, 397–402. doi:10.1002/bit.20547

Domínguez-Bocanegra, a. R., Ponce-Noyola, T., Torres-Muñoz, J. a., 2007. Astaxanthin production by Phaffia rhodozyma and *Haematococcus pluvialis*: A comparative study. Appl. Microbiol. Biotechnol. 75, 783–791. doi:10.1007/s00253-007-0889-9

Dong, L.Y., Jin, J., Lu, G., Kang, X.L., 2013. Astaxanthin attenuates the apoptosis of retinal ganglion cells in db/db mice by inhibition of oxidative stress. Mar. Drugs 11, 960–974. doi:10.3390/md11030960

Droop, M.R., 1955. Carotenogenesis in *Haematococcus pluvialis*. Nature 175, 42.

Droop, M.R., 1954. Conditions governing haematochrome formation and loss in the alga *Haematococcus pluvialis* flotow. Arch. fuer Mikrobiol. 20, 391–397. doi:10.1007/BF00690882

Droop, M.R., 1953. On the ecology of flagellates from some brackish and fresh water rockpools of finland. Acta Bot. Fenn. 51, 1–53.

Elliot, A.M., 1934. Morphology and life history of *Haematococcus pluvialis*. Arch. für Protistenkd. 82, 250–274.

Fábregas, J., Domínguez, A., García Àlvarez, D., Lamela, T., Otero, A., 1998. Induction of astaxanthin accumulation by nitrogen and magnesium deficiencies in *Haematococcus pluvialis*. Biotechnol. Lett. 20, 623–626. doi:10.1023/A:1005322416796

Fábregas, J., Domínguez, A., Maseda, A., Otero, A., 2003. Interactions between irradiance and nutrient availability during astaxanthin accumulation and degradation in *Haematococcus pluvialis*. Appl. Microbiol. Biotechnol. 61, 545–551. doi:10.1007/s00253-002-1204-4

Fan, L.; Vonshak, A.; Boussiba, S., 1994. Effect of temperature and irradiance on growth of Haematococcus pluvialis (Chlorophyceae). J. Phycol. 30, 829–833. doi:10.1111/j.0022-3646.1994.00829.x

Fan, L., Vonshak, A., 1995. The biosynthetic pathway of astaxanthin in a green alga *Haematococcus pluvialis* as indicated by inhibition with diphenylamine. Plant Cell Physiol. 36, 1519–1524.

References

Fan, L., Vonshak, A., Zarka, A., Boussiba, S., 1998. Does astaxanthin protect *Haematococcus* against light damage? Zeitschrift fur Naturforsch. - Sect. C J. Biosci. 53, 93–100.

Fogg, G.E., 1973. Phosphorus in primary aquatic plants. Water Res. 7, 77–91.

Foss, P., Storebakken, T., Austreng, E., Liaaenjensen, S., 1987. Carotenoids in diets for salmonids. V. Pigmentation of rainbow trout and sea trout with astaxanthin and astaxanthin dipalmitate in comparison with canthaxanthin. Aquaculture 65, 293–305. doi:10.1016/0044-8486(87)90242-0

Foss, P., Storebakken, T., Schiedt, K., Liaaen-Jensen, S., Austreng, E., Streiff, K., 1984. Carotenoids in diets for salmonids: I. Pigmentation of rainbow trout with the individual optical isomers of astaxanthin in comparison with cantaxahnthin. Aquaculture 41, 213–226. doi:10.1016/0044-8486(87)90242-0

Fujita, T., Satake, M., Takeshi, W., Kitjajima, C., Miki, W., Yamaguchi, K., Konosu, S., 1983. Pigmentation of Cultured Diester Red Sea Bream from Krill with Astaxanthin Oil. Bull. Japanese Soc. Sci. Fish. 49, 1855–1861.

Gao, Z., Meng, C., Chen, Y.C., Ahmed, F., Mangott, A., Schenk, P.M., Li, Y., 2014. Comparison of astaxanthin accumulation and biosynthesis gene expression of three *Haematococcus pluvialis* strains upon salinity stress. J. Appl. Phycol. doi:10.1007/s10811-014-0491-3

García-Malea, M.C., Gabriel Acién, F., Río, E. Del, Fernández, J.M., Cerón, M.C., Guerrero, M.G., Molina-Grima, E., 2009. Production of astaxanthin by *Haematococcus pluvialis*: Taking the one-step system outdoors. Biotechnol. Bioeng. 102, 651–657. doi:10.1002/bit.22076

Genin, S.N., Stewart Aitchison, J., Grant Allen, D., 2014. Design of algal film photobioreactors: Material surface energy effects on algal film productivity, colonization and lipid content. Bioresour. Technol. 155, 136–143. doi:10.1016/j.biortech.2013.12.060

Giannelli, L., Yamada, H., Katsuda, T., Yamaji, H., 2015. Effects of temperature on the astaxanthin productivity and light harvesting characteristics of the green alga *Haematococcus pluvialis*. J. Biosci. Bioeng. 119, 345–350. doi:10.1016/j.jbiosc.2014.09.002

Gieseke, A., de Beer, D., 2004. Use of microelectrodes to measure in situ microbial activities in biofilms, sediments, and microbial mats, in: Kowalchuk, G.A., de Bruijn, F.J., Head, I.M., Akkermans, A.D., van Elsas, J.D. (Eds.), Molecular Microbial Ecology Manual. Springer Netherlands, pp. 3483–3514.

Goodwin, T.W., Jamikorn, M., 1954. Studies in carotenogenesis. 11. Carotenoid synthesis in the alga *Haematococcus pluvialis*. Biochem. J. 57, 376–381.

Gross, G.J., Hazen, S.L., Lockwood, S.F., 2006. Seven day oral supplementation with Cardax (disodium disuccinate astaxanthin) provides significant cardioprotection and reduces oxidative stress in rats. Mol. Cell. Biochem. 283, 23–30. doi:10.1007/s11010-006-2217-6

Gross, M., Henry, W., Michael, C., Wen, Z., 2013. Development of a rotating algal biofilm growth system for attached microalgae growth with *in situ* biomass harvest. Bioresour. Technol. 150, 195–201. doi:10.1016/j.biortech.2013.10.016

Gross, M., Jarboe, D., Wen, Z., 2015. Biofilm-based algal cultivation systems. Appl. Microbiol. Biotechnol. 99, 5781–5789. doi:10.1007/s00253-015-6736-5

Grünewald, K., Hagen, C., 2001. β-carotene is the intermediate exported from the chloroplast during accumulation of secondary carotenoids in *Haematococcus pluvialis.* J. Appl. Phycol. 13, 89–93. doi:10.1023/A:1008183328839

Grünewald, K., Hagen, C., Braune, W., 1997. Secondary carotenoid accumulation in flagellates of the green alga *Haematococcus lacustris*. Eur. J. Phycol. 32, 387–392. doi:10.1017/S0967026297001443

Grung, M., D'Souza, F.M.L., Borowitzka, M., Liaaen-Jensen, S., 1992. Algal Carotenoids 51. Secondary carotenoids 2. *Haematococcus pluvialis* aplanospores as a source of (3 S, 3′S)-astaxanthin esters. J. Appl. Phycol. 4, 165–171. doi:10.1007/BF02442465

Hagen, C., Braune, W., Björn, L., 1994. Functional aspects of secondary carotenoides in *Haematococcus lacustris* (Volvocales). III. Action as "sunshade." J. Phycol. doi:10.1111/j.0022-3646.1994.00241.x

Hagen, C., Braune, W., Greulich, F., 1993. Functional aspects of secondary carotenoids in *Haematococcus lacustris* [Girod] Rostafinski (Volvocales) IV. Protection from photodynamic damage. J. Photochem. Photobiol. B Biol. 20, 153–160. doi:10.1016/1011-1344(93)80145-Y

Hagen, C., Siegmund, S., Braune, W., 2002. Ultrastructural and chemical changes in the cell wall of *Haematococcus pluvialis* (Volvocales, Chlorophyta) during aplanospore formation. Eur. J. Phycol. 37, 217–226. doi:10.1017/S0967026202003669

Han, D., Wang, J., Sommerfeld, M., Hu, Q., 2012. Susceptibility and protective mechanisms of motile and non motile cells of *Haematococcus pluvialis* (chlorophyceae) to photooxidative stress. J. Phycol. 48, 693–705. doi:10.1111/j.1529-8817.2012.01147.x

Harker, M., Tsavalos, A.J., Young, A.J., 1996. Factors responsible for astaxanthin formation in the chlorophyte *Haematococcus pluvialis*. Bioresour. Technol. 55, 207–214. doi:10.1016/0960-8524(95)00002-X

References

Harker, M., Tsavalos, A.J., Young, A.J., 1995. Use of response surface methodology to optimise carotenogenesis in the microalga *Haematococcus pluvialis*. J. Appl. Phycol. 7, 399–406. doi:10.1007/BF00003797

Hazen, T.E., 1899. The life history of *Sphaerella lacustris*. Mem. Torrey Bot. Club 6, 211–247. doi:10.1017/CBO9781107415324.004

Imamoglu, E., Dalay, M.C., Sukan, F.V., 2009. Influences of different stress media and high light intensities on accumulation of astaxanthin in the green alga *Haematococcus pluvialis*. N. Biotechnol. 26, 199–204. doi:10.1016/j.nbt.2009.08.007

Industry Experts, 2015. Global Astaxanthin Market – Sources , Technologies and Applications [WWW Document]. URL http://industry-experts.com/verticals/files/articles/ph009-global-astaxanthin-market-sources-technologies-and-applications.pdf (accessed 2.10.16).

Ip, P.F., Chen, F., 2005. Production of astaxanthin by the green microalga *Chlorella zofingiensis* in the dark. Process Biochem. 40, 733–738. doi:10.1016/j.procbio.2004.01.039

Jefferey, S.W., Humphrey, G.F., 1975. New spectrophotometric equations for determining chlorophylls a, b, c1 and c2 in higher plants , algae and natural phytoplankton. Biochem. und Physiol. der Pflanz. 167, 191–194.

Jeon, Y.C., Cho, C.W., Yun, Y.S., 2006. Combined effects of light intensity and acetate concentration on the growth of unicellular microalga *Haematococcus pluvialis*. Enzyme Microb. Technol. 39, 490–495. doi:10.1016/j.enzmictec.2005.12.021

Ji, B., Zhang, W., Zhang, N., Wang, J., Lutzu, G.A., Liu, T., 2013. Biofilm cultivation of the oleaginous microalgae *Pseudochlorococcum* sp. Bioprocess Biosyst. Eng. doi:10.1007/s00449-013-1109-x

Johnson, E.A., Schroeder, W.A., 1996. Biotechnology of astaxanthin production in *Phaffia rhodozyma,* in: Takeda, G., Teranishi, R., Williams, P. (Eds.), Biotechnology for Improved Foods and Flavors. pp. 39–50.

Johnson, E.A., Schroeder, W.A., 1995. Microbial Carotenoids Yield of cells on substrate. Adv. Biochem. Eng. 53, 119–178. doi:10.1007/BFb0102322

Kang, C.D., An, J.Y., Park, T.H., Sim, S.J., 2006a. Astaxanthin biosynthesis from simultaneous N and P uptake by the green alga *Haematococcus pluvialis* in primary-treated wastewater. Biochem. Eng. J. 31, 234–238. doi:10.1016/j.bej.2006.08.002

Kang, C.D., Lee, J.S., Park, T.H., Sim, S.J., 2006b. Productive encystment of *Haematococcus pluvialis* by controlling a specific irradiation rate in a photoautotrophic induction system for astaxanthin production. J. Ind. Eng. Chem. 12, 745–748.

Katsuda, T., Lababpour, A., Shimahara, K., Katoh, S., 2004. Astaxanthin production by *Haematococcus pluvialis* under illumination with LEDs. Enzyme Microb. Technol. 35, 81–86. doi:10.1016/j.enzmictec.2004.03.016

Ketchum, B.H., 1939. The develpoment and restoration of deficiencies in the phophorus and nitrogen composition of unicellular plants. J. cell. comp. Physio. 13, 373–381.

Kim, D.K., Hong, S.J., Bae, J.H., Yim, N., Jin, E., Lee, C.G., 2011. Transcriptomic analysis of *Haematococcus lacustris* during astaxanthin accumulation under high irradiance and nutrient starvation. Biotechnol. Bioprocess Eng. 16, 698–705. doi:10.1007/s12257-011-0081-z

Kobayashi, M., Kakizono, T., Nagai, S., 1993. Enhanced carotenoid biosynthesis by oxidative stress in acetate-induced cyst cells of a green unicellular alga, *Haematococcus pluvialis.* Appl. Environ. Microbiol. 59, 867–873.

Kobayashi, M., Kakizono, T., Nagai, S., 1991. Astaxanthin production by a green-alga, *Haematococcus pluvialis* accompanied with morphological changes in acetate medium. J. Ferment. Bioeng. 71, 335–339. doi:10.1016/0922-338X(91)90346-I

Kobayashi, M., Kakizono, T., Nishio, N., Nagai, S., 1992a. Effects of light intensity, light quality, and illumination cycle on astaxanthin formation in a green alga, *Haematococcus pluvialis.* J. Ferment. Bioeng. 74, 61–63.

Kobayashi, M., Kakizono, T., Nishio, N., Nagai, S., Kurimura, Y., Tsuji, Y., 1997. Antioxidant role of astaxanthin in the green alga *Haematococcus pluvialis.* Appl. Microbiol. Biotechnol. 48, 351–356. doi:10.1007/s002530051061

Kobayashi, M., Kakizono, T., Yamaguchi, K., Nishio, N., Nagai, S., 1992b. Growth and astaxanthin formation of *Haematococcus pluvialis* in heterotrophic and mixotrophic conditions. J. Ferment. Bioeng. 74, 17–20. doi:10.1016/0922-338X(92)90261-R

Lababpour, A., Hada, K., Shimahara, K., Katsuda, T., Katoh, S., 2004. Effects of nutrient supply methods and illumination with blue light emitting diodes (LEDs) on astaxanthin production by *Haematococcus pluvialis.* J. Biosci. Bioeng. 98, 452–456. doi:10.1263/jbb.98.452

Lamers, P.P., Janssen, M., De Vos, R.C.H., Bino, R.J., Wijffels, R.H., 2012. Carotenoid and fatty acid metabolism in nitrogen-starved *Dunaliella salina*, a unicellular green microalga. J. Biotechnol. 162, 21–27. doi:10.1016/j.jbiotec.2012.04.018

Lee, Y., Ding, S., 1995. Effect of Dissolved Oxygen Partial Pressure on the accumulation of astaxanthin in chemostat cultures of *Haematococcus lacustris* (Chlorophyta). J. Phycol. 31, 922–924.

References

Lee, Y.-K., Soh, C.-W., 1991. Accumulation of astaxanthin in *Haematococcus lacustris* (Chlorophyta). J. Phycol. doi:10.1111/j.0022-3646.1991.00575.x

Leu, S., Boussiba, S., 2014. Advances in the Production of High-Value Products by Microalgae. Ind. Biotechnol. 10, 169–183. doi:10.1089/ind.2013.0039

Li, J., Zhu, D., Niu, J., Shen, S., Wang, G., 2011. An economic assessment of astaxanthin production by large scale cultivation of *Haematococcus pluvialis.* Biotechnol. Adv. 29, 568–574. doi:10.1016/j.biotechadv.2011.04.001

Li, T., Piltz, B., Podola, B., Dron, A., de Beer, D., Melkonian, M., 2015a. Microscale profiling of photosynthesis-related variables in a highly productive biofilm photobioreactor. Biotechnol. Bioeng. (in press), 1–10. doi:10.1002/bit.25867

Li, T., Podola, B., de Beer, D., Melkonian, M., 2015b. A method to determine photosynthetic activity from oxygen microsensor data in biofilms subjected to evaporation.pdf. J. Microbiol. Methods 117, 100–107.

Li, T., Podola, B., Melkonian, M., 2015c. Investigating dynamic processes in a porous substrate biofilm photobioreactor - A modeling approach. Algal Res. (in press), 30–40. doi:10.1016/j.algal.2015.11.006

Li, Y., Miao, F., Geng, Y., Lu, D., Zhang, C., Zeng, M., 2012. Accurate quantification of astaxanthin from *Haematococcus* crude extract spectrophotometrically. Chinese J. Oceanol. Limnol. 30, 627–637. doi:10.1007/s00343-012-1217-5

Li, Y., Sommerfeld, M., Chen, F., Hu, Q., 2010. Effect of photon flux densities on regulation of carotenogenesis and cell viability of *Haematococcus pluvialis* (Chlorophyceae). J. Appl. Phycol. 22, 253–263. doi:10.1007/s10811-009-9453-6

Li, Y., Sommerfeld, M., Chen, F., Hu, Q., 2008. Consumption of oxygen by astaxanthin biosynthesis: A protective mechanism against oxidative stress in *Haematococcus pluvialis* (Chlorophyceae). J. Plant Physiol. 165, 1783–1797. doi:10.1016/j.jplph.2007.12.007

Liu, T., Wang, J., Hu, Q., Cheng, P., Ji, B., Liu, J., Chen, Y., Zhang, W., Chen, X., Chen, L., Gao, L., Ji, C., Wang, H., 2013. Attached cultivation technology of microalgae for efficient biomass feedstock production. Bioresour. Technol. 127, 216–222. doi:10.1016/j.biortech.2012.09.100

Lorenz, R.T., Cysewski, G.R., 2000. Commercial potential for *Haematococcus* microalgae as a natural source of astaxanthin. Trends Biotechnol. 18, 160–167. doi:10.1016/S0167-7799(00)01433-5

Mackereth, F.J., 1953. Phosphorus Utilization By *Asterionella formosa* Hass. J. Exp. Bot. 4, 296–313.

Melkonian, M., Podola, B., 2007. Method and device for cultivating eucaryotic microorganisms or blue algae and biosensor with cultivated eucaryotic microorganisms or blue algae. US 2007/0010002 A1.

Mulbry, W.W., Wilkie, A.C., 2001. Growth of benthic freshwater algae on dairy manures. J. Appl. Phycol. 13, 301–306. doi:10.1023/A:1017545116317

Murphy, T., Fleming, E., Bebout, L., Bebout, B., Berberoglu, H., 2012. A Novel Microbial Cell Cultivation Platform for Space Applications, in: 1st Annual International Space Station Research and Develop- Ment Conference. Denver, CO: American Astronomical Society (AAS). pp. 335–339.

Naguib, Y.M.A., 2000. Antioxidant activities of astaxanthin and related carotenoids. J. Agric. Food Chem. 48, 1150–1154. doi:10.1021/jf991106k

Naumann, T., Çebi, Z., Podola, B., Melkonian, M., 2013. Growing microalgae as aquaculture feeds on twin-layers: A novel solid-state photobioreactor. J. Appl. Phycol. 25, 1413–1420. doi:10.1007/s10811-012-9962-6

Noroozi, M., Omar, H., Napis, S., Hejazi, M., Soon, G., 2012. Comparative biodiversity and effect of different media on growth and astaxanthin content of nine geographical strains of *Haematococcus pluvialis*. African J. Biotechnol. 11, 15049–15059. doi:10.5897/AJB12.773

Noroozi, M., Omar, H., Tan, S.G., Napis, S., 2011. Studies on the genetic variation of the green unicellular alga *Haematococcus pluvialis* (chlorophyceae) obtained from different geographical locations using ISSR and RAPD molecular marker. Molecules 16, 2599–2608. doi:10.3390/molecules16032599

Nowack, E.C.M., Podola, B., Melkonian, M., 2005. The 96-well twin-layer system: A novel approach in the cultivation of microalgae. Protist 156, 239–251. doi:10.1016/j.protis.2005.04.003

Olaizola, M., 2003. Commercial development of microalgal biotechnology: From the test tube to the marketplace. Biomol. Eng. 20, 459–466. doi:10.1016/S1389-0344(03)00076-5

Olaizola, M., 2000. Commercial production of astaxanthin from H*aematococcus pluvialis* using 25,000-liter outdoor photobioreactors. J. Appl. Phycol. 12, 499–506. doi:10.1023/A:1008159127672

Olaizola, M., Huntley, M.E., 2003. Recent advances in commercial production of astaxanthin from microalgae, in: Fingerman, M., Nagabhushaman, R. (Eds.), Recent Advances in Marine Biotechnology. Volume 9: Biomaterials and Bioprocessing. Science Publishers, pp. 143–164.

Olivieri, G., Salatino, P., Marzocchella, A., 2014. Advances in photobioreactors for intensive microalgal production: Configurations, operating strategies and applications. J. Chem. Technol. Biotechnol. 89, 178–195. doi:10.1002/jctb.4218

Ozkan, A., Kinney, K., Katz, L., Berberoglu, H., 2012. Reduction of water and energy requirement of algae cultivation using an algae biofilm photobioreactor. Bioresour. Technol. 114, 542–548. doi:10.1016/j.biortech.2012.03.055

Park, J.S., Chyun, J.H., Kim, Y.K., Line, L.L., Chew, B.P., 2010. Astaxanthin decreased oxidative stress and inflammation and enhanced immune response in humans. Nutr. Metab. (Lond). 7, 18. doi:10.1186/1743-7075-7-18

Pérez-López, P., González-García, S., Jeffryes, C., Agathos, S.N., McHugh, E., Walsh, D., Murray, P., Moane, S., Feijoo, G., Moreira, M.T., 2014. Life cycle assessment of the production of the red antioxidant carotenoid astaxanthin by microalgae: From lab to pilot scale. J. Clean. Prod. 64, 332–344. doi:10.1016/j.jclepro.2013.07.011

Platt, T., Gallegos, C.L., Harrison, W.G., 1980. Photoinhibition of photosynthesis in natural assemblages of marine phytoplankton. J. Mar. Res. 38, 687–701.

Pocock, M. a., 1960. *Haematococcus* in Southern Africa. Trans. R. Soc. South Africa 36, 5–55. doi:10.1080/00359196009519031

Posten, C., 2009. Design principles of photo-bioreactors for cultivation of microalgae. Eng. Life Sci. 9, 165–177. doi:10.1002/elsc.200900003

Pringault, O., Garcia-Pichel, F., 2000. Monitoring of oxygenic and anoxygenic photosynthesis in a unicyanobacterial biofilm, grown in benthic gradient chamber. FEMS Microbiol. Ecol. 33, 251–258. doi:10.1016/S0168-6496(00)00068-4

Ranga Rao, a, Raghunath Reddy, R.L., Baskaran, V., Sarada, R., Ravishankar, G. a, 2010. Characterization of microalgal carotenoids by mass spectrometry and their bioavailability and antioxidant properties elucidated in rat model. J. Agric. Food Chem. 58, 8553–8559. doi:10.1021/jf101187k

Ranga, R., Sarada, Baskaran, V., Ravishankar, G. a., 2009. Identification of carotenoids from green alga Haematococcus pluvialis by HPLC and LC-MS (APCI) and their antioxidant properties. J. Microbiol. Biotechnol. 19, 1333–1341. doi:10.4014/jmb.0905.03007

Rao, A.R., Sindhuja, H.N., Dharmesh, S.M., Sankar, K.U., Sarada, R., Ravishankar, G.A., 2013. Effective inhibition of skin cancer, tyrosinase, and antioxidative properties by astaxanthin and astaxanthin esters from the green alga *Haematococcus pluvialis*. J. Agric. Food Chem. 61, 3842–3851. doi:10.1021/jf304609j

Revsbech, N.P., Jorgensen, B.B., 1983. Photosynthesis of benthic microflora measured with high spatial resolution by the oxygen microprofile method: Capabilities and limitations of the method. Limnol. Oceanogr. 28, 749–756.

Řezanka, T., Nedbalová, L., Kolouchová, I., Sigler, K., 2013. LC-MS/APCI identification of glucoside esters and diesters of astaxanthin from the snow alga *Chlamydomonas nivalis* including their optical stereoisomers. Phytochemistry 88, 34–42. doi:10.1016/j.phytochem.2013.01.003

Richmond, A., 1996. Efficient utilization of high irradiance for production of photoautotropic cell mass: a survey. J. Appl. Phycol. 8, 381–387. doi:10.1007/BF02178581

Santos, M.F., Mesquita, J.F., 1984. Ultrastructural study of *Haematococcus lacustris* (Girod .) Rostafinski (Volvocales) I . Some aspects of carotenogenesis. Cytologia (Tokyo). 49, 215–228. doi:10.1508/cytologia.49.215

Sarada, R., Tripathi, U., Ravishankar, G., 2002. Influence of stress on astaxanthin production in *Haematococcus pluvialis* grown under different culture conditions. Process Biochem. 37, 623–627. doi:10.1016/S0032-9592(01)00246-1

Schiedt, K., Foss, P., Storebakken, T., Liaaen-Jensen, S., 1989. Metabolism of carotenoids in salmonids-I. idoxanthin, a metabolite of astaxanthin in the flesh of atlantic salmon (Salmon salar, L.) under varying external conditions. Comp. Biochem. Physiol. -- Part B Biochem. 92, 277–281. doi:10.1016/0305-0491(89)90278-2

Schnurr, P.J., Allen, D.G., 2015. Factors affecting algae biofilm growth and lipid production: A review. Renew. Sustain. Energy Rev. 52, 418–429. doi:10.1016/j.rser.2015.07.090

Schnurr, P.J., Espie, G.S., Allen, D.G., 2013. Algae biofilm growth and the potential to stimulate lipid accumulation through nutrient starvation. Bioresour. Technol. 136, 337–344. doi:10.1016/j.biortech.2013.03.036

Schultze, L.K.P., Simon, M.-V., Li, T., Langenbach, D., Podola, B., Melkonian, M., 2015. High light and carbon dioxide optimize surface productivity in a Twin-Layer biofilm photobioreactor. Algal Res. 8, 37–44. doi:10.1016/j.algal.2015.01.007

Scibilia, L., Girolomoni, L., Berteotti, S., Alboresi, A., Ballottari, M., 2015. Photosynthetic response to nitrogen starvation and high light in *Haematococcus pluvialis*. Algal Res. 12, 170–181. doi:10.1016/j.algal.2015.08.024

Shi, J., Podola, B., Melkonian, M., 2007. Removal of nitrogen and phosphorus from wastewater using microalgae immobilized on twin layers: An experimental study. J. Appl. Phycol. 19, 417–423. doi:10.1007/s10811-006-9148-1

Shoaf, W.T., Lium, B.W., 1976. Improved extraction of chlorophyll a and b from algae using dimethyl sulfoxide. Limnol. Oceanogr. 21, 926–928. doi:10.4319/lo.1976.21.6.0926

Sprujit, J., 2015. Inventory of North-West European algae initiatives, Public Output report of the EnAlgae project. Swansea.

Steinbrenner, J., Linden, H., 2003. Light induction of carotenoid biosynthesis genes in the green alga *Haematococcus pluvialis* : regulation by photosynthetic redox control. Plant Mol. Biol. 52, 343–356.

Suh, I.S., Joo, H.N., Lee, C.G., 2006. A novel double-layered photobioreactor for simultaneous *Haematococcus pluvialis* cell growth and astaxanthin accumulation. J. Biotechnol. 125, 540–546. doi:10.1016/j.jbiotec.2006.03.027

Tejera, N., Cejas, J.R., Rodríguez, C., Bjerkeng, B., Jerez, S., Bolanos, A., Lorenzo, A., 2007. Pigmentation, carotenoids, lipid peroxides and lipid composition of skin of red porgy (Pagrus pagrus) fed diets supplemented with different astaxanthin sources. Aquaculture 270, 218–230. doi:10.1016/j.aquaculture.2007.01.019

Tjahjono, A.E., Hayama, Y., Kakizono, T., Terada, Y., Nishio, N., Nagai, S., 1994. Hyper-accumulation of astaxanthin in a green alga *Haematococcus pluvialis* at elevated temperatures. Biotechnol. Lett. 16, 133–138. doi:10.1007/BF01021659

Toro, J.E., 1989. The growth rate of two species of microalgae used in shellfish hatcheries cultured under two light regimes. Aquac. Fish. Manag. 20, 249–254. doi:10.1111/j.1365-2109.1989.tb00350.x

Torzillo, G., Goksan, T., Faraloni, C., Kopecky, J., Masojidek, J., 2003. Interplay between photochemical activities and pigment composition in an outdoor culture of *Haematococcus pluvialis* during the shift from the green to red stage. J. Appl. Phycol. 15, 127–136. doi:10.1023/A:1023854904163

Triki, A., Maillard, P., Gudin, C., 1997. Gametogenesis in *Haematococcus pluvialis* Flotow (Volvocales, Chlorophyta). Phycologia 36, 190–194. doi:10.2216/i0031-8884-36-3-190.1

Tsubokura, A., Yoneda, H., Mizuta, H., 1999. *Paracoccus carotinifaciens* sp. nov., a new aerobic Gram-negative astaxanthin-producing bacteriurn. Int. J. Syst. Bacteriol. 49, 277–282.

Turujman, S.A., Wamer, W.G., Wei, R.R., Albert, R.H., 1997. Rapid Liquid Chromatographic Method to Distinguish Wild Salmon from Aquacultured Salmon Fed Synthetic Astaxanthin. J. AOAC Int. 80, 622–632.

Vidhyavathi, R., Venkatachalam, L., Sarada, R., Ravishankar, G.A., 2008. Regulation of carotenoid biosynthetic genes expression and carotenoid accumulation in the green alga *Haematococcus pluvialis* under nutrient stress conditions. J. Exp. Bot. 59, 1409–1418. doi:10.1093/jxb/ern048

Vonshak, A., Richmond, A., 1988. Mass production of the blue-green alga *Spirulina*: An overview. Biomass 15, 233–247. doi:10.1016/0144-4565(88)90059-5

Wan, M., Hou, D., Li, Y., Fan, J., Huang, J., Liang, S., Wang, W., Pan, R., Wang, J., Li, S., 2014a. The effective photoinduction of *Haematococcus pluvialis* for accumulating astaxanthin with attached cultivation. Bioresour. Technol. 163, 26–32. doi:10.1016/j.biortech.2014.04.017

Wan, M., Zhang, J., Hou, D., Fan, J., Li, Y., Huang, J., Wang, J., 2014b. The effect of temperature on cell growth and astaxanthin accumulation of *Haematococcus pluvialis* during a light-dark cyclic cultivation. Bioresour. Technol. 167, 276–283.

doi:10.1016/j.biortech.2014.06.030

Wang, B., Zarka, A., Trebst, A., Boussiba, S., 2003. Astaxanthin accumulation in *Haematococcus pluvialis* (Chloropyceae) as an active photoprotective process under high irradiance. J. Phycol. 39, 1116–1124. doi:10.1111/j.0022-3646.2003.03-043.x

Wang, B., Zhang, Z., Hu, Q., Sommerfeld, M., Lu, Y., Han, D., 2014. Cellular Capacities for High-Light Acclimation and Changing Lipid Profiles across Life Cycle Stages of the Green Alga *Haematococcus pluvialis.* PLoS One 9, 1–12. doi:10.1371/journal.pone.0106679

Wang, J., Han, D., Sommerfeld, M.R., Lu, C., Hu, Q., 2013a. Effect of initial biomass density on growth and astaxanthin production of *Haematococcus pluvialis* in an outdoor photobioreactor. J. Appl. Phycol. 25, 253–260. doi:10.1007/s10811-012-9859-4

Wang, J., Sommerfeld, M.R., Lu, C., Hu, Q., 2013b. Combined effect of initial biomass density and nitrogen concentration on growth and astaxanthin production of *Haematococcus pluvialis* (Chlorophyta) in outdoor cultivation. Algae 28, 193–202.

Wang, S.-B., Chen, F., Sommerfeld, M., Hu, Q., 2004. Proteomic analysis of molecular response to oxidative stress by the green alga *Haematococcus pluvialis* (Chlorophyceae). Planta 220, 17–29. doi:10.1007/s00425-004-1323-5

Wang, W., Yu, L., Zhou, P., 2006. Effects of different fungal elicitors on growth, total carotenoids and astaxanthin formation by *Xanthophyllomyces dendrorhous*. Bioresour. Technol. 97, 26–31. doi:10.1016/j.biortech.2005.02.012

Wilmes, P., Remis, J.P., Hwang, M., Auer, M., Thelen, M.P., Banfield, J.F., 2009. Natural acidophilic biofilm communities reflect distinct organismal and functional organization. ISME J. 3, 266–270. doi:10.1038/ismej.2008.90

WILSON, L.B., 1905. A method for the rapid preparation of fresh tissues for the microscope. J. Am. Med. Assoc. XLV, 1737. doi:10.1001/jama.1905.52510230037003c

Wu, Y.H., Yang, J., Hu, H.Y., Yu, Y., 2013. Lipid-rich microalgal biomass production and nutrient removal by *Haematococcus pluvialis* in domestic secondary effluent. Ecol. Eng. 60, 155–159. doi:10.1016/j.ecoleng.2013.07.066

Yamada, S., 1990. Pigmentation of Prawn (*Penaeus japonicus*) with Carotenoids I . Effect of Dietary Astaxanthin , B-Carotene and Canthaxanthin on Pigmentation. Aquaculture 87, 323–330.

Yin, S., Wang, J., Chen, L., Liu, T., 2015. The water footprint of biofilm cultivation of *Haematococcus pluvialis* is greatly decreased by using sealed narrow chambers combined with slow aeration rate. Biotechnol. Lett. 37, 1819–1827. doi:10.1007/s10529-015-1864-7

References

Yokoyama, A., Miki, W., 1995. Composition and presumed biosynthetic pathway of carotenoids in the astaxanthin-producing bacterium *Agrobacterium aurantiacum*. FEMS Microbiol. Lett. 128, 139–144. doi:10.1016/0378-1097(95)00097-O

Yong, Y.Y.R., Lee, Y.-K., 1991. Do carotenoids play a photoprotective role in the cytoplasm of *Haematococcus lacustris* (Chlorophyta)? Phycologia 30, 257–261. doi:10.2216/i0031-8884-30-3-257.1

Yoo, J.J., Choi, S.P., Kim, B.W., Sim, S.J., 2012. Optimal design of scalable photobioreactor for phototropic culturing of *Haematococcus pluvialis*. Bioprocess Biosyst. Eng. 35, 309–315. doi:10.1007/s00449-011-0616-x

Yoshihisa, Y., Andoh, T., Matsunaga, K., Rehman, M.U., Maoka, T., Shimizu, T., 2016. Efficacy of Astaxanthin for the Treatment of Atopic Dermatitis in a Murine Model. PLoS One 11, e0152288. doi:10.1371/journal.pone.0152288

Yu, F.P., Callis, G.M., Stewart, P.S., Griebe, T., Mcfeters, G.A., 1994. Cryosectioning of biofilms for microscopic examination. Biofouling 8, 85–91. doi:10.1080/08927019409378264

Zhang, B.Y., Geng, Y.H., Li, Z.K., Hu, H.J., Li, Y.G., 2009. Production of astaxanthin from *Haematococcus* in open pond by two-stage growth one-step process. Aquaculture 295, 275–281. doi:10.1016/j.aquaculture.2009.06.043

Zhang, D., Wan, M., del Rio-Chanona, E.A., Huang, J., Wang, W., Li, Y., Vassiliadis, V.S., 2016. Dynamic modelling of *Haematococcus pluvialis* photoinduction for astaxanthin production in both attached and suspended photobioreactors. Algal Res. 13, 69–78. doi:10.1016/j.algal.2015.11.019

Zhang, D.H., Lee, Y.K., Ng, M.L., Phang, S.M., 1997. Composition and accumulation of secondary carotenoids in *Chlorococcum* sp. J. Appl. Phycol. 9, 147–155. doi:10.1023/A:1007926528388

Zhang, W., Wang, J., Wang, J., Liu, T., 2014. Attached cultivation of *Haematococcus pluvialis* for astaxanthin production. Bioresour. Technol. 158, 329–335. doi:10.1016/j.biortech.2014.02.044

Zlotinik, I., Sukenik, A., Dubinsky, Z., 1993. Physiological and photosynthetic changes durng the formation of red aplanospores in the chlorophyte *Haematococus pluvialis*. J. Phycol. 29, 463–469.

Appendix VII

125

Table 7.1. Maximum values and productivities for astaxanthin and biomass for experiments with culture medium stressors. Stress media was applied at day three and values shown here refer to a total cultivation period of 10 days.

Stress factor	Light [µmol photon m^{-2} s^{-1}]	Astaxanthin productivity [g m^{-2} d^{-1}]			Maximum astaxanthin [g m^{-2}]			Maximum astaxanthin content [% of dw]			Biomass productivity [g m^{-2} d^{-1}]			Maximum biomass [g m^{-2}]		
-	500	0.204	±	0.018	2.190	±	0.259	1.774	±	0.169	11.370	±	0.790	124.213	±	12.800
-	660	0.300	±	0.030	2.965	±	0.463	2.032	±	0.317	13.970	±	0.673	145.932	±	10.359
-	800	0.266	±	0.030	2.339	±	0.313	1.618	±	0.208	15.620	±	0.983	144.462	±	1.417
P zero	800	0.194	±	0.033	1.759	±	0.483	1.525	±	0.089	13.290	±	1.749	126.778	±	27.567
NP zero	800	0.291	±	0.027	2.712	±	0.316	2.802	±	0.461	7.457	±	0.751	97.901	±	10.130
N zero	800	0.336	±	0.030	2.738	±	0.559	2.787	±	0.380	8.982	±	1.256	97.960	±	11.500
Nzero + NaCl	800	0.270	±	0.027	2.342	±	0.457	2.888	±	0.310	6.707	±	0.880	80.538	±	7.724
NaCl	800	0.217	±	0.023	2.177	±	0.374	2.312	±	0.479	7.962	±	0.861	96.759	±	15.460
NP zero	345	0.353	±	0.022	2.852	±	0.279	2.602	±	0.254	10.410	±	0.412	109.606	±	1.294
NP zero	415	0.360	±	0.018	3.014	±	0.234	2.919	±	0.226	9.432	±	0.500	103.248	±	5.745
NP zero	485	0.316	±	0.024	2.811	±	0.516	3.017	±	0.480	6.174	±	0.337	94.370	±	5.376
NP zero	540	0.383	±	0.016	3.095	±	0.167	2.764	±	0.149	10.410	±	0.335	111.969	±	4.746
NP zero	610	0.411	±	0.023	3.409	±	0.118	2.920	±	0.101	9.513	±	0.599	116.772	±	7.400
NP zero	655	0.507	±	0.031	4.216	±	0.416	3.533	±	0.441	10.570	±	0.592	120.965	±	12.001
NP zero	740	0.424	±	0.030	3.630	±	0.531	3.613	±	0.135	8.907	±	0.834	107.638	±	7.079
NaCl	345	0.140	±	0.021	1.479	±	0.092	2.123	±	0.132	4.664	±	0.705	69.685	±	11.758
NaCl	415	0.224	±	0.011	1.995	±	0.058	2.181	±	0.063	7.586	±	0.555	91.470	±	7.535
NaCl	485	0.288	±	0.018	2.447	±	0.212	2.181	±	0.189	10.660	±	1.125	112.205	±	14.799
NaCl	540	0.213	±	0.021	1.967	±	0.227	2.185	±	0.252	6.953	±	0.793	90.026	±	12.054
NaCl	610	0.244	±	0.010	2.160	±	0.037	2.482	±	0.043	7.066	±	0.691	87.008	±	7.098
NaCl	655	0.226	±	0.019	2.057	±	0.160	2.098	±	0.163	8.845	±	0.687	98.031	±	8.526
NaCl	740	0.243	±	0.014	2.434	±	0.105	2.301	±	0.099	8.278	±	0.795	105.774	±	3.551

Erklärung

Ich versichere, dass ich die von mir vorgelegte Dissertation selbständig angefertigt, die benutzten Quellen und Hilfsmittel vollständig angegeben und die Stellen der Arbeit − einschließlich Tabellen, Karten und Abbildungen −, die anderen Werken im Wortlaut oder dem Sinn nach entnommen sind, in jedem Einzelfall als Entlehnung kenntlich gemacht habe; dass diese Dissertation noch keiner anderen Fakultät oder Universität zur Prüfungvorgelegen hat; dass sie noch nicht veröffentlicht worden ist sowie, dass ich eine solche Veröffentlichung vor Abschluss des Promotionsverfahrens nicht vornehmen werde. Die Bestimmungen der Promotionsordnung sind mir bekannt. Die von mir vorgelegte Dissertation ist von Herr Prof. Dr. Michael Melkonian betreut worden.

Köln, den 15.02.2016

Alice Costa Kiperstok

Lebenslauf

Alice Costa Kiperstok

Weyerstraßerweg 6, 50969 Köln, Tel. 0176 61377877

Email: kiperstok@gmail.com

Persönliche Angaben

Geburtsdatum: 03.06.1985
Geburtsort: Salvador
Nationalität: Brasilianisch

Ausbildung

04/2012 - aktuell	**Universität zu Köln** Doktorarbeit Thema: Optimizing immobilized cultivation of *Haematococcus pluvialis* for astaxanthin production
06/2008 – 10/2010	**Oswaldo Cruz Foundation (FIOCRUZ)**, Salvador - Brasilien Master of Science in Biologische Wissenschaften / Medizinische Biotechnologie Thema: Cardiac function evaluation in a type 2 diabetes model of a high-fat fed mouse.
03/2003 – 12/2007	**Federal University of Bahia** – Salvador - Brasilien Bachelor of Science in Biologische Wissenschaften Thema: Stem cell therapy in a mouse model of type 2 diabetes *mellitus*.
02/1997 – 12/2002	**Instituto Social da Bahia** - Salvador, Brasilien Abschluss: Certificado de conclusão do ensino médio
1996	**Castlebrook High School**, Greater Manchester, England
1993 - 1995	**Saint Paul's C of E Primary School** – Greater Manchester, England

Berufserfahrung

11/2010 – 10/2011 Federal University of Bahia
Bioenergy and catalysis laboratory (LABEC)
Junior researcher

06/2006 – 12/2007 Universidade Federal da Bahia
Clean technologies network (TECLIM)
Praktikant

01/2014 – 12/2007 Oswaldo Cruz Foundation
Tissue engineering and immunopharmacology laboratory
Praktikant